The First *Swift* BAT Gamma-Ray Burst Catalog

T. Sakamoto[1,2], S. D. Barthelmy[1], L. Barbier[1], J. R. Cummings[3,10], E. E. Fenimore[4], N. Gehrels[1], D. Hullinger[8], H. A. Krimm[6,10], C. B. Markwardt[5,10], D. M. Palmer[4], A. M. Parsons[1], G. Sato[1,7], M. Stamatikos[1,2], J. Tueller[1], T. N. Ukwatta[1,9], B. Zhang[11]

ABSTRACT

We present the first *Swift* Burst Alert Telescope (BAT) catalog of gamma-ray bursts (GRBs), which contains bursts detected by the BAT between 2004 December 19 and 2007 June 16. This catalog (hereafter BAT1 catalog) contains burst trigger time, location, 90% error radius, duration, fluence, peak flux, and time averaged spectral parameters for each of 237 GRBs, as measured by the BAT. The BAT-determined position reported here is within 1.75′ of the Swift X-ray Telescope (XRT)-determined position for 90% of these GRBs. The BAT T_{90} and T_{50} durations peak at 80 and 20 seconds, respectively. From the fluence-fluence correlation, we conclude that about 60% of the observed peak energies, $E_{\rm peak}^{\rm obs}$, of BAT GRBs could be less than 100 keV. We confirm that GRB fluence to hardness and GRB peak flux to hardness are correlated for BAT bursts in analogous ways to previous missions' results. The correlation between the photon index in a simple power-law model and $E_{\rm peak}^{\rm obs}$ is also confirmed. We also report

[1]NASA Goddard Space Flight Center, Greenbelt, MD 20771

[2]Oak Ridge Associated Universities, P.O. Box 117, Oak Ridge, Tennessee 37831-0117

[3]Joint Center for Astrophysics, University of Maryland, Baltimore County, 1000 Hilltop Circle, Baltimore, MD 21250

[4]Los Alamos National Laboratory, P.O. Box 1663, Los Alamos, NM, 87545

[5]Department of Astronomy, University of Maryland, College Park, MD 20742

[6]Universities Space Research Association, 10211 Wincopin Circle, Suite 500, Columbia, MD 21044-3432

[7]Institute of Space and Astronautical Science, JAXA, Kanagawa 229-8510, Japan

[8]Moxtek, Inc., 452 West 1260 North, Orem, UT 84057

[9]Center for Nuclear Studies, Department of Physics, The George Washington University, Washington, D.C. 20052

[10]Center for Research and Exploration in Space Science and Technology (CRESST), NASA Goddard Space Flight Center, Greenbelt, MD 20771

[11]Department of Physics and Astronomy, University of Nevada, Las Vegas, NV 89154

the current status for the on-orbit BAT calibrations based on observations of the Crab Nebula.

Subject headings: gamma rays: bursts

1. Intruduction

The *Swift* mission (Gehrels et al. 2004) has revolutionized our understanding of gamma-ray bursts (GRBs). Because of the sophisticated on-board localization capability of the *Swift* Burst Alert Telescope (BAT; Barthelmy et al. (2005a)) and the fast spacecraft pointing of *Swift*, more than 90% (30%) of *Swift* GRBs have an X-ray (optical) afterglow observation from the *Swift* X-Ray Telescope (XRT; Burrows et al. (2005a)) or the *Swift* UV/Optical Telescope (UVOT; Roming et al. (2005)) within a few hundred seconds after the trigger. *Swift* opens a new opportunity to study the host galaxies and the distance scale of the mysterious short duration GRBs.[1] (e.g., Gehrels et al. 2005; Barthelmy et al. 2005b) *Swift* allows us to use GRBs as a tool for investigation of the early universe (cf. detection of GRB 050904 at a redshift of 6.29; Cusumano et al. (2006)). *Swift* found the fourth GRB, GRB 060218, which is securely associated with a supernova (Campana et al. 2006). Furthermore, *Swift* is providing critical X-ray afterglow data (e.g., Zhang et al. 2006) which challenges the standard GRB fireball model.

Here we present the first BAT GRB catalog including 237 GRBs detected by BAT from 2004 December 19 to 2007 June 16. In §2, we describe the BAT instrument. In §3, we show the current status of the on-orbit calibration of the BAT based on the Crab observations. In §4, we describe the analysis methods for the catalog. In §5, we describe the content of the tables of the catalog and show the results of the prompt emission properties of the BAT GRBs based on the catalog. Our conclusions are summarized in §6. All quoted errors in this work are at the 90% confidence level.

2. Instrumentation

The BAT is a highly sensitive, large field of view (FOV) (1.4 sr for >50% coded FOV and 2.2 sr for >10% coded FOV), coded-aperture telescope, which detects and localizes GRBs

[1]The short burst GRB 050709, which observed and promptly localized by *HETE-2* is also a good example of a short GRB observation (Villasenor et al. 2005).

in real time. The fast and accurate BAT GRB positions with 1-3 arc-minute error radii are the key to autonomously slewing the spacecraft to point the XRT and the UVOT. The BAT GRB position, light curves, and the detector plane image (BAT scaled map) are transmitted through TDRSS to the ground within 20–200 s after the burst trigger. The BAT detector plane is composed of 32,768 pieces of CdZnTe (CZT: $4 \times 4 \times 2$ mm), and the coded-aperture mask is composed of $\sim$ 52,000 lead tiles ($5 \times 5 \times 1$ mm) with a 1-m separation between mask and detector plane. The energy range is 15-150 keV for imaging or mask weighting[2] with a non-coded response up to 350 keV.

The CZT pixels are biased to -200 V with a nominal operating temperature of 20°C. The energy scale calibration is performed automatically on the front end electronics (XA1) by injecting calibration pulses. This electronic calibration task is executed every $\sim$ 5000 s during spacecraft slews. In addition to the electronic calibration, there are two ^{241}Am tagged sources mounted below the mask for calibrating the absolute energy scale and the detector efficiency for each CZT pixel in-flight.

There are three types of triggers in the BAT flight software. Two of these are rate triggers looking for excesses in the count rate from the background, and one is an image trigger based on new significant sources found in the sky images. The rate triggers are divided into short (foreground period $\leq$ 64 ms) and long rate triggers (foreground period $\geq$ 64 ms). Each trigger criterion is a specific combination of choices of foreground interval, number of background samples, energy band and one of nine different regions of the detector plane. Currently, 494 trigger criteria have been running on-board for a long rate trigger, 36 for the short rate trigger, and 1 for the image trigger. Once a rate trigger has occurred, the BAT creates a sky image using the triggered foreground and background intervals in the specified energy band to find a significant source in the image. Failing to produce a significant image excess, the BAT will check for trigger criteria that produce a more statistically significant image. When a rate or image trigger finds a significant source in the image, a location match to the on-board source catalog is executed to exclude activity from known hard X-ray astronomical sources.[3]

For each GRB trigger, the photon-by-photon data (event data) are available with a time resolution of 100 μs. The duration of the event data was initially from T-300 s to T+300 s (T as the BAT trigger time). After March 17 2006, we have extended the duration of

---

[2]Mask weighting is a background subtraction technique based on the modulation resulting from the coded mask.

[3]If the significance of the activity of the known source is higher than the threshold value set in the on-board catalog, the activity will be reported to the GCN in real time with a different GCN notice type.

the event data which are downlinked to from T-300 s to T+1000 s. We also transmit 10 s of the event data for failed triggers.[4] In the survey mode, the BAT produces detector plane histograms (DPHs). These histograms have an 80 channel spectrum for each detector integrated typically over five minutes.[5] The DPHs are the primary data product when the GRB prompt emission lasts longer than the stop time of the event data collection (e.g. GRB 060124; Romano et al. 2006).

3. On-orbit calibration

The Crab nebula data collected for various positions in the BAT field of view were used for the on-orbit calibration. We analyzed the DPH data for this purpose. The standard BAT software (HEASoft 6.2) and the latest calibration database (CALDB: 2006-10-14) were used for processing the data. We first made the Good Time Interval (GTI) file for each observation segment (each observation ID) excluding the periods when 1) the spacecraft was not settled, 2) the spacecraft was in the South Atlantic Anomaly (SAA), and 3) the Crab was occulted by the earth, moon and/or sun. `batoccultgti` was used for excluding the time periods for case 3. `baterebin` was applied to the DPH data to correct the energy scale. The individual rows in the DPH data were processed separately to reduce the systematic uncertainty of the spacecraft attitude. A Detector Plane Image (DPI) file was created from the DPH using `batbinevt` for each individual row. The spacecraft attitude file was re-created using ftools `aspect` by specifying the observation start and stop time of the DPI. The detector enable/disable map was created using `bathotpix`. The BAT sky image was created by `batfftimage` using the DPI, the updated attitude file and the enable/disable map. `batcelldetect` was used to extract the position of the Crab. The mask weight map of the Crab was created by `batmaskwtimg` using the "true" Crab position from SIMBAD ($\mathrm{R.A._{J2000}}$ = 83.6332, $\mathrm{Dec._{J2000}}$ = 22.0144). The spectrum (PHA file) was created by `batbinevt` using the mask weight map for each row of the DPH. All of the individual PHA files at the same sky coordinate were added to create a single PHA file if the Crab was detected $> 8\sigma$ in the image in the full energy band (15–350 keV). The detector energy response file was created by `batdrmgen` for each summed PHA file.

---

[4]Failed triggers are those which caused a rate trigger, but did not also have a significant point source in the image formed with that data; or those for which the image coincided with a known source in the on-board catalog.

[5]The integration time of DPHs changes in various operational conditions, but is 300 s for most of the on-orbit operation time.

3.1. Position Accuracy

The histograms of the angular differences between the Crab detected position by `batcelldetect` and the "true" Crab position (the Crab position in SIMBAD) are shown in the top of Figure 1. The position differences are less than $1'$ for 95% of the Crab observations in both the right ascension (R.A.) and the declination (Dec.). The bottom of Figure 1 shows the BAT position errors as a function of signal to noise ratio for the Crab. The signal to noise ratio and the position error are correlated with a power-law index of -0.7 (see section 5).

3.2. Energy Response

Immediately after the first attempt to fit the Crab spectrum with the pre-launch detector energy response matrices (DRM), we noticed that there were systematic errors in the pre-launch DRM at low energies (below 25 keV) and also at high energies (above 80 keV). The investigation of these problems is still in progress. To overcome these problems, we applied corrections to force the Crab to fit a canonical model, a power-law with a photon index of 2.15 and a 15-150 keV energy flux of 2.11×10^{-8} ergs cm^{-2} s^{-1} (e.g., Jung 1989; Rothschild et al. 1998; Fiore, Guainazzi & Grandi 1999; Olive et al. 2003; Lubiński, Dubath & Paltani 2005). Due to these corrections, the BAT team has released the software tool, `batphasyserr`, and the CALDB file (swbsyserr20030101v002.fits) to apply the energy dependent systematic errors to the PHA file. The systematic errors which should be applied to the PHA file are shown in Figure 2. The Crab spectra were fitted by a simple power-law model using `Xspec 11.3.2` including the systematic errors.

Figure 3 shows the Crab photon index and the flux in the 15-150 keV band as a function of the incident angle. In the current BAT DRM (`batdrmgen v3.3` and CALDB: 20061014), the scatter of the photon index and the flux are about 5% and 10% of the canonical values. Figure 4 shows the contour maps of the Crab photon index and the flux in the 15-150 keV band over the BAT field of view. We note that the parameters tend to deviate from the canonical values towards the edge of the BAT field of view. Thus, the spectral parameters could have a larger systematic error when the source is at the edge of the field of view of BAT.

3.3. BAT GRB Response Time

Figure 5 shows the histogram of the time delay between the BAT GRB trigger time and the GCN BAT Position Notice.[6] The highest peak of the distribution is around 15 s. The BAT position has been reported on the ground within 30 s after the burst trigger for half of the BAT GRBs. Most of the longer delays (>300 s) are due to interruptions in TDRSS transmissions during regular telemetry down links to the Malindi ground station.

4. Analysis for the GRB catalog

We used the standard BAT software (HEASoft 6.1.1) and the latest calibration database (CALDB: 20061014) to process the BAT GRBs from December 2004 (GRB 041217) to June 2007 (GRB 070616).[7] The burst pipeline script, `batgrbproduct`, was used to process the BAT event data.[8] The `Xspec` spectral fitting tool (version 11.3.1) was used to fit each spectrum. Since our analysis is restricted to use only the event data, we present partial analysis based on the available event data for bursts which last longer than the end period of the event data (e.g. GRB 060124) or which have incomplete event data due to the various reasons (e.g. GRB 050507). In some cases, especially for weak short GRBs, `battblocks`, which is one of the task run in `batgrbproduct`, might fail to find the burst interval. In those cases, we fitted the mask-weighted light curve in the full BAT energy range by a liner-rise exponential decay model ("BURS" model in ftools qdp[9]) to find the burst time intervals (T_{100}, T_{90}, T_{50} and peak 1-s intervals) and created the T_{100} and peak 1-s PHA files based on these time intervals. We put comments on Table 1 for the bursts which have a problem in either the data or the processing.

For the time-averaged spectral analysis, we use the time interval from the emission start time to the emission end time (T_{100} interval). Since the BAT energy response generator, `batdrmgen`, performs the calculation for a fixed single incident angle of the source, it will be

---

[6]This GRB sample is from GRB 050215A to GRB 070616 (slightly reduced from the rest of the paper) excluding the GRBs found on the ground process.

[7]The GRB sample includes bursts which were found in the ground processing.

[8]By default, the minimum partial coding setting was 10% to remove portions of the light curve with poor sampling, and the aperture setting was CALDB:FLUX in order to avoid passive materials in the BAT field of view. Some bursts were initially in the extreme partial coded field of view (<10%). In those cases, we re-ran `batgrbproduct` specifying the options pcodethresh=0.0 and aperture=CALDB:DETECTION.

[9]http://heasarc.gsfc.nasa.gov/docs/software/ftools/others/qdp/qdp.html

a problem if the position of the source is moving during the time interval selected for the spectral analysis because of the spacecraft slew. In this situation, we created the DRMs for each five-second period during the time interval taking into account the position of the GRB in detector coordinates. We then weighted these DRMs by the five-second count rates and created the averaged DRM using `addrmf`. Since the spacecraft slews about one degree per second in response to a GRB trigger, we chose five second intervals to calculate the DRM for every five degrees.

The spectrum was fitted by a simple power-law (PL) model,

$$f(E) = K_{50}^{\rm PL} \left(\frac{E}{50\,{\rm keV}} \right)^{\alpha^{\rm PL}} \tag{1}$$

where $\alpha^{\rm PL}$ is the power-law photon index and $K_{50}^{\rm PL}$ is the normalization at 50 keV in units of photons cm^{-2} s^{-1} keV^{-1}, and by a cutoff power-law (CPL) model,

$$f(E) = K_{50}^{\rm CPL} \left(\frac{E}{50\,{\rm keV}} \right)^{\alpha^{\rm CPL}} \exp\left(\frac{-E\,(2+\alpha^{\rm CPL})}{E_{\rm peak}} \right) \tag{2}$$

where $\alpha^{\rm CPL}$ is the power-law photon index, $E_{\rm peak}$ is the peak energy in the $\nu {\rm F}_\nu$ spectrum and $K_{50}^{\rm CPL}$ is the normalization at 50 keV in units of photons cm^{-2} s^{-1} keV^{-1}. We also systematically fitted the spectrum with the Band function (Band et al. 1993). However, none of the BAT spectra show a significant improvement in χ^2 with a Band function fit compared to that of a CPL model fit. Note that this is equivalent to saying that a CPL model and a Band function represent equally well the observed spectrum. However, we only present the results based on a CPL model throughout the paper due to its simplicity in the functional form.[10] The best fit spectral model is determined based on the difference in χ^2 between a PL and a CPL fit. If $\Delta\ \chi^2$ between a PL and a CPL fit is greater than 6 ($\Delta\chi^2 \equiv \chi^2_{\rm PL} - \chi^2_{\rm CPL} > 6$), we determined that a CPL model is a better representative spectral model for the data. To quantify the significance of this improvement, we performed 10,000 spectral simulations taking into account the distributions of the power-law photon index in a PL fit, the fluence in the 15-150 keV band in a PL fit and the T_{100} duration of the BAT GRBs, and determined how many cases a CPL fit gives χ^2 improvements of equal or greater than 6 over a PL fit. The BAT DRM used in the simulation was for an incident angle of 30° which was an averaged incident angle of the BAT GRB sample (see Figure 7). We found equal or higher improvements in χ^2 in 62 simulated spectra out of 10,000. Thus, the chance probability of having an equal or higher $\Delta\chi^2$ of 6 with a CPL model when the parent distribution is a case of a PL model is 0.62%.

[10]A Band function has 4 parameters, whereas, a CPL model has 3 parameters.

The fluence and the peak flux are derived from the spectral fits. The fluences are calculated fitting the time-averaged spectrum by the best fit spectral model. The peak fluxes are calculated fitting the spectrum of the one-second interval bracketing the highest peak in the light curve (hereafter peak spectrum). Again, we used the best fit spectral model for calculating the peak fluxes. To correctly reflect the incident angle of the source during the period of the peak spectrum, the DRM for the peak spectrum was created updating the keywords of the peak spectrum file by `batupdatephakw` and running `batdrmgen` using this updated spectral file.

5. The Catalog

The first BAT catalog includes the time period between 2004 December 19 and 2007 June 16. The total number of GRBs including five untriggered GRBs[11] and four possible GRBs is 237. 237 GRBs are listed in Table 1. The first column is the GRB name. The next column is the BAT trigger number. The next column specifies the BAT trigger time in UTC in the form of *YYYY-MM-DD hh:mm:ss* where *YYYY* is year, *MM* is month, *DD* is day of month, *hh* is hour, *mm* is minute, and *ss* is second. Note that the definition of the BAT trigger time is the start time of the foreground time interval of the image from which the GRB is detected on-board. The next four columns give the locations by the ground process in equatorial (J2000) coordinate, the signal-to-noise ratio of the BAT image at the location, and the radius of the 90% confidence region in arcmin. The 90% error radius is calculated based on the signal-to-noise ratio of the image using the following equation which derived from the BAT hard X-ray survey process[12,13]

$$r_{90\%} = 10.92 \times \mathrm{SNR}^{-0.7} \ (\mathrm{arcmin}),$$

where SNR is the signal-to-noise ratio of the BAT image. However, due to the limitation of the BAT point spread function, we decided to quote the minimum allowed value of $r_{90\%}$ as $1'$ in the catalog. The next two columns specify the burst durations which contain from 5% to 95% (T_{90}) and from 25% to 75% (T_{50}) of the total burst fluence. These durations are calculated in the 15–350 keV band.[14] The next two columns are the start and stop time

[11]GRBs which found in ground processing.

[12]http://heasarc.gsfc.nasa.gov/docs/swift/analysis/bat_digest.html

[13]SWIFT-BAT-CALDB-CENTROID-v1
http://swift.gsfc.nasa.gov/docs/heasarc/caldb/swift/docs/bat/index.html

[14]The coded mask is transparent to photons above 150 keV. Thus, photons above 150 keV are treated as background in the mask-weighted method. The effective upper boundary is $\sim$ 150 keV.

from the BAT trigger time of the event data. The last column is the comments.

The energy fluences calculated in various energy bands are summarized in Table 2. The first column is the GRB name. The next column specifies the spectral model which used in deriving the fluences (PL: simple power-law model; Eq.(1), CPL: cutoff power-law model; Eq.(2)). The next five columns are the fluences in the 15-25 keV, the 25-50 keV, the 50-100 keV, the 100-150 keV, and the 15-150 keV band. The unit of the fluence is 10^{-8} ergs cm^{-2}. The last two columns specify the start and the stop time from the BAT trigger time which used to calculate the fluences. Note that since our analysis is based on the available event data, 6 bursts with the incomplete data (see the 12th column of Table 1) might not include the whole burst emission.

Table 3 and 4 summarize the 1-s peak photon and energy fluxes in various energy bands. The first column is the GRB name. The next column specifies the spectral model used in deriving the 1-s peak flux. The next five column are the 1-s peak photon and energy fluxes in the 15-25 keV, the 25-50 keV, the 50-100 keV, the 100-150 keV, and the 15-150 keV band. The unit of the flux is photons cm^{-2} s^{-1} for the peak photon flux and 10^{-8} ergs cm^{-2} s^{-1} for the peak energy flux. The last two columns specify the start and the stop time from the BAT trigger time which were used to calculate the peak fluxes.

The time-averaged spectral parameters are listed in Table 5. The first column is the GRB name. The next three columns are the photon index, the normalization at 50 keV and χ^2 of the fit for a PL model. The degree of freedom is 57 for all bursts in a PL fit. The next four columns are the photon index, $E_{\rm peak}^{\rm obs}$, the normalization at 50 keV and χ^2 of the fit in a CPL model. The degree of freedom is 56 for all bursts for a CPL fit. The spectral parameters in a CPL are only shown for the bursts which meet the criteria described in the section 4.

In the following subsections of investigating the relationship among fluences, peak fluxes, and the spectral parameters, we excluded 10 GRBs based on an incomplete data set and also those labeled as possible GRBs/SGRs (see the 12th column of Table 1).

5.1. BAT GRB Position and Sky Locations

Figure 6 shows the angular difference between the BAT ground position and the first reported XRT position.[15] The BAT ground position is within 0.95′ and 1.75′ from the XRT

[15]The XRT position is either from the on-board or from the XRT event-by-event data downloaded from the TDRSS satellite (Single-Pixel-Event-Report).

position for 68% and 90% of the bursts, respectively. The distribution of the incident angles (θ) is shown in Figure 7. The θ distribution is peaked around 30° with a spread from 0° to 60°. The sky map of the BAT 237 GRBs in galactic coordinates is shown in Figure 8.

5.2. Durations and Hardness

The histograms of T_{90} and T_{50} measured by the mask weighted light curve in the BAT full energy band are shown in Figure 9. The BAT T_{90} and T_{50} durations are peaked around 80 s and 20 s respectively. The BAT duration distributions do not show the clear bimodality seen in the BATSE sample (e.g., Kouveliotou et al. 1993) due to the smaller samples of short duration bursts (hereafter short GRBs). This is a well-known selection effect for an imaging GRB instrument like the BAT. For most of the GRB imaging instruments, two triggering processes have to be met to be determined a GRB trigger. The first step is the increase in the count rate from the background level, and the second step is the significant signal in the image. Although the short duration bursts would have triggered as an excess in the count rate, it could be very difficult to meet the criterion for a significant signal in the image because of the smaller number of photons to do the imaging compared to those of the long duration bursts (hereafter long GRBs). However, because of the large effective area and also the sophisticated flight software, the BAT has been triggering and localizing short GRBs in a much higher fraction than other GRB imaging instruments (e.g. *Beppo*SAX, *HETE-2*).

Figure 10 shows the T_{50} and T_{90} durations versus the fluence ratio between the 50-100 keV and the 25-50 keV band. Although the short GRBs tend to be systematically harder than the long GRBs, the separation in the hardness between these two classes is not obvious, at least in the BAT GRB sample. Note that there are several works that question the hardness of the BATSE short GRBs reported on the BATSE catalog (Sakamoto et al. 2006; Ohno et al. 2007; Donaghy et al. 2007). Therefore, as mentioned in Donaghy et al. (2007) and also seen in the BAT short GRB samples, the duration and the hardness are not enough criteria to distinguish between long and short GRBs.

5.3. Peak Fluxes and Fluences

Figure 11 shows the distribution of the fluence versus the peak photon flux in the 15-150 keV band. The positive correlation is seen in these two parameters (correlation coefficient of +0.912 in a 220 burst sample). The peak photon flux of about 70% of the BAT GRBs is less than 2 photons cm^{-2} s^{-1} in the 15-150 keV band. If we assume a GRB detector

with a sensitivity of 1 photons cm^{-2} s^{-1} in the 50-300 keV band (trigger band of BATSE), the peak photon flux in the 15-150 keV band is 2.5 photons cm^{-2} s^{-1} assuming the Band function parameters of $\alpha = -1$, $\beta = -2.5$, and $E^{obs}_{peak} = 100$ keV. Thus, the majority of the BAT GRBs might be too weak to trigger a typical GRB detector which is sensitive at >50 keV. This rough estimate is consistent with the observation that only 20-30% of the BAT GRBs are simultaneously triggered successfully by the currently active GRB detectors such as *Konus-Wind* and *Suzaku/WAM*.

Figure 12 shows the fluence in the 15-50 keV band versus that in the 50-150 keV band. The blue dash-dotted line is the case of the Band function parameters of $\alpha = -1$, $\beta = -2.5$, and $E^{obs}_{peak} = 100$ keV. The blue dotted line is the case of the Band function parameters of $\alpha = -1$, $\beta = -2.5$, and $E^{obs}_{peak} = 30$ keV. With the assumption of the Band parameters of $\alpha = -1$ and $\beta = -2.5$, the fraction of the long GRBs ($T_{90} > 2$ s) with $E^{obs}_{peak} < 100$ keV can be estimated to be about 60% of the total long GRB samples. On the other hand, according to the BATSE spectral catalog (Kaneko et al. 2006), there are only 3% of the long BATSE GRBs with $E^{obs}_{peak} < 100$ keV. Therefore, the E^{obs}_{peak} distribution of the BAT GRBs could be systematically lower than the BATSE E^{obs}_{peak} distribution because of the relatively lower energy coverage of the BAT.

5.4. Time-averaged Spectral Parameters

The histogram of the photon index in a PL fit is shown in Figure 13. The photon index distribution has a single broad peak which centroid around -1.6. The peak value of the PL photon index of -1.6 is close to the mean value of the low energy photon index of -1.0 and the high energy photon index of -2.5 of the typical GRB spectrum (Kaneko et al. 2006; Sakamoto et al. 2005). Since we would expect a photon index based on a PL model to be -1.0 or -2.5 if E^{obs}_{peak} is above or below the BAT energy band, this result clearly demonstrates that majority of E^{obs}_{peak} of the BAT GRBs is likely to be within the BAT energy band. The reason why the BAT can not measure E^{obs}_{peak} for the majority of GRBs is due to its narrow energy band (Sakamoto et al. in preparation). Although the sample of bursts is very limited, the short GRBs tend to have a harder PL photon index than the long GRBs. However, the PL photon index distributions have a significant overlap between the short and long GRBs.

The top panel of Figure 14 shows the photon index versus the fluence in the 15-150 keV band in a PL fit. There is a correlation between these two parameters for the long GRBs. The correlation coefficient is +0.458 for the sample of 206 bursts. The probability of such a correlation occurring by chance is < 0.001%. If we include the short duration bursts, however, the correlation becomes weaker (correlation coefficient of +0.228 for the sample of

220 bursts). Therefore, we have confirmed the fluence - hardness correlation (e.g., Lloyd et al. 2000) especially for the BAT long GRB sample. The bottom panel of Figure 14 shows the time-averaged photon index in a PL fit versus the 1-s peak energy flux in the 15-150 keV band. The correlation coefficient of these two parameters are +0.397 for the GRB sample without the short bursts (total 206 GRBs) and +0.376 for the sample with the short bursts (total 220 GRBs). The probabilities of a chance coincidence of the correlation between parameters are $< 0.001\%$ for both cases. Therefore, we also confirmed the correlation between the peak flux and the hardness either with or without the short GRBs (e.g., Lloyd et al. 2000). Note that both the fluence and the peak flux measured by the BAT are not the bolometric values and may introduce the systematic errors in the correlations.

For the limited number of GRBs (32 GRBs) which have a significant improvement in χ^2 by a CPL fit, we investigated the relationship between $E_{\rm peak}^{\rm obs}$ and other parameters. The top panel of Figure 15 shows the distribution of $E_{\rm peak}$ and the energy fluence in the 15-150 keV band. The correlation coefficient between these two parameters is +0.580 (a chance probability of 0.2%). The bottom panel of Figure 15 shows the distribution of $E_{\rm peak}$ and the 1-s peak energy flux in the 15-150 keV band. The correlation coefficient is +0.563 (a chance probability of 0.2%). Note that the fluence and the peak flux are calculated from the BAT energy range. Therefore, these values are not bolometric. Figure 16 shows the relationship between the photon index in a CPL model and $E_{\rm peak}^{\rm obs}$. The $E_{\rm peak}^{\rm obs}$ distribution is spread from 10 keV to 500 keV for the BAT GRB sample. There is no correlation between the photon index and $E_{\rm peak}^{\rm obs}$. This is consistent with the measurements of other missions (e.g., Kippen et al. 2001; Sakamoto et al. 2005).

Figure 17 shows the correlation between the photon index in a PL fit and $E_{\rm peak}^{\rm obs}$ derived from a CPL fit. As we mentioned in the first paragraph of this section, the variation in the photon indices derived from a PL fit is very likely to reflect the differences in $E_{\rm peak}^{\rm obs}$ energies which are within the BAT energy band. This correlation between the PL photon index and $E_{\rm peak}^{\rm obs}$ was also recognized by Zhang et al. (2007) and their best fit correlation is shown as a dashed line in Figure 17. Since the correlation found by Zhang et al. (2007) is based on $E_{\rm peak}$ derived from a Band function, the slight offset between the dashed line and the data could be due to the systematic difference of $E_{\rm peak}$ based on the choise of the spectral model (e.g., Kaneko et al. 2006). The detailed study of this correlation based on the spectral simulations will be presented elsewhere (Sakamoto et al. in preparation).

6. Summary

The first BAT catalog includes 237 GRBs detected by BAT during two and a half years of operation. The BAT ground positions are $< 1.75'$ from the XRT position for 90% of GRBs. We presented the observed temporal and spectral properties of the prompt emission based on the analysis of the BAT event data. Taking into account the difficulty in triggering short GRBs with the imaging instrument like BAT, the duration distributions are consistent with other missions. We showed that the BAT long GRB sample is systematically softer than that of the BATSE bright GRB sample. The correlations such as the fluence- hardness and the peak flux - hardness have been confirmed by the BAT GRB samples.

We would like to thank J. A. Nousek and J. P. Osborne for valuable comments. This research was performed while T. S. held a NASA Postdoctoral Program administered by Oak Ridge Associated Universities at NASA Goddard Space Flight Center formerly the National Research Council program.

REFERENCES

Barthelmy, S. D., et al. 2005, Space Sci. Rev., 120, 143

Barthelmy, S. D., et al. 2005, Nature, 438, 994

Band, D.L., et al., ApJ, 413, 281

Burrows, S. D., et al. 2005a, Space Sci. Rev., 120, 165

Campana, S. et al. 2006, Nature, 442, 1008

Cusumano, G. et al. 2006, Nature, 440, 164

Donaghy, T. Q. et al, submitted to ApJ (astro-ph/0605570)

Fiore, F., Guainazzi, M., Grandi, P. 1999, *Cookbook for BeppoSAX NFI Spectral Analysis* (http://heasarc.gsfc.nasa.gov/docs/sax/abc/saxabc/saxabc.html)

Gehrels, N. et al. 2004, ApJ, 611, 1005

Gehrels, N. et al. 2005, Nature, 437, 851

Jung, G.V. 1989, ApJ, 338, 972

Kaneko, Y. et al. 2006, ApJS, 166, 298

Kippen, R.M., Woods, P.M., Heise, J., in't Zant, J.J.M., Briggs, M.S., Preece, R.D. 2003, in API Conf. Proc. 662, Gamma-Ray Burst and Afterglow Astronomy 2001, ed. G.R.Ricker & R.K. Vanderspek (New York: AIP), 244

Kouveliotou, C. et al. 1993, ApJ, 413, L101

Lloyd, N.M., Petrosian, V., Mallozi, R.S. 2000, ApJ, 534, 227

Lubiński, P., Dubath, P., Paltani, S. 2005, *INTEGRAL cross-calibration status for OSA 5.1* (http://isdc.unige.ch/?Support+documents)

Ohno, M. et al. 2007, PASJ in press

Olive, J.-F. et al. 2003, in API Conf. Proc. 662, Gamma-Ray Burst and Afterglow Astronomy 2001, ed. G.R.Ricker & R.K. Vanderspek (New York: AIP), 88

Romano, P. et al. 2006, A&A, 456, 917

Roming, P.W.A. et al. 2005, Space Sci. Rev., 120, 95

Rothschild, R.E. et al. 1998, ApJ, 496, 538

Sakamoto, T. et al. 2005, ApJ, 629, 311

Sakamoto, T. et al. 2006, in API Conf. Proc. 836, Gamma-Ray Bursts in the Swift Era, ed. S.S. Holt, N. Gehrels & J.A. Nousek (New York: AIP), 43

Villasenor, J.S. et al. 2005, Nature, 437, 855

Zhang, B. et al. 2006, ApJ, 642, 354

Zhang, B. et al. 2007, ApJL, 655, 25

Table 1. BAT GRB summary

GRB Name	Trigger Number	Trigger time	R.A. (°)	Dec. (°)	SN_{img} (σ)	Error (′)	T_{90} (s)	T_{50} (s)	Start (s)	Stop (s)	Comment
041217	100116	2004-12-17 07:28:25.236	164.793	−17.942	20.4	1.3	5.8	2.7	−2.2	17.8	
041219A	100318	2004-12-19 01:42:18.000	6.154	62.847	-	7.0	-	-	-	-	No data[1]
041219B	100367	2004-12-19 15:38:48.000	167.674	−33.458	-	7.0	-	-	-	-	No data[1]
041219C	100380	2004-12-19 20:30:34.000	343.926	−76.744	34.2	1.0	4.8	1.4	−3.0	17.1	
041220	100433	2004-12-20 22:58:26.599	291.288	60.598	33.8	1.0	5.6	2.2	−299.9	302.1	
041223	100585	2004-12-23 14:06:17.956	100.204	−37.068	87.5	1.0	109.1	29.3	−299.3	302.8	
041224	100703	2004-12-24 20:20:57.698	56.192	−6.663	11.3	2.0	177.2	37.5	−299.0	303.0	
041226	100815	2004-12-26 20:34:18.976	79.689	73.329	6.2	3.0	89.7	52.8	−299.3	302.7	
041228	100970	2004-12-28 10:49:14.142	336.642	5.032	37.7	1.0	55.4	19.8	−299.5	302.6	
050117	102861	2005-01-17 12:52:36.037	358.479	65.939	54.5	1.0	166.6	83.3	−299.4	302.7	
050124	103647	2005-01-24 11:30:02.876	192.877	13.039	36.5	1.0	4.0	2.0	−299.2	302.8	
050126	103780	2005-01-26 12:00:54.073	278.115	42.384	18.5	1.4	24.8	13.6	−299.4	302.6	
050128	103906	2005-01-28 04:19:55.191	219.587	−34.765	28.3	1.1	19.2	8.0	−299.6	302.5	
050202	104298	2005-02-02 03:35:14.800	290.584	−38.730	9.1	2.3	0.27	0.10	−299.2	242.8	battblocks failed[2]
050215A	106106	2005-02-15 02:15:28.543	348.403	49.328	7.7	2.6	87.3	55.9	−119.9	302.1	
050215B	106107	2005-02-15 02:33:43.199	174.463	40.797	15.4	1.6	8.1	3.5	−60.6	122.5	
050219A	106415	2005-02-19 12:40:01.049	166.416	−40.681	34.2	1.0	23.7	10.0	−299.4	302.6	
050219B	106442	2005-02-19 21:05:51.256	81.306	−57.758	30.7	1.0	30.7	6.9	−299.7	302.4	
050223	106709	2005-02-23 03:09:06.068	271.394	−62.465	16.8	1.5	22.5	10.4	−150.0	302.6	
050306	107547	2005-03-06 03:33:11.876	282.309	−9.152	31.4	1.0	158.3	74.8	−299.3	302.8	
050315	111063	2005-03-15 20:59:42.518	306.476	−42.591	26.3	1.1	95.6	24.4	−300.0	302.1	
050318	111529	2005-03-18 15:44:37.170	49.695	−46.386	31.1	1.0	-	-	−299.6	32.4	Incomplete data[3]
050319	111622	2005-03-19 09:31:18.449	154.172	43.581	8.5	2.4	152.5	124.7	−180.0	302.2	
050326	112453	2005-03-26 09:53:56.135	6.871	−71.377	75.8	1.0	29.3	19.4	−299.6	302.5	
050401	113120	2005-04-01 14:20:15.326	247.873	2.185	29.1	1.0	33.3	25.9	−299.8	302.3	
050406	113872	2005-04-06 15:58:48.407	34.410	−50.180	8.4	2.5	5.4	2.1	−299.9	302.2	
050410	114299	2005-04-10 12:14:33.553	89.757	79.605	25.7	1.1	42.5	23.1	−299.0	243.0	
050412	114485	2005-04-12 05:44:02.894	181.099	−1.193	17.1	1.5	26.5	9.3	−200.0	302.7	
050416A	114753	2005-04-16 11:04:44.488	188.485	21.058	17.5	1.5	2.5	1.0	−300.0	302.1	
050416B	114797	2005-04-16 22:35:54.119	133.848	11.186	19.9	1.3	3.4	1.6	−299.6	302.4	
050418	114893	2005-04-18 11:00:34.629	44.334	−18.541	43.6	1.0	82.3	62.6	−299.1	302.9	
050421	115135	2005-04-21 04:11:51.617	307.341	73.678	7.5	2.7	15.0	10.0	−299.1	303.0	
050422	115214	2005-04-22 07:52:39.807	324.507	55.788	12.9	1.8	59.3	42.7	−299.3	302.8	
050502B	116116	2005-05-02 09:25:40.464	142.535	16.987	22.2	1.2	17.7	9.4	−300.0	302.1	

Table 1—Continued

GRB Name	Trigger Number	Trigger time	R.A. (°)	Dec. (°)	SN_{img} (σ)	Error (′)	T_{90} (s)	T_{50} (s)	Start (s)	Stop (s)	Comment
050505	117504	2005-05-05 23:22:21.098	141.760	30.266	21.3	1.3	58.9	26.6	−299.6	302.5	
050507	118248	2005-05-07 22:43:18.311	48.063	−11.064	10.3	2.1	-	-	−299.8	32.200	Incompete data[3]
050509A	118707	2005-05-09 01:46:28.517	310.573	54.076	22.6	1.2	11.4	4.1	−299.0	123.0	
050509B	118749	2005-05-09 04:00:19.237	189.046	28.974	8.2	2.5	0.073	0.027	−299.8	302.3	`battblocks` failed[2]
050525A	130088	2005-05-25 00:02:53.261	278.142	26.335	145.8	1.0	8.8	5.2	−300.0	303.2	
050528	130679	2005-05-28 04:06:45.128	353.524	45.957	10.5	2.1	11.3	6.8	−299.7	302.4	
050603	131560	2005-06-03 06:29:05.214	39.982	−25.175	25.0	1.1	12.4	2.8	−299.8	302.3	
050607	132247	2005-06-07 09:11:22.807	300.180	9.139	20.8	1.3	26.4	14.0	−120.0	302.7	
050701	143708	2005-07-01 11:42:59.472	227.241	−59.399	11.0	2.0	21.8	7.7	−10.1	33.0	
050712	145581	2005-07-12 14:00:27.517	77.722	64.924	14.8	1.7	51.6	26.9	−299.1	302.9	
050713A	145675	2005-07-13 04:29:02.396	320.585	77.072	29.7	1.0	124.7	10.5	−299.0	303.0	
050713B	145754	2005-07-13 12:07:17.628	307.821	60.936	10.7	2.1	54.2	22.9	−60.2	122.8	
050714B	145994	2005-07-14 22:40:32.377	169.691	−15.547	8.7	2.4	46.7	23.3	−170.0	303.0	
050715	146129	2005-07-15 22:30:26.424	155.641	−0.029	20.8	1.3	51.6	33.2	−140.0	303.0	
050716	146227	2005-07-16 12:36:03.639	338.593	38.683	30.4	1.0	69.1	35.5	−299.3	302.8	
050717	146372	2005-07-17 10:30:52.213	214.348	−50.541	53.4	1.0	85.0	27.4	−299.8	302.2	
050721	146970	2005-07-21 04:29:14.287	253.453	−28.386	12.1	1.9	98.4	30.2	−299.9	302.1	
050724	147478	2005-07-24 12:34:09.321	246.175	−27.526	12.5	1.9	96.0	70.1	−200.0	303.1	
050726	147788	2005-07-26 05:00:17.830	200.024	−32.064	13.5	1.8	49.9	18.8	−299.5	302.6	
050730	148225	2005-07-30 19:58:23.199	212.069	−3.754	20.2	1.3	156.5	62.1	−299.8	302.2	
050801	148522	2005-08-01 18:28:02.075	204.144	−21.930	16.5	1.5	19.4	6.5	−299.7	302.4	
050802	148646	2005-08-02 10:08:02.266	219.283	27.799	21.1	1.3	19.0	8.0	−80.0	302.1	
050803	148833	2005-08-03 19:14:00.344	350.650	5.788	23.3	1.2	87.9	38.1	−299.0	303.1	
050813	150139	2005-08-13 06:45:09.768	242.001	11.244	6.9	2.8	0.45	0.19	−299.4	302.6	
050814	150314	2005-08-14 11:38:56.966	264.196	46.324	11.0	2.0	150.9	55.9	−299.6	302.4	
050815	150532	2005-08-15 17:25:18.723	293.584	9.139	11.8	1.9	2.9	1.5	−299.4	122.7	
050819	151131	2005-08-19 16:23:55.132	358.751	24.871	10.9	2.0	37.7	18.0	−299.8	302.2	
050820A	151207	2005-08-20 06:34:53.115	337.416	19.560	26.1	1.1	-	-	−299.8	240.9	Incomplete data[4]
050820B	151334	2005-08-20 23:50:27.194	135.607	−72.640	75.2	1.0	12.0	3.8	−240.0	302.2	
050822	151486	2005-08-22 03:49:29.144	51.106	−46.030	14.6	1.7	103.4	44.8	−66.8	302.2	
050824	151905	2005-08-24 23:12:16.307	12.264	22.602	10.8	2.1	22.6	10.7	−220.0	303.1	
050826	152113	2005-08-26 06:18:10.289	87.761	−2.658	11.5	2.0	35.5	17.3	−300.0	302.1	
050827	152325	2005-08-27 18:57:15.118	64.294	18.219	28.6	1.0	50.0	10.7	−299.8	302.3	
050904	153514	2005-09-04 01:51:44.290	13.770	14.189	7.3	2.7	174.2	81.7	−20.0	303.1	

Table 1—Continued

GRB Name	Trigger Number	Trigger time	R.A. (°)	Dec. (°)	SN_{img} (σ)	Error (′)	T_{90} (s)	T_{50} (s)	Start (s)	Stop (s)	Comment
050906	153866	2005-09-06 10:32:04.765	52.802	−14.621	5.5	3.3	0.258	0.058	−299.5	302.5	`battblocks` failed[2]
050908	154112	2005-09-08 05:42:31.386	20.457	−12.950	17.6	1.5	19.4	6.5	−299.1	303.0	
050911	154630	2005-09-11 15:59:33.844	13.710	−38.856	8.6	2.4	16.2	13.6	−299.6	302.5	
050915A	155242	2005-09-15 11:22:42.317	81.688	−28.014	19.3	1.4	52.0	16.8	−299.0	303.0	
050915B	155284	2005-09-15 21:23:04.269	219.109	−67.411	48.8	1.0	40.9	21.0	−299.0	303.1	
050916	155408	2005-09-16 16:35:52.267	135.979	−51.406	6.6	2.9	49.5	26.4	−299.0	303.1	
050922B	156434	2005-09-22 15:02:00.257	5.790	−5.607	7.9	2.6	150.9	35.4	−299.0	303.1	
050922C	156467	2005-09-22 19:55:50.400	317.383	−8.764	55.1	1.0	4.5	1.4	−130.0	303.0	
050925	156838	2005-09-25 09:04:33.532	303.490	34.329	17.9	1.4	0.07	0.02	−299.3	302.8	Possible new SGR[6]
051001	157870	2005-10-01 11:11:36.241	350.984	−31.515	9.3	2.3	189.1	100.5	−299.0	303.1	
051006	158593	2005-10-06 20:30:33.255	110.807	9.510	18.7	1.4	34.8	10.6	−299.0	303.0	
051008	158855	2005-10-08 16:33:21.316	202.865	42.103	50.8	1.0	-	-	−299.1	33.0	Incomplete data[3]
051012	159413	2005-10-12 17:05:54.219	270.513	−52.799	9.8	2.2	-	-	0.0	20.1	Untriggered GRB
051016	159913	2005-10-16 05:23:31.350	122.814	−18.299	11.3	2.0	23.0	10.0	−299.1	302.9	
051016B	159994	2005-10-16 18:28:08.981	132.123	13.629	15.6	1.6	4.0	2.4	−299.8	302.3	
051021B	160672	2005-10-21 23:31:53.676	126.059	−45.534	22.0	1.3	46.5	19.3	−299.5	302.5	
051105	162580	2005-11-05 06:26:41.457	265.372	35.112	2.7	5.5	0.093	0.034	−60.3	122.8	`battblocks` failed[2]
051109A	163136	2005-11-09 01:12:20.522	330.316	40.850	11.8	1.9	37.2	23.4	−299.4	302.7	
051109B	163170	2005-11-09 08:39:39.370	345.469	38.663	11.6	2.0	14.3	6.0	−299.2	302.9	
051111	163438	2005-11-11 05:59:41.478	348.136	18.367	43.5	1.0	46.1	15.4	−299.3	302.8	
051113	163765	2005-11-13 15:22:34.722	187.242	−26.395	19.0	1.4	93.3	37.9	−299.6	302.5	
051114	163844	2005-11-14 04:11:28.239	226.290	60.154	11.9	1.9	-	-	−4.2	+15.8	Untriggered GRB
051117A	164268	2005-11-17 10:51:20.091	228.398	30.868	34.0	1.0	136.3	58.7	−299.9	302.1	
051117B	164279	2005-11-17 13:22:54.427	85.205	−19.286	8.8	2.4	9.0	4.8	−299.3	302.8	
051210	171931	2005-12-10 05:46:21.168	330.192	−57.622	11.9	1.9	1.3	0.6	−299.1	303.0	
051213	172516	2005-12-13 07:13:04.106	252.084	−59.233	13.1	1.8	71.1	53.2	−20.0	303.1	
051221A	173780	2005-12-21 01:51:15.612	328.715	16.888	63.2	1.0	1.40	0.55	−299.5	302.6	
051221B	173904	2005-12-21 20:03:20.090	312.378	53.041	15.6	1.6	39.9	21.7	−299.0	303.1	
051227	174738	2005-12-27 18:07:16.047	125.231	31.949	10.5	2.1	114.6	66.8	−300.0	302.1	
060102	175603	2006-01-02 21:17:27.963	328.839	−1.837	7.6	2.6	19.0	13.0	−299.9	302.2	
060105	175942	2006-01-05 06:49:27.446	297.485	46.356	36.8	1.0	54.4	25.9	−120.0	302.7	
060108	176453	2006-01-08 14:39:11.760	147.013	31.935	20.8	1.3	14.3	4.9	−299.7	302.4	
060109	176620	2006-01-09 16:54:41.230	282.735	32.011	6.2	3.0	115.4	82.9	−299.2	302.9	
060110	176702	2006-01-10 08:01:17.773	72.737	28.428	44.9	1.0	26.0	9.0	−299.7	302.4	

Table 1—Continued

GRB Name	Trigger Number	Trigger time	R.A. (°)	Dec. (°)	SN_{img} (σ)	Error (′)	T_{90} (s)	T_{50} (s)	Start (s)	Stop (s)	Comment
060111A	176818	2006-01-11 04:23:06.123	276.193	37.600	49.2	1.0	13.2	5.9	−299.1	303.0	
060111B	176918	2006-01-11 20:15:43.242	286.456	70.380	17.6	1.5	58.8	21.1	−299.2	302.9	
060115	177408	2006-01-15 13:08:00.643	54.007	17.339	11.2	2.0	139.6	92.4	−220.0	302.5	
060116	177533	2006-01-16 08:37:27.233	84.698	−5.438	14.2	1.7	105.9	31.3	−299.2	302.9	
060117	177666	2006-01-17 06:50:01.599	327.912	−59.982	62.5	1.0	16.9	10.0	−299.6	242.5	
060124	178750	2006-01-24 15:54:51.825	77.097	69.727	15.1	1.6	-	-	−40.0	302.3	Incomplete data[5]
060202	179968	2006-02-02 08:40:55.008	35.809	38.377	10.7	2.1	198.9	126.6	−299.0	303.1	
060203	180151	2006-02-03 23:55:35.005	103.463	71.841	12.8	1.8	68.2	31.5	−299.0	183.0	
060204B	180241	2006-02-04 14:34:24.092	211.805	27.675	43.1	1.0	139.4	30.1	−299.1	303.0	
060206	180455	2006-02-06 04:46:53.272	202.933	35.046	48.4	1.0	7.6	2.3	−299.3	99.2	
060210	180977	2006-02-10 04:58:49.809	57.727	27.015	30.1	1.0	255.0	43.7	−299.8	302.2	
060211A	181126	2006-02-11 09:39:10.990	58.381	21.489	17.3	1.5	126.3	80.3	−299.0	303.1	
060211B	181156	2006-02-11 15:55:14.766	75.085	14.959	13.2	1.8	27.7	7.8	−299.8	302.3	
060218	191157	2006-02-18 03:34:30.977	50.380	16.910	8.0	2.5	-	-	−50.00	303.0	Incomplete data[5]
060219	191512	2006-02-19 22:48:05.118	241.851	32.309	10.2	2.1	62.1	43.7	−299.1	302.9	
060223A	192059	2006-02-23 06:04:23.927	55.186	−17.134	24.5	1.2	11.3	5.1	−300.0	302.1	
060223B	192152	2006-02-23 19:41:04.886	254.238	−30.812	49.9	1.0	10.3	5.6	−299.9	110.0	
060306	200638	2006-03-06 00:49:10.626	41.097	−2.163	29.2	1.0	61.2	42.8	−299.7	302.5	
060312	201391	2006-03-12 01:36:12.758	45.780	12.827	38.5	1.0	50.6	16.4	−299.8	302.2	
060313	201487	2006-03-13 00:12:06.292	66.625	−10.858	48.3	1.0	0.74	0.48	−299.4	302.7	
060319	202035	2006-03-19 00:55:42.920	176.379	60.038	10.9	2.0	10.6	4.9	−60.0	303.1	
060322	202442	2006-03-22 23:00:21.120	274.230	−36.710	28.4	1.1	221.5	170.9	−239.2	962.9	
060323	202505	2006-03-23 14:32:36.031	174.421	50.000	18.0	1.4	25.4	11.8	−239.1	962.9	
060403	203755	2006-04-03 13:12:17.129	282.338	8.327	28.9	1.0	30.1	14.2	−239.2	962.9	
060413	205096	2006-04-13 18:40:22.869	291.287	13.746	12.2	1.9	147.7	38.5	−239.0	963.0	
060418	205851	2006-04-18 03:06:08.204	236.431	−3.640	34.3	1.0	103.1	25.5	−239.3	962.7	
060421	206257	2006-04-21 00:39:23.334	343.629	62.730	44.1	1.0	12.2	6.2	−239.5	962.6	
060424	206773	2006-04-24 04:16:19.520	7.359	36.787	14.6	1.7	37.5	9.7	−239.7	962.4	
060427	207281	2006-04-27 11:43:10.841	124.177	62.657	10.3	2.1	64.0	28.0	−239.0	963.1	
060428A	207364	2006-04-28 03:22:48.056	123.540	−37.167	34.6	1.0	39.5	22.2	−239.2	962.8	
060428B	207399	2006-04-28 08:54:38.839	235.369	62.016	15.2	1.6	57.9	27.4	−239.0	963.1	
060501	208050	2006-05-01 08:14:58.865	328.374	44.002	21.2	1.3	21.9	7.0	−239.0	963.1	
060502A	208169	2006-05-02 03:03:32.144	240.937	66.604	39.7	1.0	28.4	10.7	−239.3	962.8	
060502B	208275	2006-05-02 17:24:41.071	278.927	52.618	8.8	2.4	0.131	0.048	−239.2	962.8	`battblocks` failed[2]

Table 1—Continued

GRB Name	Trigger Number	Trigger time	R.A. (°)	Dec. (°)	SN_{img} (σ)	Error (′)	T_{90} (s)	T_{50} (s)	Start (s)	Stop (s)	Comment
060505	208654	2006-05-05 06:36:00.831	331.772	−27.815	4.4	3.9	-	-	0.0	10.0	Untriggered GRB
060507	208870	2006-05-07 01:53:12.230	89.911	75.250	25.4	1.1	183.3	114.3	−239.4	962.6	
060510A	209351	2006-05-10 07:43:27.647	95.860	−1.163	20.1	1.3	20.4	5.9	−239.8	408.5	
060510B	209352	2006-05-10 08:22:14.815	239.259	78.591	12.2	1.9	275.2	132.5	−239.0	963.1	
060512	209755	2006-05-12 23:13:20.730	195.748	41.209	12.2	1.9	8.5	4.3	−239.9	962.1	
060515	210084	2006-05-15 02:27:52.918	127.277	73.561	17.1	1.5	52.0	24.4	−239.1	361.9	
060516	210254	2006-05-16 06:43:34.803	71.170	−18.126	8.6	2.4	161.6	86.3	−239.0	963.0	
060522	211117	2006-05-22 02:11:18.792	322.954	2.895	17.3	1.5	71.1	42.3	−239.0	963.1	
060526	211957	2006-05-26 16:28:29.950	232.834	0.288	19.4	1.4	298.2	249.1	−239.2	962.9	
060602A	213180	2006-06-02 21:32:12.464	149.579	0.314	15.9	1.6	75.0	33.1	−239.7	722.3	
060604	213486	2006-06-04 18:19:00.012	337.224	−10.945	4.7	3.7	95.0	46.0	−239.2	842.8	
060605	213630	2006-06-05 18:15:44.618	322.128	−6.071	12.4	1.9	79.1	33.5	−239.9	600.0	
060607A	213823	2006-06-07 05:12:13.351	329.705	−22.496	40.9	1.0	102.2	24.9	−239.6	962.5	
060607B	213934	2006-06-07 23:32:44.133	42.043	14.755	25.2	1.1	31.1	12.9	−239.4	564.7	
060614	214805	2006-06-14 12:43:48.504	320.877	−53.027	37.4	1.0	108.7	43.0	−239.8	677.2	
060707	217704	2006-07-07 21:30:19.497	357.069	−17.904	19.1	1.4	66.2	34.7	−239.8	962.3	
060708	217805	2006-07-08 12:15:59.016	7.831	−33.751	31.5	1.0	10.2	3.4	−239.3	962.7	
060712	218582	2006-07-12 21:07:43.711	184.067	35.540	9.8	2.2	26.3	12.9	−239.0	739.6	
060714	219101	2006-07-14 15:12:00.283	227.855	−6.544	17.4	1.5	115.0	85.8	−239.6	962.4	
060717	219646	2006-07-17 09:07:38.901	170.857	28.982	7.6	2.6	3.0	1.0	−239.2	738.6	
060719	220020	2006-07-19 06:50:36.945	18.420	−48.381	21.7	1.3	66.9	43.4	−239.3	962.8	
060728	221627	2006-07-28 22:24:30.654	16.644	−41.390	6.2	3.0	-	-	−239.0	963.1	Possible GRB
060729	221755	2006-07-29 19:12:29.244	95.287	−62.221	4.1	4.1	115.3	21.7	−239.6	962.5	
060801	222154	2006-08-01 12:16:15.158	212.989	16.988	13.6	1.8	0.49	0.32	−239.5	962.6	
060804	222546	2006-08-04 07:28:19.825	112.219	−27.225	12.1	1.9	17.8	8.1	−239.2	962.9	
060805	222683	2006-08-05 04:47:49.167	220.928	12.580	7.4	2.7	5.3	2.5	−239.5	962.6	
060807	223217	2006-08-07 14:41:35.402	252.520	31.591	12.6	1.8	54.0	17.2	−239.8	962.3	
060813	224364	2006-08-13 22:50:22.685	111.890	−29.844	65.4	1.0	16.1	4.2	−239.1	963.0	
060814	224552	2006-08-14 23:02:19.035	221.338	20.591	48.3	1.0	145.3	61.6	−239.4	962.6	
060825	226382	2006-08-25 02:59:57.702	18.132	55.796	46.8	1.0	8.0	3.8	−239.1	962.9	
060904A	227996	2006-09-04 01:03:21.201	237.731	44.984	17.3	1.5	80.1	25.9	−239.6	962.5	
060904B	228006	2006-09-04 02:31:03.857	58.218	−0.729	35.7	1.0	171.5	145.9	−239.3	962.8	
060906	228316	2006-09-06 08:32:46.573	40.709	30.362	8.3	2.5	43.5	16.2	−239.0	963.1	
060908	228581	2006-09-08 08:57:22.344	31.828	0.335	27.5	1.1	19.3	7.4	−239.8	962.2	

Table 1—Continued

GRB Name	Trigger Number	Trigger time	R.A. (°)	Dec. (°)	SN_{img} (σ)	Error (′)	T_{90} (s)	T_{50} (s)	Start (s)	Stop (s)	Comment
060912	229185	2006-09-12 13:55:54.144	5.285	20.971	36.5	1.0	5.0	1.8	−239.6	962.5	
060919	230115	2006-09-19 07:48:38.674	276.900	−50.994	14.9	1.6	9.1	3.3	−239.1	962.9	
060923A	230662	2006-09-23 05:12:15.370	254.623	12.341	10.3	2.1	51.7	38.8	−239.8	962.2	
060923B	230702	2006-09-23 11:38:06.217	238.193	−30.907	15.2	1.6	8.6	4.2	−239.7	954.9	
060923C	230711	2006-09-23 13:33:02.537	346.122	3.943	10.8	2.1	75.8	44.6	−239.0	963.1	
060926	231231	2006-09-26 16:48:41.859	263.926	13.039	18.9	1.4	8.0	3.4	−239.3	962.8	
060927	231362	2006-09-27 14:07:35.297	329.547	5.370	41.5	1.0	22.5	15.8	−239.8	962.3	
060929	231702	2006-09-29 19:55:01.052	263.148	29.825	7.1	2.8	554.0	522.0	−239.5	962.5	
061002	231974	2006-10-02 01:03:29.592	220.356	48.726	13.9	1.7	17.6	9.2	−239.1	963.0	
061004	232339	2006-10-04 19:50:30.514	97.795	−45.903	40.3	1.0	6.2	1.9	−239.0	963.1	
061006	232585	2006-10-06 16:45:50.510	110.998	−79.195	13.4	1.8	129.9	56.44	−239.0	963.0	
061007	232683	2006-10-07 10:08:08.812	46.299	−50.496	37.2	1.0	75.3	23.0	−239.3	962.8	
061019	234516	2006-10-19 04:19:06.964	91.675	29.527	6.0	3.1	183.8	163.9	−239.5	962.6	
061021	234905	2006-10-21 15:39:07.663	145.146	−21.953	58.9	1.0	46.2	10.1	−239.2	514.8	
061027	235645	2006-10-27 10:15:02.467	270.992	−82.239	4.7	3.7	-	-	−239.0	963.1	Possible GRB
061028	235715	2006-10-28 01:26:22.466	97.193	46.290	8.1	2.5	106.2	41.6	−239.0	963.1	
061102	236430	2006-11-02 01:00:31.223	148.394	−17.022	7.6	2.6	45.6	22.3	−239.8	962.3	
061110A	238108	2006-11-10 11:47:21.318	336.284	−2.252	25.6	1.1	40.7	20.0	−239.9	962.2	
061110B	238174	2006-11-10 21:58:45.541	323.912	6.872	15.8	1.6	134.0	61.0	−239.1	963.0	
061121	239899	2006-11-21 15:22:29.006	147.228	−13.188	36.3	1.0	81.3	7.5	−239.6	962.5	
061126	240766	2006-11-26 08:47:56.420	86.615	64.204	41.1	1.0	70.8	15.3	−239.0	963.1	
061201	241840	2006-12-01 15:58:36.793	332.079	−74.568	24.2	1.2	0.76	0.43	−239.4	962.6	
061202	241963	2006-12-02 08:11:44.696	105.255	−74.602	4.2	4.0	91.2	17.3	−239.3	962.7	
061210	243690	2006-12-10 12:20:39.335	144.521	15.613	9.3	2.3	85.3	49.61	−239.0	963.1	
061217	251634	2006-12-17 03:40:08.217	160.403	−21.152	9.9	2.2	0.21	0.06	−239.9	962.2	
061218	251863	2006-12-18 04:05:05.815	149.260	−35.217	5.0	3.5	6.5	2.4	−239.5	962.6	battblocks failed[2]
061222A	252588	2006-12-22 03:28:52.110	358.254	46.524	23.6	1.2	71.4	22.0	−239.8	962.3	
061222B	252593	2006-12-22 04:11:02.350	105.353	−25.866	22.4	1.2	40.0	19.3	−239.0	903.1	
070103	254532	2007-01-03 20:46:39.412	352.581	26.823	7.5	2.7	18.6	12.2	−239.1	963.0	
070107	255029	2007-01-07 12:05:18.316	159.422	−53.202	25.0	1.1	347.3	40.0	−239.0	963.1	
070110	255445	2007-01-10 07:22:41.574	0.934	−52.978	26.0	1.1	88.4	30.3	−239.3	962.8	
070126	257741	2007-01-26 02:33:26.277	33.503	−73.553	4.7	3.7	-	-	−239.0	963.1	Possible GRB
070129	258408	2007-01-29 23:35:10.269	36.995	11.728	7.3	2.7	460.6	279.7	−239.0	963.1	
070208	259714	2007-02-08 09:10:34.281	197.891	61.942	4.9	3.6	47.7	42.0	−239.0	552.3	

Table 1—Continued

GRB Name	Trigger Number	Trigger time	R.A. (°)	Dec. (°)	SN_{img} (σ)	Error (′)	T_{90} (s)	T_{50} (s)	Start (s)	Stop (s)	Comment
070209	259803	2007-02-09 03:33:41.927	46.213	−47.376	7.1	2.8	0.09	0.03	−239.7	962.4	`battblocks` failed[2]
070219	261132	2007-02-19 01:10:16.146	260.220	69.345	12.4	1.9	16.6	8.1	−239.9	962.1	
070220	261299	2007-02-20 04:44:32.912	34.800	68.800	54.2	1.0	129.0	35.0	−239.7	962.4	
070223	261664	2007-02-23 01:15:00.682	153.453	43.132	23.1	1.2	88.5	45.8	−239.5	962.6	
070224	261880	2007-02-24 20:27:58.214	178.988	−13.355	11.4	2.0	34.5	15.6	−239.0	963.1	
070227	262347	2007-02-27 22:21:58.869	120.578	−46.302	9.1	2.3	-	-	−2.0	8.1	Untriggered GRB
070306	263361	2007-03-06 16:41:28.177	148.154	10.440	7.2	2.7	209.5	21.8	−240.0	962.1	
070318	271019	2007-03-18 07:28:56.088	48.486	−42.950	44.3	1.0	74.6	26.3	−239.9	962.2	
070328	272773	2007-03-28 03:53:53.155	65.113	−34.079	57.8	1.0	75.3	18.1	−239.0	963.1	
070330	273180	2007-03-30 22:51:31.197	269.533	−63.799	12.2	1.9	9.0	5.0	−239.1	963.0	
070406	274153	2007-04-06 00:50:39.189	198.956	16.530	8.3	3.3	1.2	0.4	−2.3	7.7	`battblocks` failed[2], Untriggered GRB
070411	275087	2007-04-11 20:12:33.316	107.342	1.061	16.5	1.5	121.5	65.1	−239.2	902.8	
070412	275119	2007-04-12 01:27:03.395	181.525	40.133	17.0	1.5	33.8	8.1	−239.3	962.8	
070419A	276205	2007-04-19 09:59:26.099	182.755	39.903	9.4	2.3	115.6	56.8	−239.0	963.1	
070419B	276212	2007-04-19 10:44:05.971	315.709	−31.266	46.0	1.0	236.4	68.7	−239.9	902.2	
070420	276321	2007-04-20 06:18:13.522	121.245	−45.564	33.8	1.0	76.5	19.3	−239.4	962.6	
070427	277356	2007-04-27 08:31:08.930	28.871	−27.603	44.3	1.0	11.1	5.7	−239.8	962.2	
070429A	277571	2007-04-29 01:35:10.078	297.695	−32.420	8.1	2.5	163.3	73.9	−239.0	963.1	
070429B	277582	2007-04-29 03:09:04.446	328.006	−38.857	13.1	1.8	0.47	0.36	−239.4	962.7	
070506	278693	2007-05-06 05:35:58.063	347.203	10.711	12.3	1.9	4.3	1.9	−239.0	963.1	
070508	278854	2007-05-08 04:18:17.835	312.832	−78.382	101.1	1.0	20.9	7.6	−239.8	962.3	
070509	278903	2007-05-09 02:48:27.305	237.874	−78.657	14.3	1.7	7.7	3.5	−239.2	962.8	
070517	279494	2007-05-17 11:20:58.391	277.556	−62.305	12.2	1.9	7.6	4.0	−239.4	962.7	
070518	279592	2007-05-18 14:26:21.204	254.219	55.289	13.5	1.8	5.5	2.9	−239.2	902.9	
070520A	279817	2007-05-20 13:05:10.032	193.255	75.005	10.1	2.2	18.1	8.9	−239.0	963.0	
070520B	279898	2007-05-20 17:44:53.264	121.886	57.588	13.1	1.8	65.8	39.1	−239.2	962.8	
070521	279935	2007-05-21 06:51:10.863	242.659	30.260	26.7	1.1	37.9	14.5	−239.8	593.7	
070529	280706	2007-05-29 12:48:28.349	283.717	20.648	14.0	1.7	109.2	55.9	−239.3	962.7	
070531	280958	2007-05-31 02:10:17.529	6.714	74.315	14.4	1.7	44.5	21.0	−239.5	962.6	
070611	282003	2007-06-11 01:57:13.890	2.004	−29.756	12.6	1.9	12.2	5.5	−239.9	962.1	
070612A	282066	2007-06-12 02:38:45.983	121.355	37.258	19.8	1.4	368.8	189.0	−239.0	963.1	
070612B	282073	2007-06-12 06:21:17.791	261.716	−8.747	25.3	1.1	13.5	6.0	−239.8	962.3	
070616	282445	2007-06-16 16:29:33.974	32.096	56.946	7.7	2.6	402.4	203.1	−239.0	963.1	

[1]The event data are not available during this very early phase of operations.

[2]`battblocks` failed because of the weak short nature of the burst.

[3]The event data of the last part of the burst emission are not available due to the downlink problem.

[4]The event data of the brightest part of the burst emission are not available due to the entering to the SAA.

[5]The burst duration was longer than the period of the event data.

[6]?

Table 2. BAT GRB energy fluence

GRB Name	Spectral Model	S(15-25)	S(25-50)	S(50-100)	S(100-150)	S(15-150)	Start (s)	Stop (s)
				(10^{-8} ergs cm^{-2})				
041217	CPL	30.6 ± 3.4	73.2 ± 3.4	109.0 ± 5.6	64.4 ± 8.3	277.0 ± 12.3	+0.8	+8.2
041219A	-	-	-	-	-	-	-	-
041219B	-	-	-	-	-	-	-	-
041219C	PL	29.6 ± 2.6	39.7 ± 2.1	39.2 ± 3.1	22.7 ± 2.9	131.0 ± 7.3	+6.7	+14.2
041220	PL	6.2 ± 0.7	10.2 ± 0.7	12.9 ± 1.2	9.1 ± 1.3	38.3 ± 2.8	−0.2	+6.8
041223	PL	143.0 ± 6.1	334.0 ± 8.3	617.0 ± 10.6	581.0 ± 16.4	1670.0 ± 27.9	−10.5	+145.9
041224	CPL	134.0 ± 12.2	261.0 ± 10.7	316.0 ± 14.6	162.0 ± 21.5	873.0 ± 34.8	−109.6	+116.3
041226	PL	3.9 ± 1.6	7.5 ± 1.8	11.4 ± 3.4	9.2 ± 4.4	32.1 ± 8.3	−1.3	+93.4
041228	PL	52.5 ± 4.6	90.5 ± 4.5	119.0 ± 6.2	86.7 ± 7.4	349.0 ± 15.2	−0.4	+70.6
050117	CPL	111.0 ± 8.1	226.0 ± 6.3	324.0 ± 9.7	221.0 ± 15.7	881.0 ± 23.3	+4.3	+215.9
050124	CPL	13.5 ± 1.8	31.5 ± 1.9	46.3 ± 3.1	27.5 ± 4.2	119.0 ± 6.6	−2.2	+3.8
050126	PL	9.4 ± 1.5	19.1 ± 1.9	30.2 ± 3.2	25.2 ± 4.1	83.8 ± 8.0	−0.3	+29.0
050128	CPL	49.0 ± 6.6	122.0 ± 6.9	199.0 ± 11.5	132.0 ± 14.5	502.0 ± 22.9	−7.6	+22.8
050202	PL	0.4 ± 0.1	0.7 ± 0.1	1.1 ± 0.2	0.8 ± 0.3	3.0 ± 0.6	+0.02	+0.15
050215A	PL	9.1 ± 2.3	17.1 ± 2.5	25.0 ± 4.5	19.6 ± 5.8	70.8 ± 10.8	−0.3	+98.3
050215B	PL	5.0 ± 0.7	6.8 ± 0.7	6.9 ± 1.2	4.0 ± 1.1	22.7 ± 2.9	−2.0	+7.2
050219A	CPL	33.4 ± 4.0	101.0 ± 4.6	175.0 ± 7.8	101.0 ± 10.6	411.0 ± 15.8	−5.8	+29.3
050219B	CPL	192.0 ± 18.7	415.0 ± 16.4	599.0 ± 24.5	379.0 ± 29.1	1580.0 ± 50.0	−35.6	+40.5
050223	PL	12.3 ± 1.7	18.3 ± 1.6	20.2 ± 2.8	12.8 ± 2.8	63.6 ± 6.5	−12.0	+16.6
050306	PL	151.0 ± 12.0	282.0 ± 13.3	404.0 ± 16.8	314.0 ± 20.8	1150.0 ± 43.4	−3.4	+187.8
050315	PL	78.6 ± 6.1	99.8 ± 4.5	92.3 ± 6.3	50.8 ± 5.6	322.0 ± 14.6	−56.1	+69.2
050318	CPL	21.3 ± 2.3	36.1 ± 2.2	35.8 ± 3.2	14.8 ± 4.6	108.0 ± 7.7	−0.6	+29.7
050319	PL	29.4 ± 4.2	39.6 ± 3.8	39.1 ± 6.5	22.7 ± 5.9	131.0 ± 14.8	−134.0	+29.0
050326	PL	89.2 ± 3.8	191.0 ± 4.6	322.0 ± 6.0	283.0 ± 8.8	886.0 ± 15.5	−9.8	+31.2
050401	PL	98.7 ± 7.9	193.0 ± 9.2	293.0 ± 11.8	237.0 ± 15.0	822.0 ± 30.6	−7.7	+29.1
050406	CPL	2.3 ± 0.6	3.4 ± 0.8	1.1 ± 0.8	< 0.07	6.8 ± 1.4	−2.5	+3.9
050410	CPL	57.8 ± 7.0	123.0 ± 6.9	157.0 ± 10.0	77.7 ± 14.0	415.0 ± 22.5	−13.8	+35.7
050412	PL	3.2 ± 0.7	9.5 ± 1.2	22.8 ± 2.0	26.2 ± 3.6	61.8 ± 5.5	−8.3	+22.2
050416A	PL	17.0 ± 1.9	12.2 ± 1.4	5.8 ± 1.4	1.8 ± 0.7	36.7 ± 3.7	−0.1	+3.0
050416B	CPL	10.5 ± 2.4	27.6 ± 2.7	44.4 ± 4.6	26.2 ± 6.5	108.0 ± 9.7	+0.1	+4.2
050418	PL	87.8 ± 5.9	142.0 ± 5.5	173.0 ± 7.6	118.0 ± 8.4	521.0 ± 18.3	−8.4	+86.4
050421	PL	2.1 ± 0.8	3.7 ± 0.9	5.0 ± 1.7	3.7 ± 1.9	14.5 ± 4.0	−0.1	+17.9
050422	PL	7.3 ± 1.4	14.3 ± 1.7	21.6 ± 3.0	17.4 ± 3.8	60.7 ± 7.4	−0.7	+62.4
050502B	PL	7.1 ± 0.9	12.3 ± 1.0	16.4 ± 1.8	12.0 ± 2.1	47.8 ± 4.2	−17.3	+3.2
050505	PL	30.3 ± 4.2	58.8 ± 4.9	88.5 ± 7.0	71.3 ± 8.7	249.0 ± 17.9	−10.1	+52.5
050507	PL	2.3 ± 0.6	4.2 ± 0.7	5.8 ± 1.3	4.4 ± 1.5	16.7 ± 3.2	+0.0	+8.2
050509A	PL	8.3 ± 1.0	10.6 ± 0.9	9.8 ± 1.5	5.4 ± 1.3	34.1 ± 3.4	−6.3	+8.1
050509B	PL	0.13 ± 0.04	0.2 ± 0.1	0.3 ± 0.1	0.2 ± 0.1	0.9 ± 0.2	−0.002	+0.048
050525A	CPL	215.0 ± 11.3	440.0 ± 8.4	568.0 ± 9.5	309.0 ± 9.4	1530.0 ± 22.1	+0.1	+12.9
050528	PL	12.4 ± 2.3	14.4 ± 2.0	12.0 ± 2.9	6.0 ± 2.2	44.8 ± 7.0	−8.2	+5.0
050603	PL	57.4 ± 4.4	130.0 ± 5.9	234.0 ± 8.9	215.0 ± 13.0	636.0 ± 22.9	−3.7	+17.7
050607	PL	12.2 ± 1.6	17.4 ± 1.4	18.3 ± 2.4	11.2 ± 2.3	59.2 ± 5.5	−0.5	+29.1
050701	PL	22.6 ± 1.9	36.9 ± 1.8	45.5 ± 2.9	31.4 ± 3.3	136.0 ± 6.8	−4.7	+28.4
050712	PL	14.6 ± 2.7	26.8 ± 2.9	37.8 ± 4.9	28.9 ± 6.0	108.0 ± 11.9	−20.4	+40.1
050713A	PL	71.2 ± 5.6	128.0 ± 5.7	178.0 ± 8.8	134.0 ± 10.9	511.0 ± 21.2	−69.4	+121.3

Table 2—Continued

GRB Name	Spectral Model	S(15-25)	S(25-50)	S(50-100)	S(100-150)	S(15-150)	Start (s)	Stop (s)
				(10^{-8} ergs cm^{-2})				
050713B	PL	37.7 ± 7.1	74.2 ± 8.3	114.0 ± 12.6	92.6 ± 16.2	318.0 ± 31.8	+5.1	+77.5
050714B	PL	18.9 ± 3.5	19.6 ± 3.1	14.4 ± 4.4	6.6 ± 3.0	59.5 ± 10.5	+18.0	+68.2
050715	PL	22.3 ± 3.1	38.6 ± 3.2	51.1 ± 5.9	37.2 ± 6.9	149.0 ± 13.8	−101.3	+53.4
050716	CPL	63.5 ± 6.8	151.0 ± 6.9	240.0 ± 11.1	163.0 ± 16.5	617.0 ± 24.3	−13.7	+76.4
050717	PL	67.3 ± 4.3	140.0 ± 5.1	228.0 ± 6.9	195.0 ± 9.9	631.0 ± 17.5	+0.1	+209.2
050721	PL	73.3 ± 9.9	106.0 ± 8.7	113.0 ± 13.6	69.9 ± 13.3	362.0 ± 31.6	−1.3	+149.6
050724	PL	20.0 ± 3.5	29.0 ± 3.0	31.3 ± 5.4	19.5 ± 5.3	99.8 ± 12.0	+0.0	+102.9
050726	PL	12.7 ± 3.5	33.6 ± 5.6	72.1 ± 7.8	75.8 ± 12.5	194.0 ± 21.2	−41.7	+15.7
050730	PL	33.0 ± 3.7	59.6 ± 3.8	82.7 ± 6.4	62.5 ± 7.9	238.0 ± 15.2	−59.8	+120.5
050801	PL	6.8 ± 1.2	9.3 ± 1.2	9.4 ± 2.1	5.5 ± 1.9	31.0 ± 4.8	+0.1	+25.7
050802	PL	28.1 ± 4.0	50.4 ± 4.2	69.1 ± 6.4	51.8 ± 7.6	200.0 ± 15.7	−3.4	+19.6
050803	PL	25.4 ± 3.0	50.2 ± 3.4	77.0 ± 5.5	62.9 ± 7.2	215.0 ± 13.5	+59.6	+165.1
050813	PL	0.5 ± 0.2	1.0 ± 0.2	1.6 ± 0.4	1.4 ± 0.6	4.4 ± 1.1	+0.0	+0.5
050814	PL	36.9 ± 5.5	56.6 ± 5.4	65.0 ± 9.4	42.5 ± 9.5	201.0 ± 22.0	−19.9	+175.5
050815	CPL	1.4 ± 0.4	3.6 ± 0.6	2.6 ± 0.9	< 0.9	7.9 ± 1.5	−0.7	+2.5
050819	PL	13.2 ± 1.9	11.7 ± 1.8	7.2 ± 2.3	2.8 ± 1.4	35.0 ± 5.5	−7.2	+40.1
050820A	PL	34.6 ± 4.0	74.2 ± 5.0	125.0 ± 9.8	110.0 ± 13.9	344.0 ± 24.2	−30.5	+237.7
050820B	CPL	19.4 ± 1.6	50.0 ± 1.6	82.5 ± 2.7	54.3 ± 4.0	206.0 ± 5.8	−0.1	+15.0
050822	PL	74.0 ± 6.9	80.3 ± 5.0	62.0 ± 7.9	29.5 ± 5.9	246.0 ± 17.2	−0.6	+133.7
050824	PL	10.4 ± 1.8	9.0 ± 1.7	5.3 ± 2.2	2.0 ± 1.3	26.6 ± 5.2	+36.6	+63.1
050826	PL	3.8 ± 1.3	8.5 ± 1.6	15.1 ± 2.8	13.9 ± 4.2	41.3 ± 7.2	+0.0	+39.6
050827	PL	24.7 ± 2.7	48.9 ± 3.1	75.2 ± 4.9	61.5 ± 6.4	210.0 ± 12.1	−31.2	+36.1
050904	PL	48.7 ± 3.7	104.0 ± 4.6	176.0 ± 7.1	154.0 ± 10.2	483.0 ± 18.0	+17.0	+217.0
050906	PL	0.2 ± 0.1	0.2 ± 0.1	0.14 ± 0.06	0.06 ± 0.04	0.6 ± 0.2	−0.03	+0.10
050908	PL	9.6 ± 1.3	14.0 ± 1.3	15.2 ± 2.2	9.5 ± 2.1	48.3 ± 5.1	−7.5	+15.8
050911	PL	6.1 ± 1.4	9.0 ± 1.4	10.1 ± 2.5	6.5 ± 2.5	31.7 ± 5.8	−1.0	+16.0
050915A	PL	10.1 ± 1.7	19.8 ± 2.1	30.3 ± 3.6	24.8 ± 4.6	85.0 ± 8.8	−8.4	+57.8
050915B	CPL	64.7 ± 5.5	106.0 ± 4.0	112.0 ± 5.3	55.5 ± 8.1	338.0 ± 13.7	−8.4	+48.3
050916	PL	16.5 ± 3.2	25.8 ± 3.2	30.4 ± 5.4	20.2 ± 5.5	92.9 ± 12.7	+7.4	+65.7
050922B	PL	57.1 ± 10.1	70.1 ± 9.4	62.5 ± 15.6	33.4 ± 12.7	223.0 ± 35.6	+31.3	+273.4
050922C	PL	18.9 ± 1.2	37.6 ± 1.4	58.1 ± 2.1	47.7 ± 2.8	162.0 ± 5.4	−3.3	+3.5
050925	CPL	0.9 ± 0.3	2.5 ± 0.3	3.2 ± 0.5	1.0 ± 0.4	7.6 ± 0.9	+0.1	+0.2
051001	PL	40.4 ± 4.5	53.2 ± 3.8	51.3 ± 6.6	29.2 ± 5.9	174.0 ± 14.7	−25.6	+196.7
051006	PL	18.3 ± 3.2	33.4 ± 3.4	46.8 ± 5.8	35.7 ± 7.0	134.0 ± 14.1	−14.4	+24.8
051008	PL	44.2 ± 3.0	102.0 ± 4.0	187.0 ± 5.5	175.0 ± 8.2	509.0 ± 14.5	−24.9	+13.3
051012	PL	8.0 ± 1.3	9.6 ± 1.1	8.4 ± 1.9	4.4 ± 1.5	30.4 ± 4.2	+0.0	+20.0
051016	PL	16.7 ± 3.9	24.3 ± 3.7	26.3 ± 5.9	16.4 ± 5.7	83.7 ± 13.8	−0.1	+26.9
051016B	PL	5.2 ± 0.7	5.6 ± 0.7	4.2 ± 1.0	2.0 ± 0.7	17.0 ± 2.2	+0.0	+4.6
051021B	CPL	10.8 ± 2.1	25.0 ± 2.5	32.5 ± 4.0	15.2 ± 5.9	83.5 ± 9.1	−4.7	+54.9
051105	PL	0.2 ± 0.1	0.5 ± 0.1	0.8 ± 0.2	0.7 ± 0.2	2.2 ± 0.4	+0.072	+0.176
051109A	PL	30.1 ± 6.5	54.8 ± 7.3	76.6 ± 10.8	58.3 ± 12.6	220.0 ± 27.2	−3.7	+41.7
051109B	PL	5.5 ± 1.0	7.6 ± 1.0	7.8 ± 1.8	4.6 ± 1.6	25.6 ± 4.1	−8.6	+8.7
051111	PL	44.9 ± 3.1	92.0 ± 3.6	147.0 ± 5.4	124.0 ± 7.4	408.0 ± 13.4	−5.9	+63.6
051113	PL	43.4 ± 5.7	69.9 ± 5.6	85.0 ± 9.0	58.0 ± 9.7	256.0 ± 21.4	−30.7	+67.3
051114	PL	1.2 ± 0.4	2.7 ± 0.5	4.7 ± 0.9	4.2 ± 1.2	12.8 ± 2.3	+0.0	+2.8

Table 2—Continued

GRB Name	Spectral Model	S(15-25)	S(25-50)	S(50-100)	S(100-150)	S(15-150)	Start (s)	Stop (s)
				(10^{-8} ergs cm^{-2})				
051117A	PL	81.7 ± 5.4	123.0 ± 4.5	139.0 ± 6.8	89.6 ± 7.2	434.0 ± 15.5	−28.7	+148.4
051117B	PL	2.5 ± 0.7	4.4 ± 0.8	6.2 ± 1.5	4.7 ± 1.7	17.7 ± 3.7	+1.4	+11.0
051210	PL	0.7 ± 0.2	1.6 ± 0.3	3.1 ± 0.5	3.0 ± 0.8	8.5 ± 1.4	−0.3	+1.2
051213	PL	12.1 ± 2.2	20.5 ± 2.4	26.6 ± 4.3	19.0 ± 4.7	78.2 ± 10.3	−10.7	+66.7
051221A	PL	13.6 ± 0.9	26.8 ± 1.0	40.9 ± 1.4	33.3 ± 1.9	115.0 ± 3.5	+0.2	+2.3
051221B	PL	10.3 ± 2.2	20.9 ± 2.6	33.0 ± 4.1	27.5 ± 5.4	91.7 ± 10.4	+49.9	+93.6
051227	PL	8.9 ± 2.1	16.9 ± 2.3	24.7 ± 4.5	19.4 ± 5.6	69.9 ± 10.8	−0.8	+122.7
060102	PL	2.3 ± 1.0	5.0 ± 1.2	8.5 ± 2.0	7.5 ± 2.9	23.4 ± 5.0	−0.9	+22.1
060105	PL	143.0 ± 6.4	342.0 ± 8.9	651.0 ± 11.5	627.0 ± 18.1	1760.0 ± 30.4	−21.0	+66.6
060108	PL	8.4 ± 1.1	11.2 ± 0.9	11.0 ± 1.7	6.3 ± 1.5	36.9 ± 3.7	−4.0	+13.2
060109	PL	13.6 ± 2.5	19.3 ± 2.5	20.3 ± 4.5	12.3 ± 4.2	65.5 ± 10.3	−1.0	+126.8
060110	PL	24.5 ± 2.0	41.3 ± 1.9	53.0 ± 3.0	37.7 ± 3.5	157.0 ± 7.0	−3.7	+34.3
060111A	CPL	17.5 ± 1.7	35.7 ± 1.6	44.7 ± 2.4	22.5 ± 3.8	120.0 ± 5.8	−0.7	+17.6
060111B	PL	12.0 ± 2.5	29.8 ± 3.5	59.5 ± 5.4	59.1 ± 8.7	160.0 ± 14.2	−2.0	+61.7
060115	CPL	28.8 ± 3.8	54.3 ± 4.2	60.6 ± 6.3	27.4 ± 9.4	171.0 ± 15.0	−49.2	+108.0
060116	PL	30.0 ± 5.7	57.5 ± 6.5	85.3 ± 10.6	67.9 ± 13.3	241.0 ± 26.1	−35.3	+86.9
060117	CPL	376.0 ± 21.4	614.0 ± 13.1	673.0 ± 14.3	360.0 ± 15.1	2020.0 ± 37.1	−2.2	+27.0
060124	PL	8.8 ± 1.4	13.2 ± 1.3	14.7 ± 2.3	9.4 ± 2.3	46.1 ± 5.3	−1.6	+13.2
060202	PL	35.8 ± 4.1	57.9 ± 4.0	70.7 ± 7.2	48.4 ± 7.8	213.0 ± 16.5	−26.1	+198.2
060203	PL	13.5 ± 3.1	23.3 ± 3.3	30.7 ± 5.3	22.2 ± 6.0	89.8 ± 12.8	−22.1	+55.7
060204B	CPL	34.3 ± 4.3	77.7 ± 4.6	114.0 ± 7.3	69.4 ± 12.7	295.0 ± 17.8	−24.3	+170.7
060206	CPL	13.1 ± 1.3	24.5 ± 1.2	29.6 ± 1.8	15.9 ± 2.7	83.1 ± 4.2	−0.6	+12.0
060210	PL	107.0 ± 10.7	192.0 ± 11.4	266.0 ± 16.5	201.0 ± 20.0	766.0 ± 40.9	−227.3	+205.8
060211A	CPL	26.8 ± 3.6	51.9 ± 3.8	55.9 ± 6.0	22.5 ± 8.1	157.0 ± 13.7	+47.8	+191.0
060211B	PL	6.4 ± 1.2	11.2 ± 1.3	15.1 ± 2.5	11.1 ± 2.9	43.8 ± 5.9	−10.5	+19.2
060218	PL	43.3 ± 4.9	50.3 ± 4.2	42.0 ± 6.7	21.3 ± 5.2	157.0 ± 15.2	+0.0	+303.0
060219	PL	14.7 ± 2.9	14.3 ± 2.5	9.7 ± 3.3	4.1 ± 2.2	42.8 ± 8.0	−57.1	+8.2
060223A	PL	11.7 ± 1.3	18.5 ± 1.2	22.2 ± 2.1	14.9 ± 2.2	67.3 ± 4.8	−2.9	+10.0
060223B	PL	21.1 ± 1.5	39.2 ± 1.6	56.0 ± 2.3	43.3 ± 2.9	160.0 ± 5.6	−7.0	+5.5
060306	PL	39.2 ± 3.4	60.0 ± 3.1	69.0 ± 5.1	45.0 ± 5.3	213.0 ± 11.8	−1.4	+66.9
060312	PL	39.0 ± 2.9	57.0 ± 2.5	61.9 ± 4.0	38.7 ± 4.0	197.0 ± 9.1	−29.2	+46.5
060313	PL	5.6 ± 0.5	16.9 ± 0.8	41.5 ± 1.6	48.4 ± 2.9	113.0 ± 4.5	+0.1	+0.9
060319	PL	7.7 ± 1.1	8.6 ± 0.9	6.8 ± 1.6	3.3 ± 1.2	26.4 ± 3.4	+1.0	+14.4
060322	CPL	71.4 ± 7.6	143.0 ± 7.2	192.0 ± 10.6	116.0 ± 17.2	522.0 ± 25.6	−51.6	+248.2
060323	PL	8.8 ± 1.4	15.7 ± 1.5	21.5 ± 2.9	16.1 ± 3.4	62.2 ± 6.7	−5.1	+23.9
060403	PL	11.0 ± 1.2	26.3 ± 1.7	49.8 ± 2.8	47.8 ± 4.2	135.0 ± 7.3	−6.2	+32.1
060413	PL	57.8 ± 4.4	95.5 ± 4.1	119.0 ± 6.3	83.4 ± 7.2	356.0 ± 14.7	+30.0	+257.4
060418	PL	138.0 ± 8.5	225.0 ± 7.7	278.0 ± 10.7	192.0 ± 12.4	833.0 ± 25.3	−82.5	+136.7
060421	PL	17.7 ± 1.4	31.7 ± 1.5	43.4 ± 2.4	32.5 ± 2.9	125.0 ± 5.7	−3.7	+16.9
060424	PL	11.3 ± 1.9	18.3 ± 1.9	22.5 ± 3.4	15.4 ± 3.7	67.6 ± 8.1	−18.8	+20.6
060427	PL	9.9 ± 2.2	14.4 ± 2.1	15.7 ± 3.9	9.9 ± 3.8	49.9 ± 8.8	−10.0	+60.0
060428A	PL	31.8 ± 2.7	42.3 ± 2.1	41.5 ± 3.5	23.9 ± 3.2	139.0 ± 7.8	−6.8	+43.0
060428B	PL	28.7 ± 3.1	27.5 ± 2.5	18.4 ± 3.5	7.8 ± 2.2	82.3 ± 8.1	−23.8	+41.9
060501	PL	15.6 ± 2.4	29.4 ± 2.7	43.0 ± 4.2	33.9 ± 5.2	122.0 ± 10.3	−1.3	+26.0
060502A	PL	29.8 ± 2.5	56.0 ± 2.8	81.3 ± 4.1	63.6 ± 5.2	231.0 ± 10.2	−5.6	+39.0

Table 2—Continued

GRB Name	Spectral Model	S(15-25)	S(25-50)	S(50-100)	S(100-150)	S(15-150)	Start (s)	Stop (s)
				(10^{-8} ergs cm^{-2})				
060502B	PL	0.3 ± 0.1	0.7 ± 0.1	1.5 ± 0.2	1.5 ± 0.3	4.0 ± 0.5	−0.03	+0.06
060505	PL	10.1 ± 3.0	20.9 ± 3.9	34.2 ± 6.8	29.3 ± 8.8	94.4 ± 17.1	−3.0	+7.0
060507	PL	84.2 ± 7.0	127.0 ± 6.3	142.0 ± 9.9	91.5 ± 10.2	445.0 ± 23.0	−11.0	+192.4
060510A	PL	117.0 ± 8.7	206.0 ± 8.8	277.0 ± 12.8	205.0 ± 15.5	805.0 ± 31.2	−7.0	+16.7
060510B	PL	73.5 ± 5.5	114.0 ± 4.8	132.0 ± 7.7	87.2 ± 8.4	407.0 ± 17.6	−16.3	+325.0
060512	PL	7.5 ± 1.3	7.7 ± 1.2	5.5 ± 1.7	2.5 ± 1.1	23.2 ± 4.0	−4.4	+5.3
060515	PL	12.4 ± 2.3	28.5 ± 3.2	51.8 ± 4.9	48.2 ± 7.1	141.0 ± 12.8	+0.2	+57.5
060516	PL	26.7 ± 4.3	32.3 ± 4.1	28.2 ± 5.2	14.9 ± 5.6	102.0 ± 15.8	−43.3	+134.0
060522	PL	16.4 ± 2.4	29.1 ± 2.6	39.4 ± 4.7	29.3 ± 5.4	114.0 ± 11.1	+0.2	+78.6
060526	PL	28.3 ± 4.7	38.1 ± 4.0	37.7 ± 7.7	21.9 ± 7.0	126.0 ± 16.5	−1.4	+310.2
060602A	PL	16.3 ± 3.1	34.8 ± 4.0	58.6 ± 6.1	51.3 ± 8.3	161.0 ± 15.7	+2.1	+86.4
060604	PL	9.0 ± 2.6	12.1 ± 2.6	12.1 ± 4.6	7.0 ± 4.1	40.2 ± 10.6	−61.2	+48.8
060605	PL	9.9 ± 1.8	17.7 ± 2.0	24.1 ± 3.8	17.9 ± 4.4	69.7 ± 9.0	−67.2	+16.0
060607A	PL	33.2 ± 2.6	62.1 ± 2.8	89.6 ± 4.6	69.8 ± 5.9	255.0 ± 11.2	−24.1	+102.3
060607B	PL	25.8 ± 3.0	43.4 ± 3.0	55.4 ± 4.9	39.4 ± 5.5	164.0 ± 11.7	−0.8	+37.1
060614	PL	463.0 ± 19.4	620.0 ± 14.0	610.0 ± 13.3	352.0 ± 13.7	2040.0 ± 36.3	−1.5	+176.5
060707	CPL	23.8 ± 4.4	51.1 ± 4.8	60.2 ± 6.8	25.0 ± 8.9	160.0 ± 15.1	−49.0	+25.4
060708	PL	8.1 ± 0.9	13.3 ± 0.9	16.5 ± 1.6	11.5 ± 1.7	49.4 ± 3.7	−0.3	+14.2
060712	PL	19.0 ± 6.3	32.4 ± 6.2	42.2 ± 8.9	30.4 ± 10.4	124.0 ± 21.7	+0.6	+29.7
060714	PL	58.7 ± 5.2	83.3 ± 4.4	87.6 ± 7.4	53.3 ± 7.2	283.0 ± 16.7	−11.7	+120.6
060717	PL	1.1 ± 0.3	1.8 ± 0.4	2.2 ± 0.7	1.5 ± 0.7	6.5 ± 1.6	−0.2	+2.8
060719	PL	30.6 ± 2.9	43.8 ± 2.4	46.7 ± 4.0	28.8 ± 4.0	150.0 ± 9.1	−0.2	+84.6
060728	PL	2.9 ± 1.2	5.5 ± 1.5	8.1 ± 2.8	6.4 ± 3.4	22.9 ± 7.0	+0.0	+64.0
060729	PL	45.6 ± 5.4	72.1 ± 5.1	85.9 ± 9.2	57.7 ± 9.8	261.0 ± 21.1	+0.9	+131.7
060801	PL	0.3 ± 0.1	1.0 ± 0.2	2.9 ± 0.4	3.8 ± 0.7	8.0 ± 1.0	+0.0	+0.6
060804	PL	10.3 ± 2.3	16.4 ± 2.4	19.7 ± 4.2	13.4 ± 4.4	59.8 ± 9.9	−12.3	+7.4
060805	PL	1.9 ± 0.5	2.3 ± 0.5	2.0 ± 0.9	1.1 ± 0.7	7.2 ± 2.0	−1.6	+4.5
060807	PL	12.5 ± 2.4	21.8 ± 2.5	29.1 ± 4.6	21.4 ± 5.3	84.8 ± 10.9	−40.8	+25.8
060813	CPL	57.8 ± 4.5	129.0 ± 4.0	206.0 ± 6.5	153.0 ± 9.3	546.0 ± 14.0	−0.5	+36.2
060814	PL	205.0 ± 8.1	368.0 ± 8.2	508.0 ± 9.3	382.0 ± 11.9	1460.0 ± 23.9	−11.7	+218.6
060825	CPL	15.5 ± 1.4	29.0 ± 1.3	34.2 ± 1.9	17.6 ± 3.1	96.3 ± 4.8	−3.6	+7.0
060904A	PL	109.0 ± 4.9	195.0 ± 4.9	267.0 ± 6.2	200.0 ± 7.9	772.0 ± 15.1	−23.9	+108.6
060904B	PL	25.4 ± 3.3	42.8 ± 3.4	54.8 ± 6.1	39.0 ± 6.8	162.0 ± 14.3	−0.9	+183.5
060906	PL	50.3 ± 4.6	67.0 ± 3.8	65.7 ± 5.9	37.9 ± 5.3	221.0 ± 13.6	−41.8	+5.9
060908	CPL	29.6 ± 2.9	67.0 ± 2.9	106.0 ± 4.9	76.9 ± 7.9	280.0 ± 11.1	−13.0	+15.5
060912	PL	23.4 ± 1.9	37.2 ± 1.7	44.5 ± 2.6	29.9 ± 2.9	135.0 ± 6.2	−0.6	+6.1
060919	PL	10.5 ± 1.8	15.6 ± 1.7	17.4 ± 2.7	11.0 ± 2.6	54.6 ± 6.4	−1.0	+9.0
060923A	PL	14.5 ± 3.1	23.5 ± 3.3	29.0 ± 5.5	20.0 ± 5.8	86.9 ± 13.3	−42.3	+11.5
060923B	PL	15.9 ± 2.4	15.9 ± 1.9	11.2 ± 2.7	5.0 ± 1.8	48.0 ± 6.2	−0.1	+9.8
060923C	PL	44.1 ± 6.8	50.9 ± 6.2	42.2 ± 9.8	21.2 ± 7.6	158.0 ± 22.4	+6.8	+90.7
060926	PL	7.5 ± 1.0	7.3 ± 0.8	5.0 ± 1.1	2.2 ± 0.8	21.9 ± 2.5	−0.1	+8.6
060927	CPL	16.8 ± 1.8	34.1 ± 1.8	41.7 ± 2.7	20.6 ± 4.5	113.0 ± 6.8	−1.0	+23.8
060929	PL	15.8 ± 5.0	23.7 ± 5.2	26.5 ± 10.0	17.0 ± 9.9	83.0 ± 23.0	−5.5	+554.5
061002	PL	12.0 ± 2.4	18.8 ± 2.2	22.1 ± 3.4	14.8 ± 3.7	67.7 ± 8.1	−2.3	+16.9
061004	PL	10.6 ± 0.9	16.0 ± 0.8	18.2 ± 1.3	11.8 ± 1.4	56.6 ± 3.1	+0.2	+8.1

Table 2—Continued

GRB Name	Spectral Model	S(15-25)	S(25-50)	S(50-100) (10^{-8} ergs cm^{-2})	S(100-150)	S(15-150)	Start (s)	Stop (s)
061006	PL	24.2 ± 3.5	38.8 ± 3.4	47.0 ± 6.1	32.0 ± 6.6	142.0 ± 14.2	−23.2	+137.7
061007	PL	342.0 ± 12.0	839.0 ± 12.8	1640.0 ± 21.1	1620.0 ± 34.0	4440.0 ± 56.2	−4.1	+231.8
061019	PL	53.5 ± 11.0	76.1 ± 10.2	80.4 ± 17.7	49.1 ± 16.8	259.0 ± 40.5	−170.6	+23.0
061021	PL	31.8 ± 2.3	66.0 ± 2.7	107.0 ± 4.0	91.0 ± 5.7	296.0 ± 10.1	−0.0	+59.9
061027	PL	6.4 ± 2.3	8.8 ± 2.4	9.1 ± 3.9	5.4 ± 3.4	29.7 ± 9.3	+0.0	+64.0
061028	PL	16.5 ± 4.1	26.4 ± 3.9	32.0 ± 7.6	21.7 ± 8.2	96.6 ± 17.2	+46.9	+166.1
061102	PL	4.0 ± 1.3	7.1 ± 1.4	9.7 ± 2.8	7.2 ± 3.3	27.9 ± 6.7	−1.0	+48.9
061110A	PL	17.1 ± 1.8	28.4 ± 1.8	35.8 ± 3.3	25.1 ± 3.8	106.0 ± 7.6	−8.8	+38.5
061110B	PL	10.2 ± 1.9	25.0 ± 2.7	49.2 ± 4.6	48.5 ± 7.3	133.0 ± 12.1	−16.5	+127.9
061121	PL	167.0 ± 6.2	325.0 ± 6.8	489.0 ± 7.6	394.0 ± 10.3	1370.0 ± 19.9	−0.8	+121.4
061126	PL	74.7 ± 5.1	153.0 ± 6.1	244.0 ± 8.8	206.0 ± 12.1	677.0 ± 22.1	−6.0	+163.4
061201	PL	1.9 ± 0.3	5.4 ± 0.6	12.4 ± 1.0	13.7 ± 1.7	33.4 ± 2.7	+0.0	+0.9
061202	PL	50.1 ± 3.7	87.7 ± 3.6	118.0 ± 5.6	86.5 ± 6.8	342.0 ± 13.3	−0.8	+147.4
061210	PL	16.0 ± 4.2	28.2 ± 4.4	38.3 ± 7.4	28.5 ± 8.9	111.0 ± 17.6	+0.2	+89.6
061217	PL	0.3 ± 0.1	0.7 ± 0.1	1.6 ± 0.3	1.7 ± 0.5	4.2 ± 0.7	+0.0	+0.3
061218	PL	1.6 ± 0.5	1.4 ± 0.5	0.8 ± 0.6	0.4 ± 0.3	4.1 ± 1.5	+0.0	+4.1
061222A	PL	90.4 ± 4.2	183.0 ± 4.8	287.0 ± 6.2	239.0 ± 8.8	799.0 ± 15.8	−2.5	+117.7
061222B	PL	48.3 ± 5.4	66.8 ± 4.9	68.2 ± 7.8	40.5 ± 7.2	224.0 ± 18.3	+35.1	+84.9
070103	PL	7.2 ± 1.2	10.0 ± 1.1	10.4 ± 2.0	6.2 ± 1.9	33.8 ± 4.6	−0.1	+20.8
070107	PL	57.2 ± 6.2	117.0 ± 7.2	186.0 ± 10.6	157.0 ± 14.8	517.0 ± 26.4	−20.6	+404.2
070110	PL	23.9 ± 2.7	41.7 ± 2.6	55.6 ± 4.7	40.8 ± 5.5	162.0 ± 10.8	−2.7	+108.2
070126	PL	3.7 ± 1.4	5.0 ± 1.6	4.8 ± 2.5	2.8 ± 2.1	16.3 ± 6.2	+0.0	+64.0
070129	PL	66.6 ± 7.7	89.8 ± 6.8	89.3 ± 12.0	52.0 ± 10.9	298.0 ± 26.7	−125.0	+374.0
070208	PL	9.4 ± 2.6	13.2 ± 2.5	13.7 ± 4.3	8.3 ± 4.0	44.5 ± 10.1	−1.0	+47.8
070209	PL	0.2 ± 0.1	0.4 ± 0.1	0.8 ± 0.2	0.8 ± 0.3	2.2 ± 0.5	+0.0	+0.14
070219	PL	5.8 ± 1.0	8.9 ± 1.0	10.4 ± 1.9	6.8 ± 2.0	31.9 ± 4.4	−1.5	+17.7
070220	PL	126.0 ± 6.4	245.0 ± 7.0	371.0 ± 9.3	300.0 ± 12.8	1040.0 ± 23.3	−17.1	+239.8
070223	PL	32.8 ± 3.2	48.7 ± 3.0	54.0 ± 5.3	34.3 ± 5.3	170.0 ± 12.0	−3.4	+98.5
070224	PL	9.5 ± 1.6	10.0 ± 1.5	7.5 ± 2.3	3.5 ± 1.6	30.5 ± 5.1	−13.8	+24.3
070227	PL	22.7 ± 6.4	40.8 ± 6.8	56.2 ± 10.2	42.3 ± 12.3	162.0 ± 24.9	+0.0	+8.0
070306	PL	85.8 ± 7.8	143.0 ± 7.4	181.0 ± 12.3	128.0 ± 14.1	538.0 ± 28.6	−118.8	+186.5
070318	PL	30.5 ± 2.5	58.8 ± 2.8	88.0 ± 4.6	70.6 ± 6.1	248.0 ± 11.2	−1.0	+103.6
070328	PL	90.4 ± 4.4	195.0 ± 5.4	330.0 ± 6.9	291.0 ± 9.9	906.0 ± 17.9	−18.0	+130.7
070330	CPL	4.5 ± 1.0	8.6 ± 1.3	4.7 ± 2.1	< 1.3	18.3 ± 3.1	−1.1	+8.9
070406	PL	0.4 ± 0.3	0.8 ± 0.3	1.3 ± 0.5	1.1 ± 0.7	3.6 ± 1.2	−0.071	+0.512
070411	PL	45.6 ± 4.4	73.5 ± 4.0	89.5 ± 6.7	61.1 ± 7.5	270.0 ± 15.5	−60.5	+109.5
070412	PL	6.2 ± 1.1	11.7 ± 1.3	17.1 ± 2.7	13.4 ± 3.3	48.4 ± 6.6	−4.1	+31.2
070419A	PL	16.5 ± 2.4	18.2 ± 2.4	14.2 ± 3.6	6.9 ± 2.6	55.8 ± 8.3	−34.7	+92.6
070419B	PL	118.0 ± 6.6	196.0 ± 6.0	248.0 ± 8.2	174.0 ± 9.8	736.0 ± 19.5	−11.7	+313.7
070420	CPL	184.0 ± 16.3	369.0 ± 13.6	512.0 ± 20.5	331.0 ± 27.6	1400.0 ± 44.8	−29.1	+100.3
070427	PL	17.2 ± 1.3	22.2 ± 1.0	20.9 ± 1.6	11.7 ± 1.4	72.0 ± 3.6	−0.2	+13.7
070429A	PL	22.0 ± 4.2	28.2 ± 3.7	26.3 ± 6.4	14.6 ± 5.5	91.0 ± 14.3	−12.4	+178.0
070429B	PL	1.1 ± 0.2	1.7 ± 0.2	2.1 ± 0.4	1.4 ± 0.4	6.3 ± 1.0	−0.2	+0.3
070506	PL	3.6 ± 0.5	5.8 ± 0.5	6.9 ± 1.0	4.7 ± 1.0	21.0 ± 2.3	+4.1	+9.0
070508	CPL	208.0 ± 11.5	452.0 ± 9.2	727.0 ± 9.9	573.0 ± 15.6	1960.0 ± 27.3	−13.8	+33.1

Table 2—Continued

GRB Name	Spectral Model	S(15-25)	S(25-50)	S(50-100) (10^{-8} ergs cm^{-2})	S(100-150)	S(15-150)	Start (s)	Stop (s)
070509	PL	5.1 ± 0.8	5.7 ± 0.7	4.5 ± 1.1	2.2 ± 0.8	17.5 ± 2.5	-1.1	$+7.9$
070517	PL	4.5 ± 0.9	6.4 ± 0.9	6.6 ± 1.5	4.0 ± 1.4	21.5 ± 3.5	$+0.6$	$+9.2$
070518	PL	3.9 ± 0.7	5.0 ± 0.6	4.7 ± 1.1	2.6 ± 0.9	16.2 ± 2.4	-1.8	$+4.5$
070520A	PL	3.8 ± 1.1	6.5 ± 1.2	8.6 ± 2.2	6.2 ± 2.5	25.0 ± 5.4	$+25.5$	$+45.4$
070520B	PL	8.1 ± 1.9	18.7 ± 2.6	34.0 ± 4.2	31.6 ± 6.3	92.5 ± 10.9	-5.0	$+71.2$
070521	CPL	86.0 ± 6.0	188.0 ± 5.0	299.0 ± 8.1	228.0 ± 12.0	801.0 ± 17.7	-14.5	$+49.7$
070529	PL	28.8 ± 5.0	58.5 ± 6.0	92.5 ± 9.8	77.3 ± 12.9	257.0 ± 24.5	-1.2	$+120.9$
070531	PL	13.0 ± 2.7	25.3 ± 3.1	38.3 ± 5.1	30.9 ± 6.5	108.0 ± 12.7	-2.4	$+46.3$
070611	PL	6.2 ± 1.3	10.4 ± 1.4	13.2 ± 2.4	9.3 ± 2.5	39.1 ± 5.7	-6.3	$+7.3$
070612A	PL	175.0 ± 16.7	286.0 ± 16.1	355.0 ± 25.3	246.0 ± 28.0	1060.0 ± 60.1	-4.7	$+417.8$
070612B	PL	23.9 ± 2.8	42.5 ± 3.0	58.1 ± 4.7	43.4 ± 5.5	168.0 ± 11.6	-6.4	$+10.3$
070616	PL	292.0 ± 12.1	501.0 ± 11.5	656.0 ± 14.0	474.0 ± 17.4	1920.0 ± 34.7	-2.6	$+602.2$

Table 3. BAT GRB 1-s peak photon flux

GRB Name	Spectral Model	F^{p}_{ph}(15-25)	F^{p}_{ph}(25-50)	F^{p}_{ph}(50-100)	F^{p}_{ph}(100-150)	F^{p}_{ph}(15-150)	Start (s)	Stop (s)
				(photons cm^{-2} s^{-1})				
041217	PL	2.11 ± 0.28	2.25 ± 0.18	1.71 ± 0.14	0.80 ± 0.11	6.86 ± 0.52	+3.3	+4.3
041219A	-	-	-	-	-	-	-	-
041219B	-	-	-	-	-	-	-	-
041219C	PL	0.96 ± 0.15	0.82 ± 0.09	0.48 ± 0.06	0.18 ± 0.04	2.45 ± 0.25	+8.1	+9.1
041220	PL	0.52 ± 0.04	0.58 ± 0.03	0.47 ± 0.02	0.23 ± 0.02	1.81 ± 0.14	0.0	+1.0
041223	PL	1.45 ± 0.14	2.12 ± 0.12	2.32 ± 0.10	1.45 ± 0.10	7.35 ± 0.32	+35.0	+36.0
041224	PL	0.80 ± 0.15	0.94 ± 0.11	0.79 ± 0.04	0.41 ± 0.03	2.94 ± 0.30	−0.1	+0.9
041226	PL	0.09 ± 0.02	0.11 ± 0.02	0.10 ± 0.02	0.05 ± 0.01	0.35 ± 0.05	+3.3	+4.3
041228	PL	0.60 ± 0.16	0.54 ± 0.04	0.33 ± 0.03	0.13 ± 0.02	1.61 ± 0.25	+22.0	+23.0
050117	PL	0.51 ± 0.04	0.70 ± 0.03	0.71 ± 0.03	0.42 ± 0.03	2.35 ± 0.17	+87.2	+88.2
050124	CPL	1.22 ± 0.23	2.01 ± 0.16	1.71 ± 0.14	0.52 ± 0.11	5.46 ± 0.38	−0.2	+0.8
050126	PL	0.20 ± 0.04	0.23 ± 0.03	0.18 ± 0.03	0.09 ± 0.02	0.71 ± 0.17	+4.1	+5.1
050128	CPL	1.67 ± 0.48	2.59 ± 0.29	2.30 ± 0.28	0.86 ± 0.18	7.42 ± 0.73	+5.6	+6.6
050202	PL	0.20 ± 0.11	0.18 ± 0.03	0.12 ± 0.02	0.05 ± 0.01	0.55 ± 0.17	−0.5	+0.5
050215A	PL	0.10 ± 0.02	0.14 ± 0.03	0.15 ± 0.02	0.10 ± 0.02	0.49 ± 0.13	+5.6	+6.6
050215B	PL	0.22 ± 0.03	0.22 ± 0.02	0.15 ± 0.02	0.07 ± 0.01	0.67 ± 0.12	−0.8	+0.2
050219A	PL	0.92 ± 0.17	1.12 ± 0.13	0.98 ± 0.10	0.52 ± 0.04	3.53 ± 0.35	+9.5	+10.5
050219B	CPL	7.55 ± 1.08	8.95 ± 0.59	6.23 ± 0.47	2.05 ± 0.29	24.80 ± 1.53	+2.9	+3.9
050223	PL	0.28 ± 0.05	0.23 ± 0.03	0.13 ± 0.02	0.05 ± 0.01	0.69 ± 0.16	+1.6	+2.6
050306	PL	1.03 ± 0.25	1.16 ± 0.18	0.93 ± 0.12	0.46 ± 0.05	3.58 ± 0.48	+107.9	+108.9
050315	PL	0.93 ± 0.15	0.63 ± 0.04	0.28 ± 0.02	0.09 ± 0.01	1.93 ± 0.22	+24.6	+25.6
050318	CPL	1.05 ± 0.14	1.18 ± 0.04	0.73 ± 0.03	0.20 ± 0.03	3.16 ± 0.20	+28.6	+29.6
050319	PL	0.71 ± 0.14	0.50 ± 0.03	0.23 ± 0.03	0.07 ± 0.01	1.52 ± 0.21	+0.4	+1.4
050326	PL	2.62 ± 0.18	3.64 ± 0.15	3.74 ± 0.12	2.24 ± 0.12	12.20 ± 0.39	−0.1	+0.9
050401	CPL	2.12 ± 0.55	3.67 ± 0.38	3.57 ± 0.37	1.37 ± 0.25	10.70 ± 0.92	+24.3	+25.3
050406	PL	0.20 ± 0.03	0.11 ± 0.02	0.04 ± 0.01	$(9.5 \pm 4.8) \times 10^{-3}$	0.36 ± 0.10	+1.2	+2.2
050410	PL	0.60 ± 0.21	0.60 ± 0.13	0.42 ± 0.10	0.18 ± 0.03	1.80 ± 0.36	+3.6	+4.6
050412	PL	0.08 ± 0.02	0.13 ± 0.02	0.16 ± 0.02	0.11 ± 0.02	0.48 ± 0.05	+1.2	+2.2
050416A	PL	2.97 ± 0.35	1.41 ± 0.15	0.41 ± 0.04	0.09 ± 0.01	4.88 ± 0.48	−0.1	+0.9
050416B	PL	1.37 ± 0.28	1.81 ± 0.23	1.75 ± 0.17	1.00 ± 0.14	5.93 ± 0.61	+0.1	+1.1
050418	PL	0.91 ± 0.14	1.15 ± 0.11	1.05 ± 0.04	0.57 ± 0.03	3.68 ± 0.28	+0.7	+1.7
050421	PL	0.07 ± 0.03	0.08 ± 0.04	0.07 ± 0.02	0.04 ± 0.01	0.26 ± 0.19	−0.1	+0.9
050422	PL	0.20 ± 0.03	0.19 ± 0.02	0.12 ± 0.02	0.05 ± 0.01	0.57 ± 0.11	+53.2	+54.2
050502B	CPL	0.36 ± 0.04	0.54 ± 0.03	0.41 ± 0.02	0.12 ± 0.02	1.42 ± 0.13	+0.2	+1.2
050505	PL	0.45 ± 0.15	0.57 ± 0.12	0.53 ± 0.04	0.29 ± 0.03	1.85 ± 0.31	+1.0	+2.0
050507	PL	0.08 ± 0.03	0.09 ± 0.02	0.08 ± 0.02	0.04 ± 0.01	0.29 ± 0.13	+4.5	+5.5
050509A	PL	0.43 ± 0.04	0.29 ± 0.02	0.13 ± 0.02	0.04 ± 0.01	0.90 ± 0.12	+0.7	+1.7
050509B	PL	0.09 ± 0.02	0.09 ± 0.02	0.07 ± 0.02	0.03 ± 0.01	0.28 ± 0.10	+0.0	+1.0
050525A	CPL	10.30 ± 0.66	14.50 ± 0.34	12.20 ± 0.27	4.64 ± 0.18	41.70 ± 0.94	+0.8	+1.8
050528	PL	0.41 ± 0.17	0.40 ± 0.10	0.27 ± 0.04	0.11 ± 0.02	1.18 ± 0.30	+3.4	+4.4
050603	CPL	3.23 ± 0.53	6.51 ± 0.44	7.90 ± 0.52	3.86 ± 0.43	21.50 ± 1.07	−0.2	+0.8
050607	PL	0.29 ± 0.04	0.31 ± 0.02	0.24 ± 0.02	0.11 ± 0.01	0.95 ± 0.14	+0.9	+1.9
050701	PL	0.80 ± 0.10	0.89 ± 0.03	0.71 ± 0.03	0.34 ± 0.02	2.74 ± 0.18	+7.4	+8.4
050712	PL	0.24 ± 0.11	0.18 ± 0.03	0.09 ± 0.02	0.03 ± 0.01	0.55 ± 0.18	+17.4	+18.4
050713A	PL	1.29 ± 0.17	1.50 ± 0.12	1.25 ± 0.05	0.63 ± 0.04	4.67 ± 0.33	+1.1	+2.1

Table 3—Continued

GRB Name	Spectral Model	F^{P}_{ph}(15-25)	F^{P}_{ph}(25-50)	F^{P}_{ph}(50-100)	F^{P}_{ph}(100-150)	F^{P}_{ph}(15-150)	Start (s)	Stop (s)
				(photons cm^{-2} s^{-1})				
050713B	PL	0.47 ± 0.27	0.52 ± 0.18	0.41 ± 0.13	0.20 ± 0.10	1.60 ± 0.50	+8.6	+9.6
050714B	PL	0.24 ± 0.14	0.17 ± 0.04	0.08 ± 0.03	0.03 ± 0.01	0.52 ± 0.22	+55.2	+56.2
050715	PL	0.39 ± 0.04	0.35 ± 0.02	0.22 ± 0.02	0.09 ± 0.01	1.05 ± 0.14	+40.4	+41.4
050716	PL	0.68 ± 0.19	0.72 ± 0.12	0.53 ± 0.05	0.24 ± 0.03	2.18 ± 0.35	+12.2	+13.2
050717	PL	1.47 ± 0.15	1.91 ± 0.12	1.82 ± 0.05	1.02 ± 0.04	6.23 ± 0.31	+2.8	+3.8
050721	CPL	0.52 ± 0.28	1.01 ± 0.21	0.64 ± 0.16	0.07 ± 0.04	2.24 ± 0.46	+3.7	+4.7
050724	PL	1.19 ± 0.19	1.09 ± 0.10	0.70 ± 0.04	0.28 ± 0.03	3.26 ± 0.30	+0.0	+1.0
050726	PL	0.31 ± 0.17	0.42 ± 0.14	0.41 ± 0.05	0.24 ± 0.04	1.38 ± 0.38	+1.1	+2.1
050730	PL	0.15 ± 0.03	0.17 ± 0.03	0.15 ± 0.02	0.07 ± 0.02	0.55 ± 0.14	+5.0	+6.0
050801	PL	0.44 ± 0.04	0.48 ± 0.02	0.37 ± 0.02	0.18 ± 0.02	1.46 ± 0.14	+0.1	+1.1
050802	PL	0.82 ± 0.23	0.90 ± 0.16	0.70 ± 0.12	0.34 ± 0.04	2.75 ± 0.44	+0.0	+1.0
050803	PL	0.26 ± 0.03	0.30 ± 0.02	0.26 ± 0.02	0.13 ± 0.01	0.96 ± 0.11	+147.1	+148.1
050813	PL	0.27 ± 0.11	0.30 ± 0.04	0.25 ± 0.03	0.12 ± 0.02	0.94 ± 0.23	−0.2	+0.8
050814	PL	0.19 ± 0.12	0.22 ± 0.05	0.19 ± 0.03	0.10 ± 0.02	0.71 ± 0.25	+8.7	+9.7
050815	PL	0.20 ± 0.03	0.18 ± 0.02	0.12 ± 0.02	0.05 ± 0.01	0.55 ± 0.12	−0.1	+0.9
050819	PL	0.16 ± 0.04	0.13 ± 0.02	0.07 ± 0.04	0.03 ± 0.01	0.38 ± 0.12	+9.5	+10.5
050820A	PL	0.56 ± 0.05	0.74 ± 0.04	0.72 ± 0.04	0.41 ± 0.04	2.45 ± 0.23	+229.5	+230.5
050820B	CPL	0.74 ± 0.05	1.28 ± 0.04	1.33 ± 0.04	0.59 ± 0.03	3.95 ± 0.18	+8.6	+9.6
050822	PL	1.00 ± 0.14	0.75 ± 0.04	0.37 ± 0.03	0.12 ± 0.01	2.24 ± 0.22	+47.6	+48.6
050824	PL	0.21 ± 0.04	0.17 ± 0.03	0.09 ± 0.02	0.03 ± 0.01	0.50 ± 0.15	+53.1	+54.1
050826	PL	0.14 ± 0.04	0.13 ± 0.02	0.08 ± 0.02	0.03 ± 0.01	0.38 ± 0.13	+1.4	+2.4
050827	PL	0.45 ± 0.05	0.57 ± 0.04	0.53 ± 0.03	0.29 ± 0.02	1.84 ± 0.20	+0.3	+1.3
050904	PL	0.15 ± 0.04	0.19 ± 0.03	0.18 ± 0.03	0.10 ± 0.02	0.62 ± 0.17	+27.4	+28.4
050906[†]	PL	-	-	-	-	-	-	-
050908	PL	0.23 ± 0.03	0.23 ± 0.02	0.17 ± 0.02	0.07 ± 0.01	0.70 ± 0.14	+1.7	+2.7
050911	PL	0.57 ± 0.13	0.44 ± 0.03	0.23 ± 0.03	0.08 ± 0.01	1.33 ± 0.20	−0.1	+0.9
050915A	PL	0.16 ± 0.03	0.23 ± 0.03	0.24 ± 0.02	0.14 ± 0.02	0.77 ± 0.14	+13.7	+14.7
050915B	PL	0.82 ± 0.12	0.77 ± 0.04	0.51 ± 0.03	0.21 ± 0.02	2.31 ± 0.21	−3.1	−2.1
050916	PL	0.21 ± 0.12	0.21 ± 0.04	0.15 ± 0.03	0.07 ± 0.02	0.65 ± 0.23	+43.7	+44.7
050922B	PL	0.30 ± 0.19	0.33 ± 0.13	0.26 ± 0.05	0.12 ± 0.03	1.01 ± 0.36	+98.6	+99.6
050922C	PL	2.08 ± 0.17	2.35 ± 0.12	1.90 ± 0.05	0.94 ± 0.04	7.26 ± 0.32	−0.1	+0.9
050925	CPL	2.62 ± 0.81	4.17 ± 0.53	2.74 ± 0.45	0.49 ± 0.19	10.00 ± 1.19	−0.4	+0.6
051001	PL	0.17 ± 0.03	0.16 ± 0.02	0.11 ± 0.02	0.05 ± 0.01	0.49 ± 0.11	+130.4	+131.4
051006	PL	0.34 ± 0.13	0.48 ± 0.11	0.50 ± 0.04	0.30 ± 0.04	1.62 ± 0.30	+2.6	+3.6
051008	PL	1.25 ± 0.17	1.66 ± 0.13	1.61 ± 0.10	0.92 ± 0.05	5.44 ± 0.35	+2.9	+3.9
051012	PL	0.17 ± 0.04	0.17 ± 0.02	0.13 ± 0.02	0.06 ± 0.01	0.53 ± 0.13	+4.5	+5.5
051016	PL	0.47 ± 0.23	0.46 ± 0.14	0.32 ± 0.10	0.14 ± 0.03	1.39 ± 0.38	+4.9	+5.9
051016B	PL	0.56 ± 0.10	0.44 ± 0.03	0.23 ± 0.02	0.08 ± 0.01	1.30 ± 0.16	+0.1	+1.1
051021B	PL	0.25 ± 0.04	0.26 ± 0.03	0.20 ± 0.02	0.09 ± 0.02	0.80 ± 0.14	−0.7	+0.3
051105	PL	0.06 ± 0.02	0.09 ± 0.05	0.10 ± 0.02	0.06 ± 0.02	0.32 ± 0.12	−0.4	+0.6
051109A	PL	1.28 ± 0.37	1.30 ± 0.24	0.93 ± 0.16	0.42 ± 0.11	3.94 ± 0.69	+0.7	+1.7
051109B	PL	0.24 ± 0.04	0.18 ± 0.02	0.09 ± 0.02	0.03 ± 0.01	0.55 ± 0.13	+0.0	+1.0
051111	PL	0.67 ± 0.10	0.83 ± 0.04	0.75 ± 0.03	0.41 ± 0.03	2.66 ± 0.21	−0.3	+0.7
051113	PL	0.77 ± 0.18	0.75 ± 0.11	0.51 ± 0.05	0.22 ± 0.03	2.25 ± 0.32	+0.3	+1.3
051114	PL	0.14 ± 0.03	0.20 ± 0.03	0.22 ± 0.02	0.14 ± 0.02	0.70 ± 0.15	+0.3	+1.3

Table 3—Continued

GRB Name	Spectral Model	F^{p}_{ph}(15-25)	F^{p}_{ph}(25-50)	F^{p}_{ph}(50-100)	F^{p}_{ph}(100-150)	F^{p}_{ph}(15-150)	Start (s)	Stop (s)
				(photons cm^{-2} s^{-1})				
051117A	PL	0.45 ± 0.05	0.31 ± 0.03	0.14 ± 0.02	0.04 ± 0.01	0.95 ± 0.16	+2.6	+3.6
051117B	PL	0.15 ± 0.03	0.16 ± 0.02	0.12 ± 0.02	0.05 ± 0.01	0.49 ± 0.14	+1.4	+2.4
051210	PL	0.16 ± 0.03	0.22 ± 0.02	0.23 ± 0.02	0.14 ± 0.02	0.75 ± 0.12	+0.1	+1.1
051213	PL	0.11 ± 0.03	0.14 ± 0.03	0.14 ± 0.02	0.08 ± 0.02	0.48 ± 0.14	+48.9	+49.9
051221A	PL	3.36 ± 0.22	3.86 ± 0.15	3.19 ± 0.10	1.60 ± 0.04	12.00 ± 0.39	+0.2	+1.2
051221B	PL	0.09 ± 0.03	0.15 ± 0.12	0.18 ± 0.03	0.12 ± 0.03	0.54 ± 0.20	+58.9	+59.9
051227	PL	0.22 ± 0.03	0.29 ± 0.02	0.28 ± 0.02	0.16 ± 0.02	0.95 ± 0.12	+0.0	+1.0
060102	PL	0.06 ± 0.02	0.10 ± 0.03	0.13 ± 0.02	0.09 ± 0.02	0.38 ± 0.12	+0.1	+1.1
060105	PL	1.64 ± 0.16	2.23 ± 0.14	2.25 ± 0.11	1.32 ± 0.05	7.44 ± 0.36	+30.8	+31.8
060108	PL	0.29 ± 0.03	0.26 ± 0.02	0.16 ± 0.02	0.06 ± 0.01	0.77 ± 0.12	+0.6	+1.6
060109	PL	0.16 ± 0.03	0.16 ± 0.02	0.10 ± 0.02	0.04 ± 0.01	0.47 ± 0.12	+90.2	+91.2
060110	CPL	0.50 ± 0.05	0.68 ± 0.03	0.53 ± 0.03	0.17 ± 0.03	1.89 ± 0.16	+1.3	+2.3
060111A	CPL	0.46 ± 0.04	0.63 ± 0.03	0.47 ± 0.03	0.15 ± 0.02	1.71 ± 0.15	+4.3	+5.3
060111B	PL	0.29 ± 0.12	0.41 ± 0.10	0.43 ± 0.04	0.27 ± 0.04	1.40 ± 0.27	+0.4	+1.4
060115	PL	0.25 ± 0.03	0.28 ± 0.02	0.23 ± 0.02	0.11 ± 0.01	0.87 ± 0.12	+94.9	+95.9
060116	PL	0.40 ± 0.18	0.37 ± 0.11	0.24 ± 0.04	0.10 ± 0.02	1.11 ± 0.32	+36.1	+37.1
060117	CPL	14.50 ± 1.17	17.40 ± 0.55	12.30 ± 0.41	4.13 ± 0.25	48.30 ± 1.56	+11.1	+12.1
060124	PL	0.33 ± 0.05	0.30 ± 0.03	0.19 ± 0.03	0.08 ± 0.02	0.89 ± 0.18	+0.2	+1.2
060202	PL	0.18 ± 0.15	0.17 ± 0.03	0.11 ± 0.03	0.05 ± 0.02	0.51 ± 0.17	−6.5	−5.5
060203	PL	0.19 ± 0.03	0.20 ± 0.03	0.14 ± 0.02	0.07 ± 0.02	0.60 ± 0.19	+25.9	+26.9
060204B	PL	0.42 ± 0.04	0.44 ± 0.03	0.33 ± 0.02	0.15 ± 0.02	1.35 ± 0.15	+5.0	+6.0
060206	CPL	0.87 ± 0.12	1.04 ± 0.03	0.69 ± 0.03	0.19 ± 0.02	2.79 ± 0.17	+2.1	+3.1
060210	PL	0.70 ± 0.14	0.86 ± 0.10	0.76 ± 0.04	0.41 ± 0.03	2.72 ± 0.28	+0.0	+1.0
060211A	PL	0.13 ± 0.03	0.14 ± 0.02	0.10 ± 0.02	0.05 ± 0.01	0.42 ± 0.12	+145.6	+146.6
060211B	PL	0.23 ± 0.03	0.24 ± 0.02	0.18 ± 0.02	0.08 ± 0.01	0.73 ± 0.13	+1.8	+2.8
060218	PL	0.15 ± 0.04	0.07 ± 0.04	0.02 ± 0.01	$(5 \pm 3) \times 10^{-3}$	0.25 ± 0.11	+275.0	+276.0
060219	PL	0.33 ± 0.13	0.17 ± 0.03	0.05 ± 0.02	$(11 \pm 6) \times 10^{-3}$	0.56 ± 0.17	+4.1	+5.1
060223A	PL	0.47 ± 0.05	0.45 ± 0.03	0.30 ± 0.03	0.13 ± 0.02	1.35 ± 0.18	+0.1	+1.1
060223B	PL	0.62 ± 0.04	0.86 ± 0.04	0.87 ± 0.03	0.52 ± 0.03	2.87 ± 0.20	+3.0	+4.0
060306	CPL	1.73 ± 0.24	2.10 ± 0.14	1.56 ± 0.11	0.58 ± 0.05	5.97 ± 0.35	+0.2	+1.2
060312	PL	0.54 ± 0.04	0.51 ± 0.02	0.34 ± 0.02	0.14 ± 0.01	1.53 ± 0.14	+5.6	+6.6
060313	PL	2.02 ± 0.17	3.27 ± 0.17	4.02 ± 0.15	2.77 ± 0.17	12.10 ± 0.45	+0.0	+1.0
060319	PL	0.52 ± 0.05	0.36 ± 0.02	0.16 ± 0.02	0.05 ± 0.01	1.09 ± 0.14	+4.1	+5.1
060322	PL	0.73 ± 0.12	0.69 ± 0.03	0.46 ± 0.03	0.19 ± 0.02	2.08 ± 0.20	+182.2	+183.2
060323	PL	0.39 ± 0.05	0.26 ± 0.03	0.11 ± 0.02	0.03 ± 0.01	0.78 ± 0.15	+2.5	+3.5
060403	PL	0.17 ± 0.02	0.27 ± 0.02	0.31 ± 0.02	0.20 ± 0.02	0.95 ± 0.13	+1.8	+2.8
060413	PL	0.38 ± 0.04	0.31 ± 0.02	0.17 ± 0.02	0.06 ± 0.01	0.93 ± 0.12	+90.2	+91.2
060418	PL	2.18 ± 0.21	2.17 ± 0.12	1.51 ± 0.05	0.66 ± 0.03	6.52 ± 0.35	+27.5	+28.5
060421	PL	0.80 ± 0.04	0.94 ± 0.03	0.80 ± 0.03	0.41 ± 0.02	2.94 ± 0.18	+2.3	+3.3
060424	PL	0.62 ± 0.11	0.54 ± 0.03	0.33 ± 0.03	0.13 ± 0.02	1.61 ± 0.19	+0.1	+1.1
060427	PL	0.12 ± 0.04	0.09 ± 0.02	0.05 ± 0.02	0.02 ± 0.01	0.27 ± 0.13	+5.0	+6.0
060428A	PL	1.05 ± 0.13	0.76 ± 0.03	0.36 ± 0.03	0.12 ± 0.01	2.28 ± 0.20	+4.2	+5.2
060428B	PL	0.36 ± 0.05	0.21 ± 0.03	0.07 ± 0.02	0.02 ± 0.01	0.66 ± 0.15	+20.8	+21.8
060501	PL	0.44 ± 0.12	0.60 ± 0.10	0.60 ± 0.04	0.35 ± 0.03	1.98 ± 0.26	+0.4	+1.4
060502A	PL	0.36 ± 0.04	0.50 ± 0.04	0.51 ± 0.03	0.30 ± 0.03	1.69 ± 0.21	−0.1	+0.9

Table 3—Continued

GRB Name	Spectral Model	F^{p}_{ph}(15-25)	F^{p}_{ph}(25-50)	F^{p}_{ph}(50-100)	F^{p}_{ph}(100-150)	F^{p}_{ph}(15-150)	Start (s)	Stop (s)
				(photons cm^{-2} s^{-1})				
060502B	PL	0.12 ± 0.02	0.17 ± 0.02	0.20 ± 0.02	0.13 ± 0.02	0.62 ± 0.12	−0.5	+0.5
060505	PL	0.64 ± 0.30	0.82 ± 0.23	0.77 ± 0.19	0.43 ± 0.16	2.65 ± 0.63	+0.0	+1.0
060507	PL	0.48 ± 0.12	0.43 ± 0.04	0.26 ± 0.03	0.10 ± 0.02	1.27 ± 0.22	+1.2	+2.2
060510A	PL	4.71 ± 0.65	4.85 ± 0.40	3.53 ± 0.32	1.60 ± 0.23	14.70 ± 1.13	+0.3	+1.3
060510B	PL	0.18 ± 0.03	0.19 ± 0.02	0.14 ± 0.02	0.06 ± 0.01	0.57 ± 0.11	+136.2	+137.2
060512	PL	0.54 ± 0.14	0.25 ± 0.04	0.07 ± 0.02	$(15 \pm 5) \times 10^{-3}$	0.88 ± 0.20	+3.3	+4.3
060515	PL	0.16 ± 0.04	0.24 ± 0.04	0.26 ± 0.03	0.16 ± 0.03	0.82 ± 0.20	+5.6	+6.6
060516	PL	< 0.28	0.11 ± 0.10	0.06 ± 0.03	0.02 ± 0.01	0.34 ± 0.23	+128.6	+129.6
060522	PL	0.25 ± 0.04	0.18 ± 0.03	0.08 ± 0.02	0.03 ± 0.01	0.55 ± 0.15	+4.4	+5.4
060526	PL	0.49 ± 0.04	0.54 ± 0.03	0.43 ± 0.03	0.21 ± 0.02	1.67 ± 0.18	+0.1	+1.1
060602A	PL	0.10 ± 0.03	0.16 ± 0.04	0.18 ± 0.03	0.12 ± 0.02	0.56 ± 0.20	+18.0	+19.0
060604	PL	0.13 ± 0.04	0.11 ± 0.02	0.07 ± 0.03	0.03 ± 0.01	0.34 ± 0.13	−32.2	−31.2
060605	PL	0.09 ± 0.05	0.13 ± 0.04	0.15 ± 0.04	0.09 ± 0.03	0.46 ± 0.12	+2.1	+3.1
060607A	PL	0.35 ± 0.03	0.43 ± 0.02	0.40 ± 0.02	0.22 ± 0.02	1.40 ± 0.13	−1.0	+0.0
060607B	PL	0.46 ± 0.13	0.48 ± 0.04	0.35 ± 0.04	0.16 ± 0.02	1.46 ± 0.25	+8.6	+9.6
060614	PL	4.12 ± 0.45	3.85 ± 0.26	2.51 ± 0.19	1.04 ± 0.13	11.50 ± 0.74	−1.3	−0.3
060707	PL	0.35 ± 0.13	0.34 ± 0.04	0.23 ± 0.03	0.10 ± 0.02	1.01 ± 0.23	+2.0	+3.0
060708	PL	0.58 ± 0.04	0.63 ± 0.02	0.49 ± 0.02	0.23 ± 0.02	1.94 ± 0.14	+1.1	+2.1
060712	PL	0.84 ± 0.42	0.53 ± 0.19	0.21 ± 0.12	0.06 ± 0.02	1.64 ± 0.60	+16.8	+17.8
060714	PL	0.42 ± 0.03	0.42 ± 0.02	0.30 ± 0.02	0.13 ± 0.01	1.28 ± 0.13	+75.4	+76.4
060717	PL	0.23 ± 0.03	0.18 ± 0.02	0.10 ± 0.02	0.03 ± 0.01	0.54 ± 0.11	+0.8	+1.8
060719	CPL	0.78 ± 0.14	0.86 ± 0.04	0.44 ± 0.03	0.08 ± 0.02	2.16 ± 0.20	+0.4	+1.4
060728[†]	-	-	-	-	-	-	-	-
060729	PL	0.49 ± 0.04	0.39 ± 0.02	0.21 ± 0.02	0.07 ± 0.01	1.17 ± 0.13	+92.0	+93.0
060801	PL	0.17 ± 0.03	0.31 ± 0.03	0.45 ± 0.03	0.34 ± 0.03	1.27 ± 0.16	−0.2	+0.8
060804	PL	0.33 ± 0.16	0.37 ± 0.11	0.29 ± 0.04	0.14 ± 0.03	1.13 ± 0.29	+4.5	+5.5
060805	PL	0.14 ± 0.03	0.11 ± 0.02	0.06 ± 0.02	0.02 ± 0.01	0.34 ± 0.11	+0.7	+1.7
060807	PL	0.23 ± 0.04	0.26 ± 0.03	0.22 ± 0.03	0.11 ± 0.02	0.83 ± 0.16	−0.1	+0.9
060813	PL	2.24 ± 0.20	2.77 ± 0.14	2.49 ± 0.11	1.34 ± 0.05	8.84 ± 0.39	+3.6	+4.6
060814	PL	2.08 ± 0.16	2.35 ± 0.11	1.90 ± 0.04	0.94 ± 0.03	7.27 ± 0.29	+15.4	+16.4
060825	CPL	0.71 ± 0.11	0.97 ± 0.03	0.74 ± 0.03	0.24 ± 0.03	2.66 ± 0.17	+0.1	+1.1
060904A	PL	1.23 ± 0.10	1.52 ± 0.04	1.38 ± 0.03	0.74 ± 0.03	4.87 ± 0.20	+55.3	+56.3
060904B	PL	0.64 ± 0.11	0.77 ± 0.04	0.67 ± 0.03	0.35 ± 0.03	2.44 ± 0.21	+1.2	+2.2
060906	PL	0.91 ± 0.18	0.65 ± 0.05	0.31 ± 0.04	0.10 ± 0.02	1.97 ± 0.28	−24.9	−23.9
060908	CPL	0.58 ± 0.14	1.01 ± 0.10	1.02 ± 0.05	0.42 ± 0.04	3.03 ± 0.25	+1.0	+2.0
060912	PL	3.19 ± 0.28	2.88 ± 0.15	1.79 ± 0.11	0.72 ± 0.04	8.58 ± 0.44	+0.0	+1.0
060919	CPL	0.43 ± 0.18	0.78 ± 0.13	0.70 ± 0.11	0.21 ± 0.04	2.12 ± 0.30	−0.5	+0.5
060923A	PL	0.41 ± 0.14	0.43 ± 0.05	0.32 ± 0.04	0.15 ± 0.03	1.32 ± 0.26	+0.0	+1.0
060923B	PL	0.85 ± 0.23	0.47 ± 0.11	0.16 ± 0.03	0.04 ± 0.01	1.52 ± 0.33	+4.9	+5.9
060923C	PL	0.50 ± 0.23	0.31 ± 0.13	0.12 ± 0.04	0.03 ± 0.02	0.96 ± 0.36	+27.5	+28.5
060926	PL	0.58 ± 0.05	0.35 ± 0.02	0.13 ± 0.02	0.04 ± 0.01	1.09 ± 0.14	+0.4	+1.4
060927	CPL	0.55 ± 0.05	0.90 ± 0.03	0.88 ± 0.03	0.38 ± 0.03	2.70 ± 0.17	+0.2	+1.2
060929	PL	0.12 ± 0.03	0.14 ± 0.02	0.11 ± 0.02	0.05 ± 0.01	0.42 ± 0.13	+2.5	+3.5
061002	PL	0.30 ± 0.16	0.27 ± 0.04	0.17 ± 0.03	0.07 ± 0.02	0.81 ± 0.26	−1.4	−0.4
061004	PL	0.91 ± 0.05	0.85 ± 0.03	0.55 ± 0.02	0.23 ± 0.01	2.54 ± 0.16	+2.7	+3.7

Table 3—Continued

GRB Name	Spectral Model	F^{P}_{ph}(15-25)	F^{P}_{ph}(25-50)	F^{P}_{ph}(50-100)	F^{P}_{ph}(100-150)	F^{P}_{ph}(15-150)	Start (s)	Stop (s)
				(photons cm^{-2} s^{-1})				
061006	PL	1.04 ± 0.05	1.52 ± 0.04	1.65 ± 0.03	1.03 ± 0.04	5.24 ± 0.21	−23.2	−22.2
061007	PL	2.42 ± 0.15	3.95 ± 0.15	4.87 ± 0.12	3.36 ± 0.14	14.60 ± 0.37	+45.1	+46.1
061019	PL	0.86 ± 0.28	0.71 ± 0.15	0.40 ± 0.12	0.15 ± 0.03	2.12 ± 0.44	+2.5	+3.5
061021	PL	1.56 ± 0.14	1.92 ± 0.10	1.71 ± 0.04	0.92 ± 0.04	6.11 ± 0.27	+2.4	+3.4
061027[†]	-	-	-	-	-	-	-	-
061028	PL	0.16 ± 0.04	0.20 ± 0.04	0.18 ± 0.03	0.10 ± 0.02	0.65 ± 0.19	+79.9	+80.9
061102	PL	0.04 ± 0.01	0.06 ± 0.02	0.08 ± 0.02	0.05 ± 0.01	0.23 ± 0.05	+3.4	+4.4
061110A	PL	0.20 ± 0.03	0.18 ± 0.02	0.11 ± 0.02	0.05 ± 0.01	0.53 ± 0.12	+9.7	+10.7
061110B	PL	0.10 ± 0.02	0.13 ± 0.02	0.14 ± 0.02	0.08 ± 0.02	0.45 ± 0.11	+3.3	+4.3
061121	PL	4.94 ± 0.24	6.47 ± 0.18	6.21 ± 0.13	3.52 ± 0.12	21.10 ± 0.46	+74.5	+75.5
061126	PL	2.00 ± 0.17	2.86 ± 0.14	3.04 ± 0.12	1.86 ± 0.12	9.76 ± 0.38	+6.7	+7.7
061201	PL	0.72 ± 0.13	1.09 ± 0.12	1.25 ± 0.05	0.81 ± 0.05	3.86 ± 0.31	+0.0	+1.0
061202	PL	0.74 ± 0.04	0.82 ± 0.03	0.64 ± 0.02	0.31 ± 0.02	2.51 ± 0.17	+75.0	+76.0
061210	PL	0.97 ± 0.19	1.49 ± 0.18	1.72 ± 0.15	1.13 ± 0.15	5.31 ± 0.47	+0.0	+1.0
061217	PL	0.28 ± 0.05	0.42 ± 0.05	0.47 ± 0.04	0.30 ± 0.04	1.49 ± 0.24	−0.4	+0.6
061218	PL	0.15 ± 0.04	0.08 ± 0.04	0.02 ± 0.01	$(5 \pm 3) \times 10^{-3}$	0.26 ± 0.12	+1.5	+2.5
061222A	CPL	1.64 ± 0.15	2.58 ± 0.05	2.78 ± 0.11	1.52 ± 0.05	8.53 ± 0.26	+86.5	+87.5
061222B	PL	0.81 ± 0.23	0.51 ± 0.12	0.21 ± 0.04	0.06 ± 0.02	1.59 ± 0.36	+59.2	+60.2
070103	CPL	0.38 ± 0.10	0.46 ± 0.04	0.19 ± 0.03	0.02 ± 0.01	1.04 ± 0.15	−0.1	+0.9
070107	PL	0.43 ± 0.11	0.59 ± 0.05	0.59 ± 0.03	0.35 ± 0.03	1.97 ± 0.23	−7.2	−6.2
070110	PL	0.22 ± 0.04	0.20 ± 0.02	0.13 ± 0.02	0.05 ± 0.01	0.60 ± 0.12	−0.2	+0.8
070126[†]	-	-	-	-	-	-	-	-
070129	PL	0.23 ± 0.03	0.18 ± 0.02	0.10 ± 0.02	0.03 ± 0.01	0.55 ± 0.12	+310.6	+311.6
070208	PL	0.39 ± 0.15	0.30 ± 0.04	0.16 ± 0.03	0.05 ± 0.02	0.90 ± 0.22	−0.3	+0.7
070209	PL	0.10 ± 0.03	0.12 ± 0.02	0.11 ± 0.02	0.06 ± 0.01	0.38 ± 0.13	−0.4	+0.6
070219	PL	0.29 ± 0.04	0.23 ± 0.02	0.12 ± 0.02	0.04 ± 0.01	0.67 ± 0.13	+1.3	+2.3
070220	PL	1.54 ± 0.15	1.86 ± 0.11	1.63 ± 0.04	0.85 ± 0.04	5.88 ± 0.29	+11.9	+12.9
070223	PL	0.22 ± 0.04	0.23 ± 0.03	0.17 ± 0.02	0.08 ± 0.02	0.69 ± 0.15	+34.3	+35.3
070224	PL	0.14 ± 0.04	0.12 ± 0.02	0.06 ± 0.03	0.02 ± 0.01	0.34 ± 0.11	−13.8	−12.8
070227	PL	1.84 ± 0.72	1.55 ± 0.43	0.89 ± 0.29	0.34 ± 0.16	4.62 ± 1.27	+1.0	+2.0
070306	PL	1.40 ± 0.13	1.36 ± 0.04	0.92 ± 0.03	0.39 ± 0.02	4.07 ± 0.21	+98.3	+99.3
070318	PL	0.52 ± 0.04	0.57 ± 0.03	0.45 ± 0.02	0.21 ± 0.02	1.76 ± 0.15	+1.9	+2.9
070328	PL	1.02 ± 0.12	1.30 ± 0.05	1.22 ± 0.04	0.67 ± 0.03	4.22 ± 0.24	+0.8	+1.8
070330	PL	0.36 ± 0.04	0.29 ± 0.02	0.16 ± 0.02	0.06 ± 0.01	0.88 ± 0.14	−0.1	+0.9
070406	PL	0.11 ± 0.03	0.12 ± 0.02	0.09 ± 0.02	0.04 ± 0.01	0.37 ± 0.11	−0.1	+0.9
070411	PL	0.30 ± 0.03	0.30 ± 0.02	0.21 ± 0.02	0.10 ± 0.01	0.91 ± 0.13	+70.2	+71.2
070412	PL	0.19 ± 0.03	0.21 ± 0.02	0.17 ± 0.02	0.08 ± 0.01	0.66 ± 0.12	+5.3	+6.3
070419A[†]	PL	-	-	-	-	0.2 ± 0.1	−1.1	−0.1
070419B	PL	0.40 ± 0.05	0.45 ± 0.03	0.36 ± 0.03	0.17 ± 0.02	1.38 ± 0.17	−0.3	+0.7
070420	PL	2.34 ± 0.41	2.36 ± 0.27	1.67 ± 0.20	0.74 ± 0.13	7.12 ± 0.76	+1.4	+2.4
070427	PL	0.59 ± 0.04	0.45 ± 0.02	0.23 ± 0.02	0.08 ± 0.01	1.34 ± 0.13	+6.8	+7.8
070429A	PL	0.13 ± 0.04	0.14 ± 0.03	0.10 ± 0.02	0.04 ± 0.01	0.41 ± 0.15	+4.0	+5.0
070429B	PL	0.66 ± 0.14	0.59 ± 0.04	0.36 ± 0.03	0.14 ± 0.02	1.76 ± 0.24	−0.5	+0.6
070506	CPL	0.33 ± 0.04	0.41 ± 0.03	0.19 ± 0.03	0.02 ± 0.01	0.96 ± 0.13	+6.2	+7.2
070508	CPL	5.09 ± 0.40	7.63 ± 0.23	7.58 ± 0.23	3.75 ± 0.17	24.10 ± 0.61	+10.8	+11.8

Table 3—Continued

GRB Name	Spectral Model	F^{p}_{ph}(15-25)	F^{p}_{ph}(25-50)	F^{p}_{ph}(50-100)	F^{p}_{ph}(100-150)	F^{p}_{ph}(15-150)	Start (s)	Stop (s)
				(photons cm^{-2} s^{-1})				
070509	PL	0.25 ± 0.03	0.23 ± 0.02	0.14 ± 0.02	0.06 ± 0.01	0.68 ± 0.12	−0.3	+0.7
070517	PL	0.42 ± 0.11	0.32 ± 0.03	0.16 ± 0.02	0.05 ± 0.01	0.95 ± 0.17	+1.4	+2.4
070518	PL	0.33 ± 0.04	0.22 ± 0.02	0.09 ± 0.02	0.03 ± 0.01	0.68 ± 0.13	+0.1	+1.1
070520A	PL	0.18 ± 0.05	0.15 ± 0.03	0.08 ± 0.04	0.03 ± 0.01	0.44 ± 0.15	+35.8	+36.8
070520B	PL	0.07 ± 0.02	0.12 ± 0.03	0.14 ± 0.02	0.10 ± 0.02	0.43 ± 0.14	+0.7	+1.7
070521	CPL	1.35 ± 0.16	2.08 ± 0.11	2.09 ± 0.11	1.01 ± 0.05	6.53 ± 0.27	+30.5	+31.5
070529	PL	0.39 ± 0.17	0.46 ± 0.13	0.39 ± 0.10	0.20 ± 0.04	1.43 ± 0.36	+2.0	+3.0
070531	PL	0.22 ± 0.05	0.30 ± 0.04	0.30 ± 0.03	0.18 ± 0.03	1.00 ± 0.22	+1.1	+2.1
070611	PL	0.33 ± 0.01	0.28 ± 0.07	0.16 ± 0.05	0.06 ± 0.03	0.82 ± 0.21	+2.8	+3.8
070612A	PL	0.42 ± 0.19	0.48 ± 0.14	0.40 ± 0.05	0.20 ± 0.04	1.51 ± 0.38	+10.4	+11.4
070612B	CPL	0.49 ± 0.22	0.93 ± 0.17	0.83 ± 0.14	0.22 ± 0.12	2.47 ± 0.39	−0.2	+0.8
070616	PL	0.53 ± 0.04	0.62 ± 0.03	0.52 ± 0.02	0.27 ± 0.02	1.93 ± 0.14	+139.7	+140.7

[†]The signal-to-noise ratio of the peak spectrum is too low to perform a spectral fit.

Table 4. BAT GRB 1-s peak energy flux

GRB Name	Spectral Model	F^{p}_{enc}(15-25)	F^{p}_{enc}(25-50)	F^{p}_{ene}(50-100)	F^{p}_{enc}(100-150)	F^{p}_{ene}(15-150)	Start (s)	Stop (s)
				(10^{-8} ergs cm^{-2} s^{-1})				
041217	PL	6.5 ± 0.8	12.8 ± 1.0	19.4 ± 1.7	15.7 ± 2.1	54.4 ± 4.2	+3.3	+4.3
041219A	-	-	-	-	-	-	-	-
041219B	-	-	-	-	-	-	-	-
041219C	PL	2.9 ± 0.5	4.6 ± 0.5	5.4 ± 0.7	3.6 ± 0.7	16.6 ± 1.8	+1.5	+2.5
041220	PL	1.6 ± 0.2	3.3 ± 0.3	5.4 ± 0.5	4.6 ± 0.7	15.0 ± 1.3	−0.0	+1.0
041223	PL	4.6 ± 0.4	12.3 ± 0.7	26.9 ± 1.2	28.8 ± 2.1	72.6 ± 3.3	+35.0	+36.0
041224	PL	2.5 ± 0.5	5.4 ± 0.6	9.1 ± 1.0	8.0 ± 1.4	25.0 ± 2.6	−0.1	+0.9
041226	PL	0.3 ± 0.1	0.6 ± 0.2	1.1 ± 0.4	1.1 ± 0.5	3.1 ± 0.9	+3.3	+4.2
041228	PL	1.9 ± 0.5	3.0 ± 0.5	3.8 ± 0.8	2.6 ± 0.8	11.2 ± 1.8	+22.0	+23.0
050117	PL	1.6 ± 0.2	4.1 ± 0.4	8.2 ± 0.6	8.3 ± 1.0	22.2 ± 1.7	+87.2	+88.2
050124	CPL	3.9 ± 0.7	11.6 ± 0.9	19.2 ± 1.6	10.1 ± 2.1	44.8 ± 3.3	−0.2	+0.8
050126	PL	0.6 ± 0.3	1.3 ± 0.3	2.1 ± 0.6	1.8 ± 0.8	5.8 ± 1.5	+4.1	+5.1
050128	CPL	5.3 ± 1.5	15.0 ± 1.6	26.1 ± 3.2	16.7 ± 3.7	63.0 ± 5.9	+5.6	+6.6
050202	PL	0.6 ± 0.3	1.0 ± 0.3	1.3 ± 0.5	0.9 ± 0.6	3.9 ± 1.3	−0.5	+0.5
050215A	PL	0.3 ± 0.2	0.8 ± 0.3	1.8 ± 0.5	1.9 ± 0.7	4.9 ± 1.2	+5.6	+6.6
050215B	PL	0.7 ± 0.2	1.2 ± 0.2	1.8 ± 0.4	1.3 ± 0.5	5.0 ± 1.1	−0.8	+0.2
050219A	PL	2.8 ± 0.5	6.4 ± 0.7	11.3 ± 1.2	10.3 ± 1.6	30.8 ± 3.1	+9.5	+10.5
050219B	CPL	23.2 ± 3.3	51.1 ± 3.4	69.8 ± 5.3	39.7 ± 5.8	184.0 ± 10.5	+2.9	+3.8
050223	PL	0.9 ± 0.3	1.3 ± 0.3	1.5 ± 0.6	0.9 ± 0.6	4.6 ± 1.3	+1.6	+2.5
050306	PL	3.2 ± 0.8	6.6 ± 1.0	10.6 ± 1.5	9.0 ± 1.9	29.4 ± 3.8	+107.9	+108.9
050315	PL	2.8 ± 0.4	3.5 ± 0.4	3.1 ± 0.6	1.7 ± 0.5	11.1 ± 1.4	+24.6	+25.6
050318	CPL	3.3 ± 0.4	6.7 ± 0.5	8.2 ± 0.7	3.9 ± 1.1	22.0 ± 1.7	+28.6	+29.6
050319	PL	2.2 ± 0.4	2.8 ± 0.4	2.6 ± 0.6	1.4 ± 0.5	9.0 ± 1.4	+0.4	+1.4
050326	PL	8.1 ± 0.6	21.1 ± 0.8	43.3 ± 1.4	44.2 ± 2.3	117.0 ± 3.8	−0.1	+0.9
050401	CPL	6.6 ± 1.7	21.4 ± 2.2	40.7 ± 4.2	26.6 ± 5.0	95.4 ± 7.7	+24.3	+25.3
050406	PL	0.6 ± 0.2	0.6 ± 0.2	0.4 ± 0.3	0.18 ± 0.17	1.8 ± 0.7	+1.2	+2.2
050410	PL	1.9 ± 0.6	3.4 ± 0.7	4.7 ± 1.2	3.6 ± 1.4	13.6 ± 2.8	+3.6	+4.6
050412	PL	0.2 ± 0.1	0.7 ± 0.2	1.9 ± 0.4	2.2 ± 0.7	5.1 ± 1.0	+1.2	+2.2
050416A	PL	8.9 ± 1.1	7.6 ± 0.8	4.5 ± 0.9	1.7 ± 0.5	22.6 ± 2.4	−0.1	+0.9
050416B	PL	4.3 ± 0.9	10.4 ± 1.3	20.2 ± 2.0	19.8 ± 2.9	54.7 ± 5.3	+0.1	+1.1
050418	PL	2.9 ± 0.4	6.6 ± 0.6	12.1 ± 1.0	11.3 ± 1.4	32.8 ± 2.5	+0.7	+1.7
050421	PL	0.24 ± 0.20	0.5 ± 0.3	0.8 ± 0.4	0.7 ± 0.6	2.2 ± 1.1	−0.1	+0.9
050422	PL	0.6 ± 0.2	1.1 ± 0.2	1.4 ± 0.4	1.0 ± 0.4	4.1 ± 0.9	+53.2	+54.2
050502B	CPL	1.1 ± 0.2	3.1 ± 0.3	4.6 ± 0.5	2.2 ± 0.9	11.1 ± 1.2	+0.2	+1.2
050505	PL	1.4 ± 0.4	3.3 ± 0.7	6.1 ± 0.9	5.7 ± 1.3	16.6 ± 2.5	+1.0	+2.0
050507	PL	0.24 ± 0.19	0.5 ± 0.3	0.9 ± 0.4	0.8 ± 0.6	2.5 ± 1.1	+4.5	+5.5
050509A	PL	1.3 ± 0.2	1.6 ± 0.2	1.5 ± 0.4	0.8 ± 0.3	5.2 ± 0.9	+0.7	+1.7
050509B	PL	0.3 ± 0.2	0.5 ± 0.2	0.8 ± 0.4	0.6 ± 0.4	2.2 ± 0.9	+0.0	+1.0
050525A	CPL	32.5 ± 2.0	83.8 ± 1.9	138.0 ± 3.0	90.2 ± 3.7	345.0 ± 6.0	+0.8	+1.8
050528	PL	1.3 ± 0.5	2.2 ± 0.6	3.0 ± 0.9	2.2 ± 1.0	8.7 ± 2.2	+3.4	+4.4
050603	CPL	10.3 ± 1.6	38.4 ± 2.5	91.3 ± 5.9	75.5 ± 8.7	216.0 ± 11.6	−0.2	+0.8
050607	PL	0.9 ± 0.2	1.8 ± 0.3	2.7 ± 0.5	2.2 ± 0.6	7.6 ± 1.2	+0.9	+1.9
050701	PL	2.5 ± 0.3	5.1 ± 0.4	8.1 ± 0.7	6.8 ± 0.9	22.4 ± 1.6	+7.4	+8.4
050712	PL	0.7 ± 0.3	1.0 ± 0.3	1.1 ± 0.6	0.6 ± 0.5	3.4 ± 1.3	+17.4	+18.4
050713A	PL	4.0 ± 0.5	8.6 ± 0.7	14.3 ± 1.2	12.4 ± 1.6	39.3 ± 2.9	+1.1	+2.0

Table 4—Continued

GRB Name	Spectral Model	F^{p}_{cnc}(15-25)	F^{p}_{cnc}(25-50)	F^{p}_{cnc}(50-100)	F^{p}_{cnc}(100-150)	F^{p}_{cnc}(15-150)	Start (s)	Stop (s)
				(10^{-8} ergs cm^{-2} s^{-1})				
050713B	PL	1.5 ± 0.8	2.9 ± 1.0	4.7 ± 1.6	3.9 ± 1.9	12.9 ± 3.9	+8.7	+9.7
050714B	PL	0.7 ± 0.4	1.0 ± 0.4	0.9 ± 0.7	< 1.23	3.1 ± 1.6	+55.2	+56.2
050715	PL	1.2 ± 0.2	2.0 ± 0.3	2.5 ± 0.5	1.7 ± 0.5	7.4 ± 1.2	+40.4	+41.4
050716	PL	2.1 ± 0.6	4.1 ± 0.7	6.0 ± 1.1	4.8 ± 1.3	17.0 ± 2.8	+12.2	+13.2
050717	PL	4.6 ± 0.5	11.0 ± 0.7	21.0 ± 1.1	20.2 ± 1.7	56.8 ± 2.9	+2.8	+3.8
050721	CPL	1.8 ± 0.9	5.9 ± 1.2	6.9 ± 1.8	1.40 ± 1.38	15.8 ± 3.3	+3.7	+4.7
050724	PL	3.7 ± 0.6	6.2 ± 0.6	7.8 ± 1.0	5.5 ± 1.1	23.2 ± 2.3	+0.0	+1.0
050726	PL	1.0 ± 0.5	2.4 ± 0.8	4.8 ± 1.1	4.7 ± 1.6	12.9 ± 3.1	+1.1	+2.0
050730	PL	0.5 ± 0.2	1.0 ± 0.3	1.7 ± 0.5	1.5 ± 0.7	4.6 ± 1.2	+5.0	+6.0
050801	PL	1.4 ± 0.2	2.7 ± 0.3	4.2 ± 0.5	3.5 ± 0.6	11.8 ± 1.2	+0.1	+1.1
050802	PL	2.5 ± 0.7	5.1 ± 0.9	8.0 ± 1.4	6.6 ± 1.7	22.2 ± 3.5	+0.0	+1.0
050803	PL	0.8 ± 0.2	1.8 ± 0.2	3.0 ± 0.4	2.6 ± 0.6	8.2 ± 1.1	+147.1	+148.1
050813	PL	0.8 ± 0.3	1.7 ± 0.4	2.9 ± 0.8	2.5 ± 1.0	7.9 ± 2.0	+0.0	+0.6
050814	PL	0.6 ± 0.4	1.3 ± 0.5	2.2 ± 0.8	2.0 ± 1.0	6.1 ± 2.1	+8.7	+9.7
050815	PL	0.6 ± 0.2	1.0 ± 0.2	1.3 ± 0.4	1.0 ± 0.4	4.0 ± 1.0	−0.1	+0.9
050819	PL	0.5 ± 0.2	0.7 ± 0.2	0.8 ± 0.6	0.5 ± 0.4	2.5 ± 1.0	+9.5	+10.5
050820A	PL	1.8 ± 0.3	4.3 ± 0.4	8.4 ± 1.0	8.2 ± 1.5	22.6 ± 2.6	+229.5	+230.5
050820B	CPL	2.4 ± 0.3	7.5 ± 0.4	15.3 ± 0.9	11.5 ± 1.3	36.6 ± 1.8	+8.6	+9.6
050822	PL	3.1 ± 0.4	4.2 ± 0.4	4.1 ± 0.7	2.4 ± 0.6	13.7 ± 1.6	+47.6	+48.6
050824	PL	0.6 ± 0.3	0.9 ± 0.3	1.0 ± 0.5	0.6 ± 0.5	3.2 ± 1.2	+53.1	+54.1
050826	PL	0.4 ± 0.2	0.7 ± 0.2	0.9 ± 0.7	0.6 ± 0.5	2.7 ± 1.1	+1.4	+2.4
050827	PL	1.4 ± 0.3	3.3 ± 0.4	6.1 ± 0.7	5.8 ± 1.0	16.5 ± 1.8	+0.3	+1.3
050904	PL	0.5 ± 0.2	1.1 ± 0.4	2.1 ± 0.6	1.9 ± 0.9	5.6 ± 1.6	+27.4	+28.4
050906[†]	-	-	-	-	-	-	-	-
050908	PL	0.7 ± 0.2	1.3 ± 0.3	1.9 ± 0.5	1.4 ± 0.5	5.3 ± 1.1	+1.7	+2.7
050911	PL	1.8 ± 0.4	2.5 ± 0.4	2.6 ± 0.7	1.6 ± 0.6	8.3 ± 1.6	−0.1	+0.9
050915A	PL	0.5 ± 0.2	1.3 ± 0.3	2.8 ± 0.5	2.9 ± 0.8	7.4 ± 1.3	+13.7	+14.7
050915B	PL	2.5 ± 0.4	4.4 ± 0.4	5.7 ± 0.7	4.2 ± 0.8	16.8 ± 1.6	−3.1	−2.1
050916	PL	0.7 ± 0.4	1.2 ± 0.4	1.7 ± 0.7	1.3 ± 0.8	5.0 ± 1.8	+43.7	+44.7
050922B	PL	0.9 ± 0.6	1.9 ± 0.7	2.9 ± 1.1	2.4 ± 1.4	8.2 ± 2.8	+98.6	+99.6
050922C	PL	6.5 ± 0.5	13.4 ± 0.6	21.6 ± 1.1	18.4 ± 1.4	59.9 ± 2.7	−0.1	+0.9
050925	CPL	8.4 ± 2.5	24.1 ± 3.1	30.0 ± 5.0	9.3 ± 3.7	71.7 ± 8.5	+0.1	+0.2
051001	PL	0.5 ± 0.2	0.9 ± 0.2	1.3 ± 0.4	0.9 ± 0.4	3.7 ± 0.9	+130.4	+131.4
051006	PL	1.1 ± 0.4	2.8 ± 0.6	5.8 ± 1.0	5.9 ± 1.6	15.6 ± 2.7	+2.6	+3.6
051008	PL	4.0 ± 0.5	9.6 ± 0.7	18.6 ± 1.4	18.2 ± 1.9	50.2 ± 3.1	+2.9	+3.9
051012	PL	0.5 ± 0.2	1.0 ± 0.3	1.4 ± 0.5	1.1 ± 0.6	4.1 ± 1.1	+4.5	+5.5
051016	PL	1.4 ± 0.7	2.6 ± 0.8	3.6 ± 1.2	2.7 ± 1.4	10.4 ± 2.8	+4.9	+5.9
051016B	PL	1.7 ± 0.3	2.4 ± 0.3	2.5 ± 0.5	1.5 ± 0.5	8.2 ± 1.2	+0.1	+1.1
051021B	PL	0.8 ± 0.2	1.5 ± 0.3	2.2 ± 0.5	1.8 ± 0.7	6.3 ± 1.3	−0.7	+0.3
051105	PL	0.20 ± 0.16	0.5 ± 0.3	1.1 ± 0.4	1.2 ± 0.7	3.1 ± 1.1	−0.4	+0.6
051109A	PL	4.0 ± 1.1	7.4 ± 1.4	10.6 ± 1.9	8.2 ± 2.2	30.2 ± 4.9	+0.7	+1.6
051109B	PL	0.7 ± 0.2	1.0 ± 0.3	1.0 ± 0.5	0.6 ± 0.4	3.4 ± 1.1	+0.1	+1.0
051111	PL	2.1 ± 0.3	4.8 ± 0.4	8.7 ± 0.8	8.0 ± 1.1	23.6 ± 2.0	−0.3	+0.7
051113	PL	2.4 ± 0.6	4.2 ± 0.6	5.8 ± 1.1	4.3 ± 1.2	16.7 ± 2.5	+0.3	+1.3
051114	PL	0.5 ± 0.2	1.2 ± 0.3	2.5 ± 0.6	2.7 ± 1.0	6.8 ± 1.6	+0.3	+1.3

Table 4—Continued

GRB Name	Spectral Model	F^{p}_{cne}(15-25)	F^{p}_{cne}(25-50)	F^{p}_{cne}(50-100)	F^{p}_{cne}(100-150)	F^{p}_{cne}(15-150)	Start (s)	Stop (s)
				(10^{-8} ergs cm^{-2} s^{-1})				
051117A	PL	1.4 ± 0.3	1.7 ± 0.3	1.6 ± 0.5	0.9 ± 0.4	5.5 ± 1.2	+2.6	+3.6
051117B	PL	0.5 ± 0.2	0.9 ± 0.3	1.4 ± 0.5	1.1 ± 0.6	3.8 ± 1.2	+1.4	+2.4
051210	PL	0.5 ± 0.2	1.3 ± 0.3	2.7 ± 0.4	2.8 ± 0.7	7.3 ± 1.2	+0.1	+1.1
051213	PL	0.3 ± 0.2	0.8 ± 0.3	1.7 ± 0.5	1.7 ± 0.7	4.5 ± 1.2	+48.9	+49.9
051221A	PL	10.5 ± 0.7	22.1 ± 0.8	36.4 ± 1.2	31.5 ± 1.7	100.0 ± 3.1	+0.2	+1.2
051221B	PL	0.29 ± 0.26	0.9 ± 0.7	2.1 ± 0.6	2.4 ± 1.1	5.7 ± 1.7	+58.9	+59.9
051227	PL	0.7 ± 0.2	1.7 ± 0.3	3.2 ± 0.5	3.2 ± 0.7	8.8 ± 1.2	−0.0	+1.0
060102	PL	0.19 ± 0.16	0.6 ± 0.3	1.5 ± 0.4	1.8 ± 0.8	4.1 ± 1.2	+0.1	+1.1
060105	PL	5.1 ± 0.5	12.9 ± 0.8	26.0 ± 1.3	26.1 ± 2.0	70.1 ± 3.4	+30.8	+31.8
060108	PL	0.9 ± 0.2	1.4 ± 0.2	1.8 ± 0.4	1.2 ± 0.4	5.3 ± 1.0	+0.6	+1.6
060109	PL	0.5 ± 0.2	0.9 ± 0.2	1.2 ± 0.4	0.8 ± 0.4	3.4 ± 1.0	+90.2	+91.2
060110	CPL	1.6 ± 0.3	3.9 ± 0.4	5.9 ± 0.6	3.4 ± 1.0	14.8 ± 1.5	+1.3	+2.3
060111A	CPL	1.5 ± 0.3	3.6 ± 0.4	5.3 ± 0.6	2.8 ± 1.0	13.2 ± 1.4	+4.3	+5.3
060111B	PL	0.9 ± 0.4	2.4 ± 0.6	5.0 ± 0.9	5.2 ± 1.5	13.6 ± 2.5	+0.4	+1.4
060115	PL	0.8 ± 0.2	1.6 ± 0.2	2.6 ± 0.5	2.2 ± 0.6	7.1 ± 1.1	+94.9	+95.9
060116	PL	1.2 ± 0.5	2.1 ± 0.6	2.7 ± 1.0	1.9 ± 1.1	8.0 ± 2.4	+36.1	+37.1
060117	CPL	44.4 ± 3.5	99.0 ± 3.0	138.0 ± 4.5	80.1 ± 5.0	363.0 ± 9.2	+11.1	+12.1
060124	PL	1.0 ± 0.3	1.7 ± 0.3	2.1 ± 0.6	1.5 ± 0.7	6.3 ± 1.5	+0.2	+1.2
060202	PL	0.6 ± 0.5	1.0 ± 0.3	1.3 ± 0.6	0.9 ± 0.7	3.7 ± 1.4	−6.5	−5.5
060203	PL	0.6 ± 0.3	1.1 ± 0.4	1.6 ± 0.6	1.3 ± 0.7	4.6 ± 1.4	+25.9	+26.9
060204B	PL	1.3 ± 0.2	2.5 ± 0.3	3.7 ± 0.6	3.0 ± 0.7	10.5 ± 1.4	+5.0	+6.0
060206	CPL	2.7 ± 0.4	5.9 ± 0.4	7.6 ± 0.6	3.7 ± 0.9	20.0 ± 1.4	+2.1	+3.1
060210	PL	2.2 ± 0.4	4.9 ± 0.6	8.8 ± 0.9	8.1 ± 1.3	23.9 ± 2.4	−0.0	+1.0
060211A	PL	0.4 ± 0.2	0.8 ± 0.2	1.2 ± 0.4	0.9 ± 0.5	3.3 ± 1.1	+145.6	+146.6
060211B	PL	0.7 ± 0.2	1.4 ± 0.2	2.1 ± 0.5	1.6 ± 0.6	5.8 ± 1.1	+1.8	+2.8
060218	PL	0.4 ± 0.2	0.4 ± 0.3	< 0.6	< 0.4	1.2 ± 0.7	+275.0	+276.0
060219	PL	1.0 ± 0.4	0.9 ± 0.4	0.5 ± 0.4	< 0.6	2.6 ± 1.0	+4.1	+5.1
060223A	PL	1.4 ± 0.3	2.5 ± 0.3	3.4 ± 0.6	2.5 ± 0.7	9.9 ± 1.4	+0.1	+1.1
060223B	PL	1.9 ± 0.3	5.0 ± 0.4	10.1 ± 0.7	10.2 ± 1.1	27.2 ± 1.9	+3.0	+4.0
060306	CPL	5.4 ± 0.7	12.0 ± 0.8	17.6 ± 1.3	11.3 ± 1.8	46.4 ± 2.8	+0.2	+1.2
060312	PL	1.7 ± 0.2	2.9 ± 0.3	3.9 ± 0.5	2.8 ± 0.6	11.2 ± 1.2	+5.6	+6.6
060313	PL	6.4 ± 0.5	19.1 ± 1.0	47.0 ± 1.8	54.9 ± 3.3	127.0 ± 5.1	+0.1	+1.0
060319	PL	1.6 ± 0.3	2.0 ± 0.3	1.8 ± 0.5	0.9 ± 0.4	6.2 ± 1.0	+4.1	+5.1
060322	PL	2.3 ± 0.4	3.9 ± 0.4	5.1 ± 0.6	3.7 ± 0.7	15.1 ± 1.5	+182.2	+183.2
060323	PL	1.2 ± 0.3	1.4 ± 0.3	1.2 ± 0.5	0.6 ± 0.4	4.4 ± 1.2	+2.5	+3.5
060403	PL	0.6 ± 0.2	1.6 ± 0.3	3.6 ± 0.5	4.0 ± 0.8	9.6 ± 1.3	+1.8	+2.8
060413	PL	1.2 ± 0.2	1.8 ± 0.2	1.9 ± 0.4	1.2 ± 0.4	6.1 ± 1.0	+90.2	+91.2
060418	PL	6.8 ± 0.6	12.3 ± 0.7	17.1 ± 1.1	13.0 ± 1.4	49.1 ± 2.7	+27.5	+28.5
060421	PL	2.5 ± 0.3	5.4 ± 0.4	9.1 ± 0.6	8.1 ± 0.9	25.1 ± 1.6	+2.3	+3.3
060424	PL	1.9 ± 0.3	3.0 ± 0.4	3.7 ± 0.6	2.5 ± 0.7	11.1 ± 1.5	+0.1	+1.1
060427	PL	0.4 ± 0.3	0.5 ± 0.3	0.5 ± 0.4	< 0.9	1.7 ± 1.1	+5.0	+6.0
060428A	PL	3.2 ± 0.4	4.2 ± 0.4	4.0 ± 0.6	2.3 ± 0.5	13.7 ± 1.4	+4.2	+5.2
060428B	PL	1.1 ± 0.3	1.1 ± 0.3	0.8 ± 0.4	0.4 ± 0.3	3.4 ± 1.0	+20.8	+21.8
060501	PL	1.4 ± 0.4	3.5 ± 0.6	6.9 ± 0.9	6.9 ± 1.3	18.6 ± 2.3	+0.4	+1.4
060502A	PL	1.2 ± 0.3	2.9 ± 0.4	5.9 ± 0.7	6.0 ± 1.1	16.0 ± 1.9	−0.1	+0.9

Table 4—Continued

GRB Name	Spectral Model	F^{p}_{cnc}(15-25)	F^{p}_{cnc}(25-50)	F^{p}_{cnc}(50-100)	F^{p}_{cnc}(100-150)	F^{p}_{cnc}(15-150)	Start (s)	Stop (s)
				(10^{-8} ergs cm^{-2} s^{-1})				
060502B	PL	0.4 ± 0.2	1.0 ± 0.3	2.3 ± 0.4	2.6 ± 0.8	6.2 ± 1.2	−0.5	+0.5
060505	PL	2.0 ± 0.9	4.7 ± 1.3	8.8 ± 2.2	8.4 ± 3.3	24.0 ± 5.8	+0.0	+1.0
060507	PL	1.5 ± 0.4	2.4 ± 0.4	2.9 ± 0.7	2.0 ± 0.7	8.8 ± 1.7	+1.2	+2.2
060510A	PL	14.7 ± 2.0	27.5 ± 2.2	40.0 ± 3.7	31.4 ± 4.6	114.0 ± 9.1	+0.3	+1.3
060510B	PL	0.6 ± 0.2	1.1 ± 0.2	1.6 ± 0.4	1.2 ± 0.5	4.4 ± 1.0	+136.2	+137.2
060512	PL	1.6 ± 0.4	1.4 ± 0.4	0.8 ± 0.4	0.3 ± 0.2	4.1 ± 1.2	+3.3	+4.3
060515	PL	0.5 ± 0.3	1.4 ± 0.4	3.0 ± 0.7	3.2 ± 1.1	8.1 ± 1.9	+5.6	+6.6
060516	PL	0.43 ± 0.42	0.6 ± 0.5	< 1.5	< 1.4	2.2 ± 1.7	+128.6	+129.6
060522	PL	0.8 ± 0.3	1.0 ± 0.3	0.9 ± 0.5	0.5 ± 0.4	3.2 ± 1.1	+4.4	+5.4
060526	PL	1.5 ± 0.3	3.1 ± 0.3	4.9 ± 0.6	4.2 ± 0.8	13.7 ± 1.6	+0.1	+1.1
060602A	PL	0.3 ± 0.2	0.9 ± 0.4	2.1 ± 0.6	2.4 ± 1.0	5.7 ± 1.7	+18.0	+19.0
060604	PL	0.4 ± 0.2	0.6 ± 0.2	0.8 ± 0.5	0.51 ± 0.50	2.3 ± 1.1	−32.2	−31.2
060605	PL	0.3 ± 0.1	0.8 ± 0.2	1.7 ± 0.4	1.8 ± 0.7	4.6 ± 1.2	+2.1	+3.1
060607A	PL	1.1 ± 0.2	2.5 ± 0.3	4.6 ± 0.5	4.3 ± 0.7	12.4 ± 1.2	−1.0	+0.0
060607B	PL	1.4 ± 0.4	2.7 ± 0.5	4.0 ± 0.8	3.2 ± 1.0	11.4 ± 2.0	+8.6	+9.6
060614	PL	12.7 ± 1.4	21.7 ± 1.4	28.2 ± 2.2	20.3 ± 2.5	83.0 ± 5.4	−1.3	−0.3
060707	PL	1.1 ± 0.4	1.9 ± 0.4	2.6 ± 0.7	1.9 ± 0.8	7.4 ± 1.7	+2.0	+3.0
060708	PL	1.8 ± 0.2	3.6 ± 0.3	5.6 ± 0.5	4.6 ± 0.6	15.6 ± 1.2	+1.1	+2.1
060712	PL	2.5 ± 1.3	2.9 ± 1.0	2.3 ± 1.8	1.2 ± 1.0	8.9 ± 3.4	+16.8	+17.7
060714	PL	1.3 ± 0.2	2.4 ± 0.2	3.4 ± 0.4	2.6 ± 0.5	9.7 ± 1.1	+75.4	+76.4
060717	PL	0.7 ± 0.2	1.0 ± 0.2	1.1 ± 0.4	0.7 ± 0.3	3.4 ± 0.9	+0.8	+1.8
060719	CPL	2.4 ± 0.4	4.8 ± 0.5	4.8 ± 0.7	1.6 ± 0.8	13.6 ± 1.5	+0.4	+1.4
060728[†]	-	-	-	-	-	-	-	-
060729	PL	1.5 ± 0.2	2.2 ± 0.2	2.4 ± 0.4	1.5 ± 0.4	7.5 ± 1.0	+92.0	+93.0
060801	PL	0.5 ± 0.2	1.8 ± 0.4	5.3 ± 0.6	6.9 ± 1.2	14.5 ± 1.9	+0.0	+0.6
060804	PL	1.0 ± 0.5	2.1 ± 0.6	3.3 ± 0.9	2.8 ± 1.3	9.3 ± 2.3	+4.5	+5.5
060805	PL	0.4 ± 0.2	0.6 ± 0.2	0.7 ± 0.4	0.4 ± 0.3	2.2 ± 0.9	+0.7	+1.7
060807	PL	0.7 ± 0.2	1.5 ± 0.3	2.6 ± 0.6	2.2 ± 0.8	7.0 ± 1.5	−0.1	+0.9
060813	PL	7.0 ± 0.6	15.9 ± 0.8	28.6 ± 1.3	26.4 ± 1.9	78.0 ± 3.4	+3.6	+4.6
060814	PL	6.5 ± 0.5	13.4 ± 0.6	21.7 ± 1.0	18.4 ± 1.3	60.0 ± 2.4	+15.4	+16.4
060825	CPL	2.2 ± 0.3	5.6 ± 0.4	8.3 ± 0.7	4.5 ± 1.1	20.7 ± 1.6	+0.1	+1.1
060904A	PL	3.9 ± 0.3	8.8 ± 0.4	15.8 ± 0.7	14.6 ± 1.1	43.0 ± 1.8	+55.3	+56.3
060904B	PL	2.0 ± 0.3	4.4 ± 0.4	7.7 ± 0.8	6.9 ± 1.1	21.1 ± 1.9	+1.2	+2.2
060906	PL	2.8 ± 0.5	3.6 ± 0.5	3.4 ± 0.8	1.9 ± 0.7	11.8 ± 1.9	−24.9	−23.9
060908	CPL	1.8 ± 0.4	5.9 ± 0.6	11.7 ± 1.2	8.2 ± 1.8	27.7 ± 2.4	+1.0	+2.0
060912	PL	9.8 ± 0.8	16.2 ± 0.8	20.2 ± 1.3	14.0 ± 1.4	60.2 ± 3.2	+0.0	+1.0
060919	CPL	1.4 ± 0.5	4.6 ± 0.7	7.9 ± 1.2	4.0 ± 1.6	17.8 ± 2.5	−0.5	+0.5
060923A	PL	1.3 ± 0.4	2.5 ± 0.5	3.6 ± 0.9	2.9 ± 1.1	10.3 ± 2.1	+0.0	+1.0
060923B	PL	2.6 ± 0.7	2.5 ± 0.6	1.8 ± 0.8	0.8 ± 0.5	7.6 ± 1.9	+4.9	+5.9
060923C	PL	1.5 ± 0.7	1.7 ± 0.7	1.4 ± 1.0	< 1.6	5.2 ± 2.5	+27.6	+28.5
060926	PL	1.8 ± 0.3	1.9 ± 0.3	1.4 ± 0.4	0.7 ± 0.3	5.8 ± 0.9	+0.4	+1.4
060927	CPL	1.8 ± 0.3	5.2 ± 0.4	10.0 ± 0.8	7.4 ± 1.3	24.3 ± 1.7	+0.2	+1.2
060929	PL	0.4 ± 0.2	0.8 ± 0.3	1.2 ± 0.5	1.1 ± 0.6	3.5 ± 1.2	+2.5	+3.5
061002	PL	0.9 ± 0.5	1.5 ± 0.5	1.9 ± 0.8	1.4 ± 0.8	5.8 ± 1.8	−1.4	−0.4
061004	PL	2.8 ± 0.3	4.8 ± 0.3	6.2 ± 0.5	4.5 ± 0.6	18.3 ± 1.3	+2.7	+3.7

Table 4—Continued

GRB Name	Spectral Model	F^{p}_{cnc}(15-25)	F^{p}_{cnc}(25-50)	F^{p}_{cnc}(50-100)	F^{p}_{cnc}(100-150)	F^{p}_{cnc}(15-150)	Start (s)	Stop (s)
				(10^{-8} ergs cm^{-2} s^{-1})				
061006	PL	3.3 ± 0.3	8.8 ± 0.5	19.2 ± 0.8	20.4 ± 1.4	51.6 ± 2.2	−23.2	−22.2
061007	PL	7.7 ± 0.5	23.1 ± 0.8	56.9 ± 1.5	66.7 ± 2.8	154.0 ± 4.2	+45.1	+46.1
061019	PL	2.6 ± 0.8	4.0 ± 0.8	4.5 ± 1.4	2.9 ± 1.3	14.0 ± 3.2	+2.6	+3.5
061021	PL	4.9 ± 0.4	11.0 ± 0.6	19.7 ± 1.0	18.0 ± 1.5	53.6 ± 2.5	+2.4	+3.4
061027[†]	-	-	-	-	-	-	-	-
061028	PL	0.5 ± 0.3	1.2 ± 0.4	2.1 ± 0.6	2.0 ± 0.9	5.8 ± 1.7	+79.9	+80.9
061102	PL	< 0.13	0.4 ± 0.2	0.9 ± 0.4	1.0 ± 0.6	2.4 ± 1.0	+3.4	+4.4
061110A	PL	0.6 ± 0.2	1.0 ± 0.2	1.3 ± 0.5	0.9 ± 0.5	3.8 ± 1.1	+9.7	+10.7
061110B	PL	0.3 ± 0.2	0.8 ± 0.2	1.6 ± 0.4	1.6 ± 0.7	4.2 ± 1.1	+3.3	+4.3
061121	PL	15.4 ± 0.7	37.3 ± 1.0	71.6 ± 1.5	69.4 ± 2.5	194.0 ± 4.0	+74.5	+75.5
061126	PL	6.3 ± 0.5	16.5 ± 0.8	35.2 ± 1.4	36.9 ± 2.4	94.9 ± 3.8	+6.7	+7.7
061201	PL	2.2 ± 0.4	6.3 ± 0.7	14.5 ± 1.2	16.1 ± 2.0	39.2 ± 3.2	+0.0	+0.9
061202	PL	2.3 ± 0.3	4.7 ± 0.3	7.3 ± 0.6	6.0 ± 0.8	20.3 ± 1.4	+75.0	+76.0
061210	PL	3.0 ± 0.6	8.7 ± 1.0	20.1 ± 1.8	22.4 ± 3.0	54.1 ± 4.8	+0.2	+0.8
061217	PL	0.9 ± 0.3	2.5 ± 0.5	5.5 ± 0.9	6.0 ± 1.6	14.9 ± 2.6	+0.0	+0.3
061218	PL	0.5 ± 0.2	0.4 ± 0.3	< 0.6	< 0.4	1.2 ± 0.7	+1.5	+2.5
061222A	CPL	5.2 ± 0.5	15.1 ± 0.6	32.2 ± 1.2	30.0 ± 1.9	82.4 ± 2.6	+86.5	+87.5
061222B	PL	2.5 ± 0.7	2.8 ± 0.7	2.3 ± 1.0	1.1 ± 0.7	8.7 ± 2.4	+59.2	+60.1
070103	CPL	1.2 ± 0.3	2.6 ± 0.4	2.0 ± 0.7	< 1.1	6.1 ± 1.2	−0.1	+0.9
070107	PL	1.4 ± 0.3	3.4 ± 0.5	6.9 ± 0.8	6.9 ± 1.0	18.6 ± 2.1	−7.2	−6.2
070110	PL	0.7 ± 0.2	1.1 ± 0.2	1.4 ± 0.4	1.0 ± 0.5	4.2 ± 1.0	−0.2	+0.8
070126[†]	-	-	-	-	-	-	-	-
070129	PL	0.7 ± 0.2	1.0 ± 0.2	1.1 ± 0.4	0.7 ± 0.4	3.5 ± 1.0	+310.6	+311.6
070208	PL	1.2 ± 0.5	1.7 ± 0.4	1.8 ± 0.8	1.1 ± 0.9	5.7 ± 1.7	−0.3	+0.7
070209	PL	0.3 ± 0.2	0.7 ± 0.3	1.2 ± 0.4	1.1 ± 0.6	3.3 ± 1.1	−0.4	+0.6
070219	PL	0.9 ± 0.2	1.2 ± 0.2	1.3 ± 0.4	0.8 ± 0.4	4.3 ± 1.0	+1.3	+2.3
070220	PL	4.8 ± 0.5	10.7 ± 0.6	18.7 ± 1.0	16.8 ± 1.4	51.0 ± 2.5	+11.9	+12.9
070223	PL	0.7 ± 0.2	1.3 ± 0.3	1.9 ± 0.6	1.5 ± 0.7	5.4 ± 1.3	+34.3	+35.3
070224	PL	0.4 ± 0.2	0.6 ± 0.2	0.7 ± 0.6	0.5 ± 0.4	2.2 ± 1.0	−13.8	−12.8
070227	PL	5.7 ± 2.2	8.7 ± 2.4	10.0 ± 3.3	6.6 ± 3.1	30.9 ± 8.5	+1.0	+2.0
070306	PL	4.3 ± 0.4	7.7 ± 0.4	10.4 ± 0.7	7.7 ± 0.8	30.1 ± 1.7	+98.3	+99.3
070318	PL	1.6 ± 0.2	3.3 ± 0.3	5.1 ± 0.6	4.2 ± 0.8	14.2 ± 1.4	+1.9	+2.9
070328	PL	3.2 ± 0.4	7.5 ± 0.5	14.0 ± 0.8	13.3 ± 1.3	38.0 ± 2.2	+0.8	+1.8
070330	PL	1.1 ± 0.3	1.6 ± 0.3	1.8 ± 0.5	1.2 ± 0.4	5.7 ± 1.1	−0.1	+0.9
070406	PL	0.4 ± 0.3	0.7 ± 0.2	1.1 ± 0.4	0.9 ± 0.5	3.0 ± 1.0	−0.1	+0.9
070411	PL	0.9 ± 0.2	1.7 ± 0.2	2.4 ± 0.5	1.9 ± 0.6	6.9 ± 1.1	+70.2	+71.2
070412	PL	0.6 ± 0.2	1.2 ± 0.2	1.9 ± 0.5	1.6 ± 0.6	5.4 ± 1.2	+5.3	+6.3
070419A[†]	PL	-	-	-	-	1.9 ± 1.0	−1.1	−0.1
070419B	PL	1.2 ± 0.3	2.6 ± 0.3	4.1 ± 0.6	3.4 ± 0.8	11.3 ± 1.5	−0.3	+0.7
070420	PL	7.3 ± 1.2	13.4 ± 1.5	18.9 ± 2.3	14.5 ± 2.6	54.1 ± 5.8	+1.4	+2.4
070427	PL	1.8 ± 0.3	2.5 ± 0.2	2.5 ± 0.4	1.5 ± 0.4	8.3 ± 1.0	+6.8	+7.8
070429A	PL	0.4 ± 0.3	0.8 ± 0.3	1.1 ± 0.5	0.8 ± 0.6	3.1 ± 1.2	+4.0	+5.0
070429B	PL	2.1 ± 0.4	3.3 ± 0.4	4.0 ± 0.8	2.8 ± 0.8	12.2 ± 1.9	−0.2	+0.3
070506	CPL	1.0 ± 0.2	2.4 ± 0.4	2.1 ± 0.6	< 1.1	5.9 ± 1.1	+6.2	+7.2
070508	CPL	16.1 ± 1.2	44.4 ± 1.3	87.1 ± 2.6	73.7 ± 3.5	221.0 ± 5.1	+10.8	+11.8

Table 4—Continued

GRB Name	Spectral Model	F^{p}_{cnc}(15-25)	F^{p}_{cnc}(25-50)	F^{p}_{cnc}(50-100)	F^{p}_{cnc}(100-150)	F^{p}_{cne}(15-150)	Start (s)	Stop (s)
				(10^{-8} ergs cm^{-2} s^{-1})				
070509	PL	0.8 ± 0.2	1.3 ± 0.2	1.6 ± 0.4	1.2 ± 0.4	4.8 ± 1.0	−0.3	+0.7
070517	PL	1.3 ± 0.3	1.8 ± 0.3	1.8 ± 0.5	1.1 ± 0.5	5.9 ± 1.2	+1.4	+2.4
070518	PL	1.0 ± 0.3	1.2 ± 0.3	1.0 ± 0.4	0.5 ± 0.3	3.8 ± 1.0	+0.1	+1.1
070520A	PL	0.6 ± 0.3	0.8 ± 0.3	0.9 ± 0.7	0.6 ± 0.5	2.9 ± 1.2	+35.8	+36.8
070520B	PL	0.23 ± 0.16	0.7 ± 0.3	1.7 ± 0.5	1.9 ± 0.8	4.5 ± 1.4	+0.7	+1.7
070521	CPL	4.3 ± 0.5	12.1 ± 0.6	24.0 ± 1.2	19.8 ± 1.9	60.2 ± 2.6	+30.5	+31.5
070529	PL	1.2 ± 0.5	2.6 ± 0.7	4.4 ± 1.2	3.9 ± 1.6	12.1 ± 3.1	+2.0	+3.0
070531	PL	0.7 ± 0.3	1.7 ± 0.5	3.5 ± 0.7	3.6 ± 1.2	9.5 ± 1.9	+1.1	+2.1
070611	PL	1.0 ± 0.4	1.5 ± 0.4	1.8 ± 0.7	1.1 ± 0.6	5.4 ± 1.5	+2.8	+3.7
070612A	PL	1.3 ± 0.6	2.8 ± 0.8	4.6 ± 1.1	4.0 ± 1.5	12.7 ± 3.0	+10.4	+11.4
070612B	CPL	1.6 ± 0.7	5.4 ± 1.0	9.3 ± 1.7	4.3 ± 2.4	20.7 ± 3.6	−0.2	+0.8
070616	PL	1.6 ± 0.2	3.5 ± 0.3	5.9 ± 0.5	5.2 ± 0.8	16.3 ± 1.4	+139.7	+140.7

[†]The signal-to-noise ratio of the peak spectrum is too low to perform a spectral fit.

Table 5. BAT time-averaged spectral parameters

GRB	$\alpha^{\rm PL}$	$K_{50}^{\rm PL}$	χ^2	$\alpha^{\rm CPL}$	$E_{\rm peak}^{\rm obs}$	$K_{50}^{\rm CPL}$	χ^2
041217	-1.46 ± 0.07	407.0 ± 15.2	74.9	-0.7 ± 0.3	95^{+27}_{-14}	907^{+363}_{-243}	54.8
041219A	-	-	-	-	-	-	-
041219B	-	-	-	-	-	-	-
041219C	-2.02 ± 0.10	70.9 ± 4.1	53.4	-	-	-	-
041220	-1.66 ± 0.12	58.8 ± 4.0	28.9	-	-	-	-
041223	-1.11 ± 0.03	103.0 ± 1.9	24.3	-	-	-	-
041224	-1.72 ± 0.06	43.8 ± 1.5	56.1	-1.1 ± 0.3	74^{+16}_{-9}	92^{+34}_{-23}	36.7
041226	-1.40 ± 0.43	3.5 ± 0.8	85.1	-	-	-	-
041228	-1.60 ± 0.08	52.5 ± 2.2	68.3	-	-	-	-
050117	-1.50 ± 0.04	44.9 ± 1.0	38.8	-1.2 ± 0.2	143^{+108}_{-33}	63^{+13}_{-11}	29.6
050124	-1.47 ± 0.08	213.0 ± 10.5	58.7	-0.7 ± 0.4	95^{+39}_{-16}	468^{+234}_{-146}	45.4
050126	-1.34 ± 0.15	29.3 ± 2.5	79.8	-	-	-	-
050128	-1.37 ± 0.07	172.0 ± 7.5	59.3	$-0.7^{+0.4}_{-0.3}$	113^{+46}_{-19}	348^{+141}_{-95}	44.8
050202	-1.44 ± 0.32	246.0 ± 44.9	55.4	-	-	-	-
050215A	-1.46 ± 0.26	7.5 ± 1.0	51.1	-	-	-	-
050215B	-1.99 ± 0.19	26.9 ± 3.5	53.4	-	-	-	-
050219A	-1.31 ± 0.06	123.0 ± 4.3	103.2	-0.1 ± 0.3	92^{+12}_{-8}	410^{+147}_{-102}	45.5
050219B	-1.53 ± 0.05	224.0 ± 6.8	86.6	$-1.0^{+0.3}_{-0.2}$	108^{+35}_{-16}	393^{+108}_{-81}	69.0
050223	-1.85 ± 0.17	24.2 ± 2.5	59.6	-	-	-	-
050306	-1.48 ± 0.07	63.2 ± 2.4	59.9	-	-	-	-
050315	-2.11 ± 0.09	27.6 ± 1.3	52.6	-	-	-	-
050318	-1.90 ± 0.10	41.5 ± 2.3	56.6	-	-	-	-
050319	-2.02 ± 0.19	8.7 ± 1.0	45.5	-	-	-	-
050326	-1.25 ± 0.04	216.0 ± 3.9	42.1	-	-	-	-
050401	-1.40 ± 0.07	231.0 ± 8.8	37.1	-	-	-	-
050406	-2.43 ± 0.35	12.6 ± 3.6	82.7	-	-	-	-
050410	-1.65 ± 0.08	94.1 ± 4.3	78.5	-0.8 ± 0.4	74^{+19}_{-9}	240^{+129}_{-78}	61.3
050412	-0.74 ± 0.17	16.9 ± 1.6	34.4	-	-	-	-
050416A	-3.08 ± 0.22	97.6 ± 17.1	58.8	-	-	-	-
050416B	-1.36 ± 0.13	279.0 ± 21.5	67.4	$-0.4^{+0.7}_{-0.6}$	94^{+66}_{-19}	758^{+796}_{-352}	59.7
050418	-1.71 ± 0.07	59.4 ± 2.0	35.2	-	-	-	-
050421	-1.56 ± 0.43	8.6 ± 2.2	65.5	-	-	-	-
050422	-1.41 ± 0.19	10.0 ± 1.1	55.4	-	-	-	-
050502B	-1.59 ± 0.14	24.9 ± 2.0	54.6	-	-	-	-
050505	-1.41 ± 0.12	41.3 ± 2.9	47.8	-	-	-	-
050507	-1.53 ± 0.29	21.5 ± 3.8	63.6	-	-	-	-
050509A	-2.11 ± 0.18	25.6 ± 2.8	59.1	-	-	-	-
050509B	-1.57 ± 0.38	184.0 ± 46.6	44.0	-	-	-	-
050525A	-1.76 ± 0.00	1340.0 ± 0.0	166.4	-1.0 ± 0.1	82^{+4}_{-3}	2740^{+303}_{-267}	17.9
050528	-2.27 ± 0.26	35.8 ± 6.5	63.2	-	-	-	-
050603	-1.16 ± 0.06	289.0 ± 10.3	71.1	-	-	-	-
050607	-1.92 ± 0.16	21.7 ± 2.1	61.1	-	-	-	-
050701	-1.70 ± 0.09	44.5 ± 2.1	64.4	-	-	-	-
050712	-1.50 ± 0.18	18.8 ± 1.9	61.4	-	-	-	-
050713a	-1.53 ± 0.08	28.4 ± 1.1	70.8	-	-	-	-
050713b	-1.39 ± 0.17	45.3 ± 4.3	68.6	-	-	-	-

Table 5—Continued

GRB	α^{PL}	K_{50}^{PL}	χ^2	α^{CPL}	E_{peak}^{obs}	K_{50}^{CPL}	χ^2
050714b	-2.45 ± 0.30	12.0 ± 2.7	45.3	-	-	-	-
050715	-1.60 ± 0.15	10.3 ± 0.9	56.3	-	-	-	-
050716	-1.37 ± 0.06	72.1 ± 2.5	52.5	-0.8 ± 0.3	123^{+61}_{-24}	127^{+42}_{-30}	39.4
050717	-1.30 ± 0.05	30.5 ± 0.8	48.5	-	-	-	-
050721	-1.90 ± 0.15	26.1 ± 2.3	76.3	-	-	-	-
050724	-1.89 ± 0.22	10.6 ± 1.3	58.2	-	-	-	-
050726	-0.90 ± 0.21	30.2 ± 3.8	70.3	-	-	-	-
050730	-1.53 ± 0.11	14.0 ± 0.8	41.5	-	-	-	-
050801	-1.99 ± 0.25	13.1 ± 2.1	58.9	-	-	-	-
050802	-1.54 ± 0.13	92.2 ± 6.9	52.6	-	-	-	-
050803	-1.38 ± 0.11	21.1 ± 1.2	60.7	-	-	-	-
050813	-1.28 ± 0.37	86.0 ± 20.0	70.5	-	-	-	-
050814	-1.80 ± 0.17	11.2 ± 1.2	66.0	-	-	-	-
050815	-1.81 ± 0.24	32.3 ± 5.5	75.6	$0.9^{+1.9}_{-1.4}$	44^{+9}_{-6}	1300^{+13900}_{-1110}	62.1
050819	-2.71 ± 0.29	6.9 ± 1.6	57.1	-	-	-	-
050820A	-1.25 ± 0.12	12.8 ± 0.8	59.4	-	-	-	-
050820B	-1.34 ± 0.04	144.0 ± 3.5	89.6	-0.6 ± 0.2	111^{+21}_{-13}	298^{+69}_{-54}	48.7
050822	-2.37 ± 0.14	18.9 ± 1.7	57.4	-	-	-	-
050824	-2.76 ± 0.38	9.2 ± 2.8	49.9	-	-	-	-
050826	-1.16 ± 0.31	10.2 ± 1.6	58.7	-	-	-	-
050827	-1.38 ± 0.10	32.2 ± 1.7	40.2	-	-	-	-
050904	-1.25 ± 0.07	24.1 ± 0.9	50.6	-	-	-	-
050906	-2.46 ± 0.43	44.9 ± 17.1	61.0	-	-	-	-
050908	-1.88 ± 0.17	22.5 ± 2.4	55.1	-	-	-	-
050911	-1.84 ± 0.28	20.3 ± 3.7	44.8	-	-	-	-
050915A	-1.39 ± 0.17	13.2 ± 1.2	65.4	-	-	-	-
050915B	-1.90 ± 0.06	67.4 ± 2.2	55.5	-1.4 ± 0.3	61^{+17}_{-8}	115^{+43}_{-30}	46.0
050916	-1.76 ± 0.21	17.3 ± 2.3	53.8	-	-	-	-
050922B	-2.17 ± 0.26	9.8 ± 1.8	51.5	-	-	-	-
050922C	-1.37 ± 0.06	246.0 ± 7.8	44.9	-	-	-	-
050925	-1.76 ± 0.16	763.0 ± 90.2	87.2	$0.4^{+1.1}_{-0.9}$	61^{+9}_{-7}	7940^{+16000}_{-4870}	68.0
051001	-2.05 ± 0.15	8.5 ± 0.8	43.3	-	-	-	-
051006	-1.51 ± 0.17	36.3 ± 3.5	74.7	-	-	-	-
051008	-1.13 ± 0.05	129.0 ± 3.9	55.0	-	-	-	-
051012	-2.19 ± 0.24	16.2 ± 2.6	78.7	-	-	-	-
051016	-1.89 ± 0.27	33.7 ± 5.6	58.1	-	-	-	-
051016B	-2.40 ± 0.23	37.9 ± 6.3	67.9	-	-	-	-
051021B	-1.55 ± 0.14	16.0 ± 1.3	56.9	$-0.6^{+0.8}_{-0.6}$	72^{+45}_{-14}	50^{+70}_{-30}	49.7
051105	-1.22 ± 0.30	206.0 ± 38.9	43.1	-	-	-	-
051109A	-1.51 ± 0.20	51.1 ± 6.1	63.7	-	-	-	-
051109B	-1.97 ± 0.24	16.1 ± 2.7	63.5	-	-	-	-
051111	-1.32 ± 0.06	59.7 ± 1.9	47.1	-	-	-	-
051113	-1.72 ± 0.14	28.3 ± 2.3	51.0	-	-	-	-
051114	-1.21 ± 0.28	45.2 ± 7.2	45.8	-	-	-	-
051117A	-1.82 ± 0.07	26.6 ± 0.9	46.7	-	-	-	-
051117B	-1.53 ± 0.31	19.5 ± 3.7	60.9	-	-	-	-

Table 5—Continued

GRB	$\alpha^{\rm PL}$	$K_{50}^{\rm PL}$	χ^2	$\alpha^{\rm CPL}$	$E_{\rm peak}^{\rm obs}$	$K_{50}^{\rm CPL}$	χ^2
051210	-1.06 ± 0.28	54.9 ± 8.5	62.4	-	-	-	-
051213	-1.63 ± 0.20	10.8 ± 1.3	53.4	-	-	-	-
051221A	-1.39 ± 0.06	558.0 ± 16.5	55.2	-	-	-	-
051221B	-1.34 ± 0.19	21.5 ± 2.3	56.3	-	-	-	-
051227	-1.45 ± 0.24	5.9 ± 0.8	55.8	-	-	-	-
060102	-1.23 ± 0.39	10.1 ± 2.0	58.7	-	-	-	-
060105	-1.07 ± 0.04	191.0 ± 3.6	32.5	-	-	-	-
060108	-2.03 ± 0.17	23.1 ± 2.5	51.5	-	-	-	-
060109	-1.93 ± 0.24	5.6 ± 0.9	75.6	-	-	-	-
060110	-1.64 ± 0.08	44.3 ± 1.9	46.1	-	-	-	-
060111A	-1.65 ± 0.07	75.1 ± 2.8	69.0	-0.9 ± 0.3	74^{+19}_{-10}	173^{+76}_{-50}	50.4
060111B	-1.01 ± 0.17	23.3 ± 2.1	62.3	-	-	-	-
060115	-1.75 ± 0.12	12.6 ± 0.9	52.6	$-1.0^{+0.6}_{-0.5}$	63^{+36}_{-11}	31^{+29}_{-14}	45.8
060116	-1.43 ± 0.18	20.5 ± 2.1	63.2	-	-	-	-
060117	-1.93 ± 0.03	775.0 ± 12.4	67.0	-1.5 ± 0.1	70^{+7}_{-5}	1170^{+162}_{-138}	35.6
060124	-1.84 ± 0.19	33.9 ± 3.9	54.9	-	-	-	-
060202	-1.71 ± 0.13	10.3 ± 0.8	64.5	-	-	-	-
060203	-1.61 ± 0.23	12.3 ± 1.7	64.9	-	-	-	-
060204B	-1.44 ± 0.09	16.5 ± 0.8	47.0	-0.8 ± 0.4	100^{+75}_{-21}	32^{+18}_{-11}	38.9
060206	-1.71 ± 0.08	74.2 ± 3.1	64.6	-1.2 ± 0.3	78^{+38}_{-13}	137^{+62}_{-40}	55.3
060210	-1.53 ± 0.09	18.7 ± 1.0	64.9	-	-	-	-
060211A	-1.77 ± 0.11	12.9 ± 0.9	71.5	$-0.9^{+0.6}_{-0.5}$	58^{+18}_{-8}	39^{+38}_{-18}	60.6
060211B	-1.57 ± 0.21	15.7 ± 1.9	45.2	-	-	-	-
060218	-2.26 ± 0.17	5.5 ± 0.6	51.3	-	-	-	-
060219	-2.56 ± 0.34	6.4 ± 1.6	59.6	-	-	-	-
060223A	-1.74 ± 0.12	56.2 ± 3.9	61.5	-	-	-	-
060223B	-1.49 ± 0.07	134.0 ± 4.5	42.7	-	-	-	-
060306	-1.80 ± 0.10	33.9 ± 1.8	53.2	-	-	-	-
060312	-1.88 ± 0.09	28.2 ± 1.3	49.2	-	-	-	-
060313	-0.70 ± 0.07	1050.0 ± 40.6	49.9	-	-	-	-
060319	-2.33 ± 0.25	20.4 ± 3.4	58.8	-	-	-	-
060322	-1.58 ± 0.07	19.2 ± 0.8	64.6	$-1.1^{+0.3}_{-0.4}$	96^{+90}_{-18}	34^{+12}_{-11}	57.5
060323	-1.54 ± 0.18	22.8 ± 2.2	56.9	-	-	-	-
060403	-1.08 ± 0.09	33.4 ± 1.7	54.7	-	-	-	-
060413	-1.68 ± 0.08	16.9 ± 0.7	42.9	-	-	-	-
060418	-1.70 ± 0.06	41.0 ± 1.2	44.7	-	-	-	-
060421	-1.55 ± 0.08	64.8 ± 2.8	59.2	-	-	-	-
060424	-1.71 ± 0.19	18.5 ± 2.1	61.4	-	-	-	-
060427	-1.87 ± 0.29	7.8 ± 1.4	43.3	-	-	-	-
060428A	-2.03 ± 0.11	30.3 ± 1.8	40.3	-	-	-	-
060428B	-2.58 ± 0.19	12.3 ± 1.7	66.7	$-0.8^{+1.6}_{-1.2}$	23^{+5}_{-13}	192^{+2140}_{-152}	59.1
060501	-1.45 ± 0.14	46.8 ± 3.8	56.3	-	-	-	-
060502A	-1.46 ± 0.08	54.1 ± 2.3	55.7	-	-	-	-
060502B	-0.98 ± 0.19	408.0 ± 48.9	39.0	-	-	-	-
060505	-1.29 ± 0.28	95.4 ± 15.8	58.1	-	-	-	-
060507	-1.83 ± 0.09	23.8 ± 1.2	65.4	-	-	-	-

Table 5—Continued

GRB	$\alpha^{\rm PL}$	$K_{50}^{\rm PL}$	χ^2	$\alpha^{\rm CPL}$	$E_{\rm peak}^{\rm obs}$	$K_{50}^{\rm CPL}$	χ^2
060510A	-1.57 ± 0.07	362.0 ± 13.4	54.0	-	-	-	-
060510B	-1.78 ± 0.08	12.9 ± 0.5	35.1	-	-	-	-
060512	-2.48 ± 0.30	24.1 ± 5.5	36.1	-	-	-	-
060515	-1.14 ± 0.15	23.8 ± 2.1	75.2	-	-	-	-
060516	-2.19 ± 0.25	6.1 ± 1.1	51.5	-	-	-	-
060522	-1.56 ± 0.15	15.5 ± 1.4	70.6	-	-	-	-
060526	-2.01 ± 0.24	4.4 ± 0.6	56.0	-	-	-	-
060602A	-1.25 ± 0.16	19.1 ± 1.8	38.6	-	-	-	-
060604	-2.01 ± 0.42	4.0 ± 1.1	48.3	-	-	-	-
060605	-1.55 ± 0.20	8.9 ± 1.0	81.0	-	-	-	-
060607A	-1.47 ± 0.08	21.1 ± 0.9	52.1	-	-	-	-
060607B	-1.65 ± 0.12	46.6 ± 3.1	65.5	-	-	-	-
060614	-2.02 ± 0.04	124.0 ± 2.2	46.3	-	-	-	-
060707	-1.71 ± 0.13	24.6 ± 2.0	70.5	$-0.6^{+0.7}_{-0.6}$	63^{+21}_{-10}	85^{+103}_{-42}	60.5
060708	-1.68 ± 0.12	36.9 ± 2.6	62.3	-	-	-	-
060712	-1.62 ± 0.33	45.6 ± 7.7	59.2	-	-	-	-
060714	-1.93 ± 0.11	23.2 ± 1.4	64.5	-	-	-	-
060717	-1.70 ± 0.37	23.4 ± 5.5	48.9	-	-	-	-
060719	-1.91 ± 0.11	19.2 ± 1.2	66.6	-	-	-	-
060728	-1.44 ± 0.44	3.7 ± 1.0	72.9	-	-	-	-
060729	-1.75 ± 0.14	21.6 ± 1.7	47.8	-	-	-	-
060801	-0.47 ± 0.24	107.0 ± 15.8	57.4	-	-	-	-
060804	-1.73 ± 0.26	32.9 ± 5.2	58.8	-	-	-	-
060805	-2.20 ± 0.42	12.6 ± 4.0	57.0	-	-	-	-
060807	-1.58 ± 0.21	13.6 ± 1.6	53.1	-	-	-	-
060813	-1.36 ± 0.04	155.0 ± 3.6	54.1	-1.0 ± 0.2	168^{+117}_{-39}	218^{+45}_{-35}	43.5
060814	-1.53 ± 0.03	67.3 ± 1.1	30.1	-	-	-	-
060825	-1.72 ± 0.07	103.0 ± 3.9	64.8	-1.2 ± 0.3	73^{+28}_{-11}	199^{+89}_{-58}	53.7
060904A	-1.55 ± 0.04	61.8 ± 1.2	43.6	-	-	-	-
060904B	-1.64 ± 0.14	9.4 ± 0.8	45.9	-	-	-	-
060906	-2.03 ± 0.11	50.1 ± 3.2	62.5	-	-	-	-
060908	-1.35 ± 0.06	103.0 ± 3.4	50.7	-1.0 ± 0.3	151^{+184}_{-41}	153^{+50}_{-36}	44.2
060912	-1.74 ± 0.09	219.0 ± 9.7	61.1	-	-	-	-
060919	-1.85 ± 0.19	59.1 ± 6.8	74.4	-	-	-	-
060923A	-1.70 ± 0.23	17.5 ± 2.6	72.6	-	-	-	-
060923B	-2.50 ± 0.25	48.7 ± 8.4	56.9	-	-	-	-
060923C	-2.27 ± 0.24	19.9 ± 3.4	53.7	-	-	-	-
060926	-2.54 ± 0.23	24.8 ± 4.0	58.5	-	-	-	-
060927	-1.65 ± 0.08	52.3 ± 2.4	70.4	-0.9 ± 0.4	72^{+25}_{-11}	123^{+72}_{-42}	57.5
060929	-1.83 ± 0.44	1.6 ± 0.4	48.7	-	-	-	-
061002	-1.76 ± 0.21	38.2 ± 4.4	64.5	-	-	-	-
061004	-1.81 ± 0.10	78.1 ± 4.1	36.5	-	-	-	-
061006	-1.72 ± 0.17	9.5 ± 0.9	49.5	-	-	-	-
061007	-1.03 ± 0.03	176.0 ± 2.6	27.0	-	-	-	-
061019	-1.92 ± 0.26	14.6 ± 2.3	54.0	-	-	-	-
061021	-1.30 ± 0.06	50.0 ± 1.6	43.7	-	-	-	-

Table 5—Continued

GRB	$\alpha^{\rm PL}$	$K_{50}^{\rm PL}$	χ^2	$\alpha^{\rm CPL}$	$E_{\rm peak}^{\rm obs}$	$K_{50}^{\rm CPL}$	χ^2
061027	-1.96 ± 0.46	5.0 ± 1.6	65.5	-	-	-	-
061028	-1.73 ± 0.30	8.8 ± 1.5	46.7	-	-	-	-
061102	-1.56 ± 0.37	6.0 ± 1.3	55.6	-	-	-	-
061110A	-1.67 ± 0.12	24.2 ± 1.6	40.2	-	-	-	-
061110B	-1.03 ± 0.16	8.6 ± 0.7	68.2	-	-	-	-
061121	-1.41 ± 0.03	117.0 ± 1.8	26.7	-	-	-	-
061126	-1.32 ± 0.06	40.7 ± 1.3	41.6	-	-	-	-
061201	-0.81 ± 0.15	336.0 ± 27.4	61.6	-	-	-	-
061202	-1.58 ± 0.07	24.6 ± 0.9	73.6	-	-	-	-
061210	-1.56 ± 0.28	13.2 ± 1.9	70.3	-	-	-	-
061217	-0.86 ± 0.30	131.0 ± 21.7	48.9	-	-	-	-
061218	-2.75 ± 0.63	9.2 ± 7.1	59.6	-	-	-	-
061222A	-1.35 ± 0.04	68.0 ± 1.4	42.3	-	-	-	-
061222B	-1.97 ± 0.13	48.8 ± 4.1	67.9	-	-	-	-
070103	-1.95 ± 0.21	17.6 ± 2.5	47.5	-	-	-	-
070107	-1.33 ± 0.10	12.4 ± 0.6	59.3	-	-	-	-
070110	-1.58 ± 0.12	15.6 ± 1.0	50.5	-	-	-	-
070126	-2.03 ± 0.51	2.8 ± 1.1	46.8	-	-	-	-
070129	-2.01 ± 0.15	6.5 ± 0.6	62.8	-	-	-	-
070208	-1.94 ± 0.36	9.9 ± 2.3	61.5	-	-	-	-
070209	-1.00 ± 0.38	146.0 ± 34.6	75.0	-	-	-	-
070219	-1.78 ± 0.22	18.0 ± 2.4	57.4	-	-	-	-
070220	-1.40 ± 0.04	42.0 ± 0.9	42.6	-	-	-	-
070223	-1.85 ± 0.12	18.1 ± 1.3	50.8	-	-	-	-
070224	-2.42 ± 0.30	8.2 ± 1.8	77.0	-	-	-	-
070227	-1.53 ± 0.27	215.0 ± 31.3	52.5	-	-	-	-
070306	-1.66 ± 0.10	19.0 ± 0.9	61.2	-	-	-	-
070318	-1.42 ± 0.08	24.6 ± 1.0	50.1	-	-	-	-
070328	-1.24 ± 0.04	60.7 ± 1.3	36.7	-	-	-	-
070330	-2.06 ± 0.22	24.0 ± 3.6	66.7	-	-	-	-
070406	-1.38 ± 0.60	30.7 ± 9.2	34.3	-	-	-	-
070411	-1.72 ± 0.10	17.2 ± 0.9	56.4	-	-	-	-
070412	-1.45 ± 0.20	14.3 ± 1.7	64.2	-	-	-	-
070419A	-2.35 ± 0.25	4.5 ± 0.8	69.2	-	-	-	-
070419B	-1.66 ± 0.05	24.3 ± 0.6	29.6	-	-	-	-
070420	-1.56 ± 0.05	117.0 ± 3.4	60.7	-1.2 ± 0.2	120^{+76}_{-24}	176^{+47}_{-36}	51.1
070427	-2.08 ± 0.10	56.0 ± 3.0	36.4	-	-	-	-
070429A	-2.10 ± 0.27	5.2 ± 0.9	73.8	-	-	-	-
070429B	-1.72 ± 0.23	132.0 ± 19.8	41.5	-	-	-	-
070506	-1.73 ± 0.17	46.1 ± 4.8	55.8	-	-	-	-
070508	-1.35 ± 0.03	432.0 ± 6.3	38.4	-1.1 ± 0.1	260^{+203}_{-68}	522^{+56}_{-49}	27.8
070509	-2.33 ± 0.25	20.2 ± 3.6	42.2	-	-	-	-
070517	-1.94 ± 0.25	27.4 ± 4.6	60.1	-	-	-	-
070518	-2.11 ± 0.25	27.7 ± 4.5	63.9	-	-	-	-
070520A	-1.60 ± 0.33	13.4 ± 2.7	56.9	-	-	-	-
070520B	-1.14 ± 0.21	11.7 ± 1.3	58.7	-	-	-	-

Table 5—Continued

GRB	$\alpha^{\rm PL}$	$K_{50}^{\rm PL}$	χ^2	$\alpha^{\rm CPL}$	$E_{\rm peak}^{\rm obs}$	$K_{50}^{\rm CPL}$	χ^2
070521	-1.36 ± 0.04	130.0 ± 2.6	57.5	-1.1 ± 0.2	209^{+234}_{-60}	166^{+30}_{-24}	50.1
070529	-1.34 ± 0.16	21.5 ± 1.9	51.0	-	-	-	-
070531	-1.41 ± 0.20	22.9 ± 2.5	54.6	-	-	-	-
070611	-1.66 ± 0.22	30.9 ± 4.3	53.4	-	-	-	-
070612A	-1.69 ± 0.10	27.2 ± 1.5	54.8	-	-	-	-
070612B	-1.55 ± 0.11	107.0 ± 7.0	46.1	-	-	-	-
070616	-1.61 ± 0.04	34.1 ± 0.6	55.0	-	-	-	-

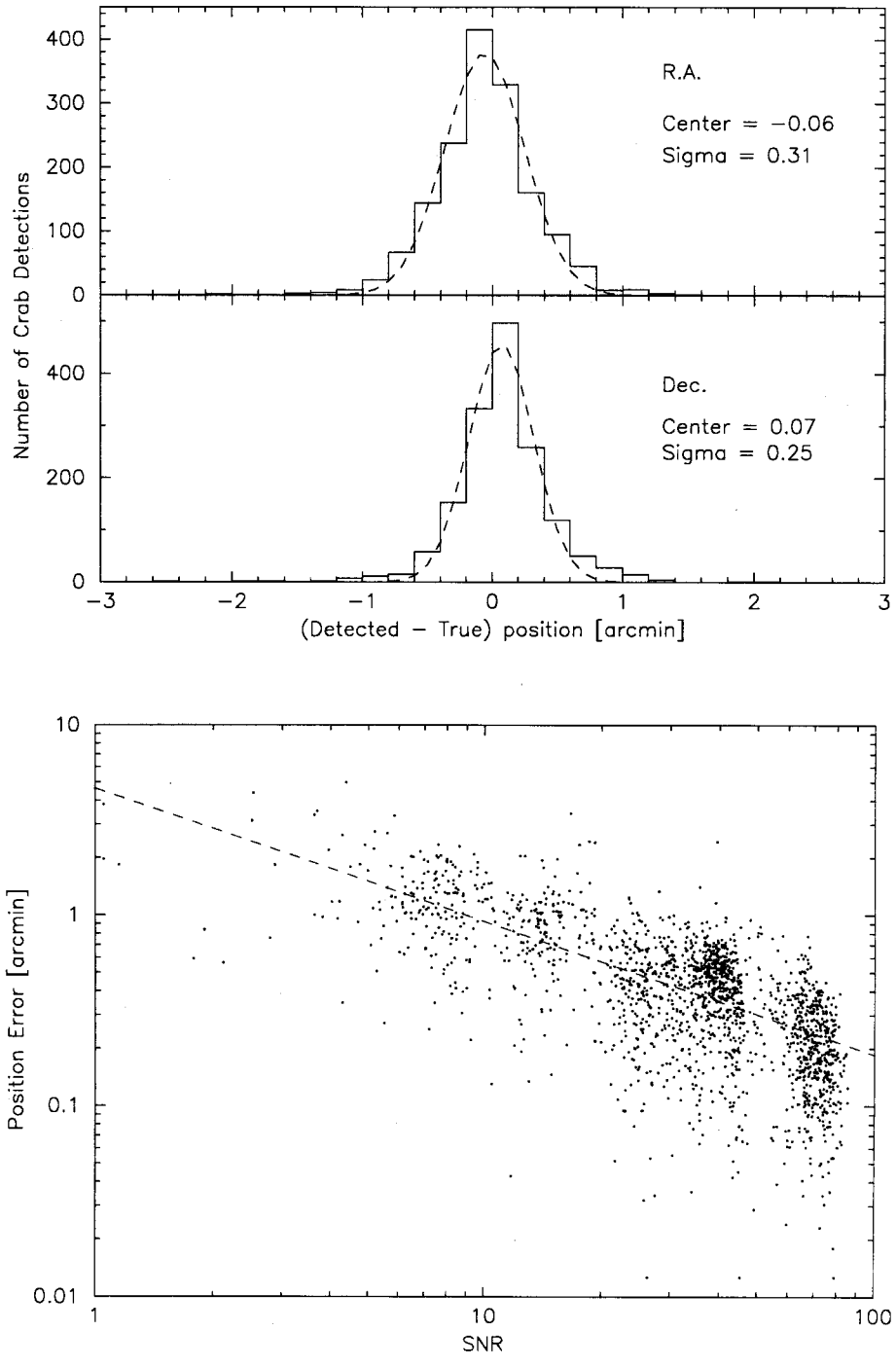

Fig. 1.— Top: The difference in R.A. (top) and Dec. (bottom) between the BAT detected ($> 8\sigma$) and the SIMBAD ('true') Crab position. The dotted line is the best fit gaussian model. The centroid and sigma of the best fit gaussian are $-0.07'$ and $0.33'$ for R.A., and $0.08'$ and $0.27'$ for Dec., respectively. Bottom: BAT position errors as a function of signal to noise ratio for the Crab. The red dashed line is the position error $\propto \mathrm{SNR}^{-0.7}$.

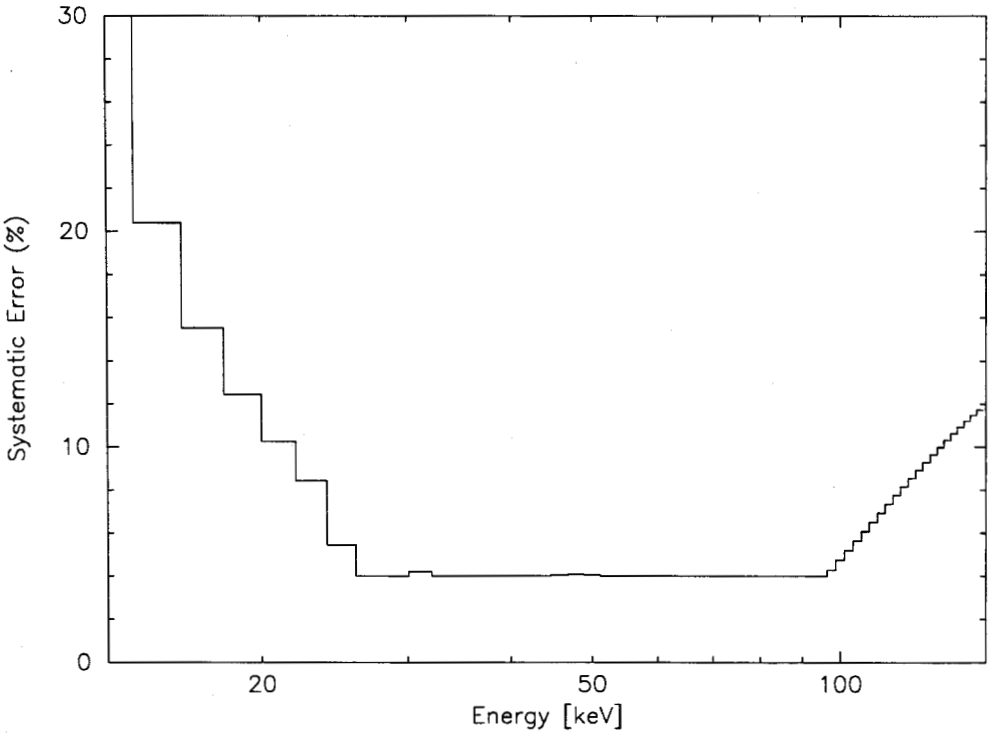

Fig. 2.— Systematic error as a function of energy. The systematic error vectors must be applied to the BAT spectral file created by the BAT software, HEASoft 6.2 and CALDB: 2006-10-14, due to the current uncertainly in the energy calibration.

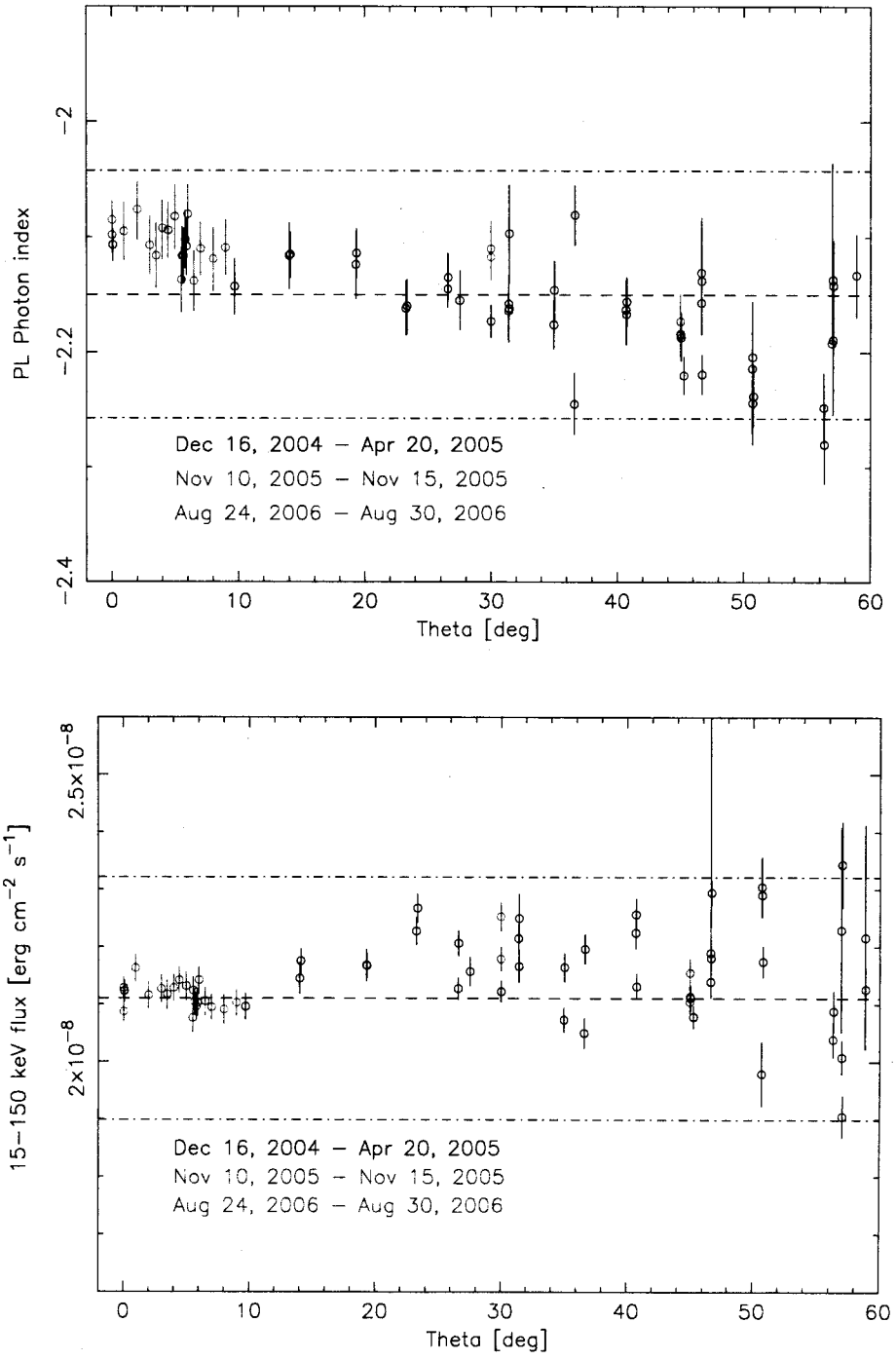

Fig. 3.— The power-law photon index (top) and the flux in the 15-150 keV band as a function of the incident angle (θ) of the Crab observed December 2004-April 2005 (black), November 2005 (red), and August 2006 (blue). The horizontal dashed lines are the Crab canonical values of -2.15 for the photon index and 2.11×10^{-8} ergs cm^{-2} s^{-1} for the flux. The dashed dotted lines are $\pm 5\%$ of the photon index and $\pm 10\%$ of the flux canonical values.

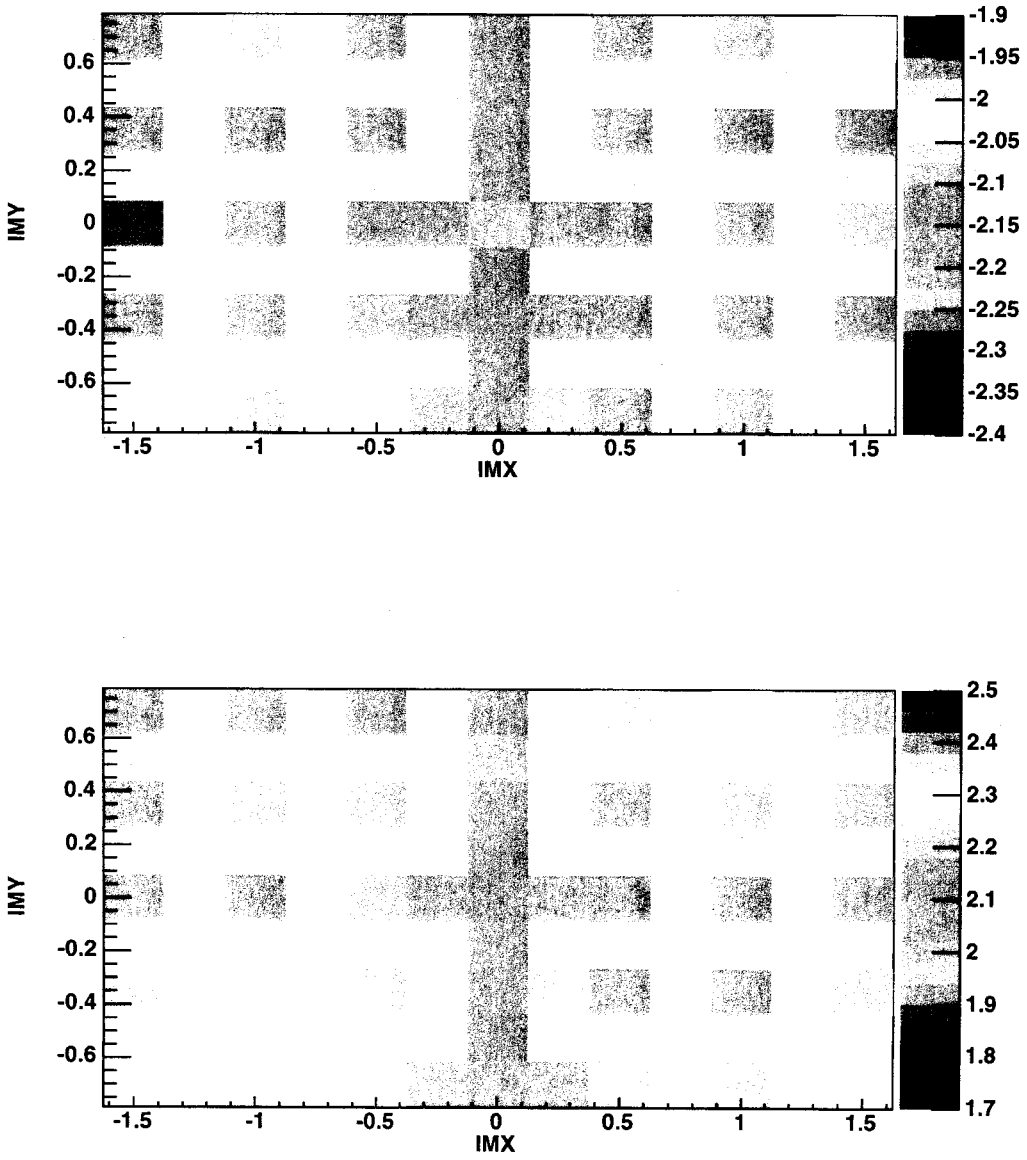

Fig. 4.— The contour maps (sparsely sampled) of the Crab photon index (top) and the flux in the 15-150 keV band in units of 10^{-8} ergs cm^{-2} s^{-1} (bottom) in the BAT field of view in tangent plane coordinates (IMX and IMY).

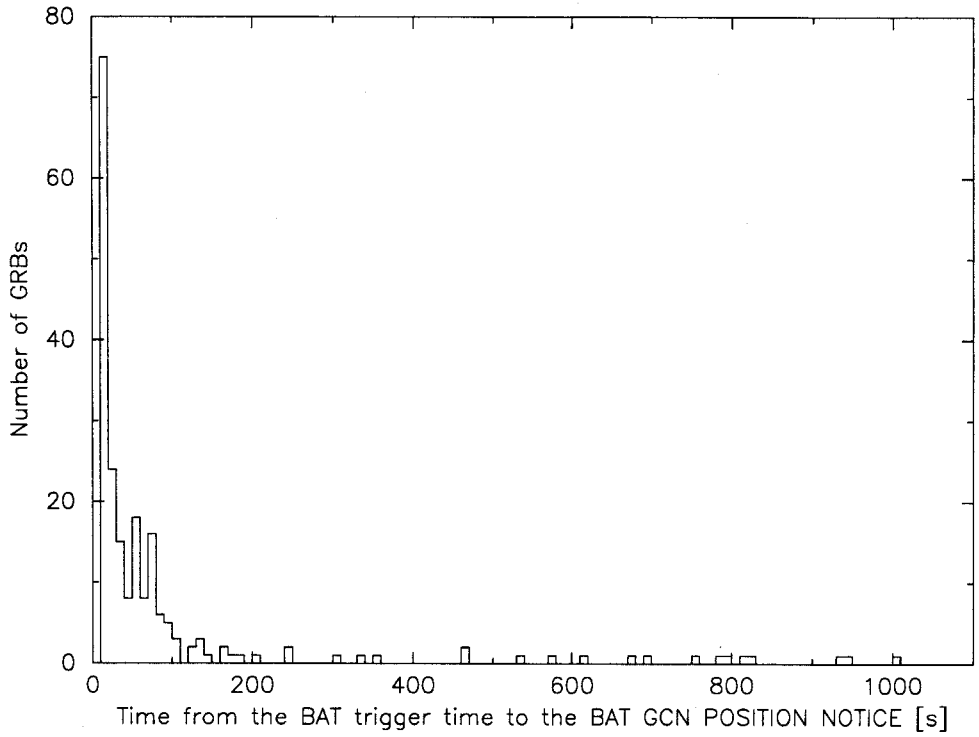

Fig. 5.— The time delay from the BAT trigger time to the GCN BAT Position Notice (the BAT burst sample from GRB 050215A to GRB 070616 excluding the GRBs found in ground processing).

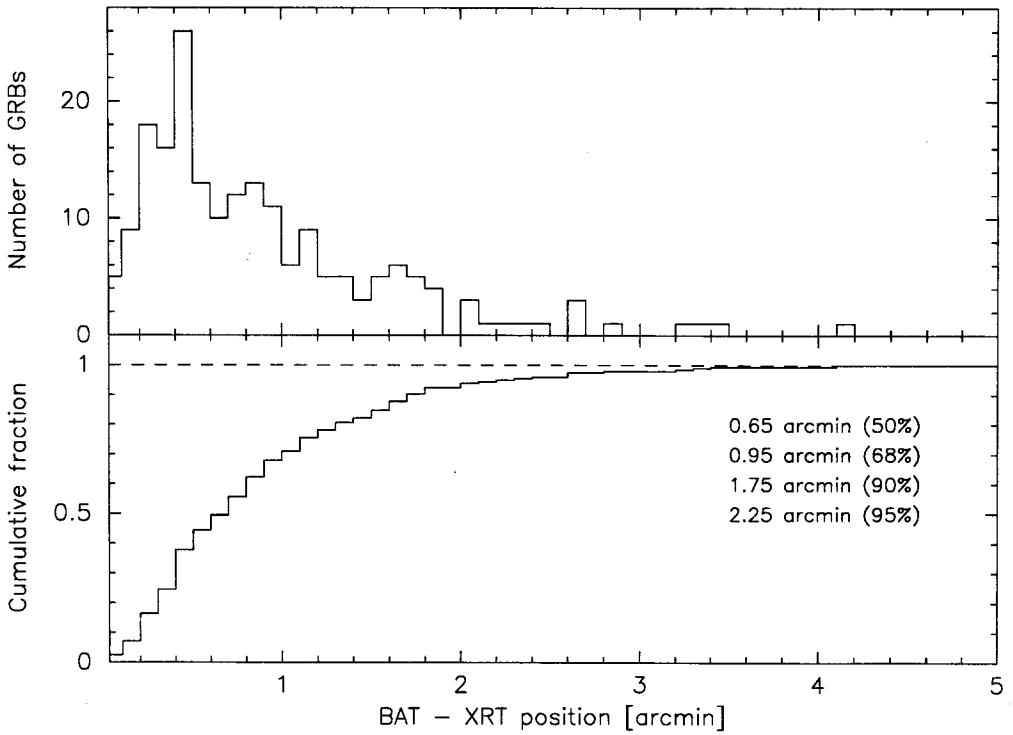

Fig. 6.— The histogram (top) and the cumulative fraction (bottom) of the angular difference between the BAT ground position and the XRT position. 68% and 90% of BAT ground positions are within 0.95′ and 1.75′ from the XRT position, respectively.

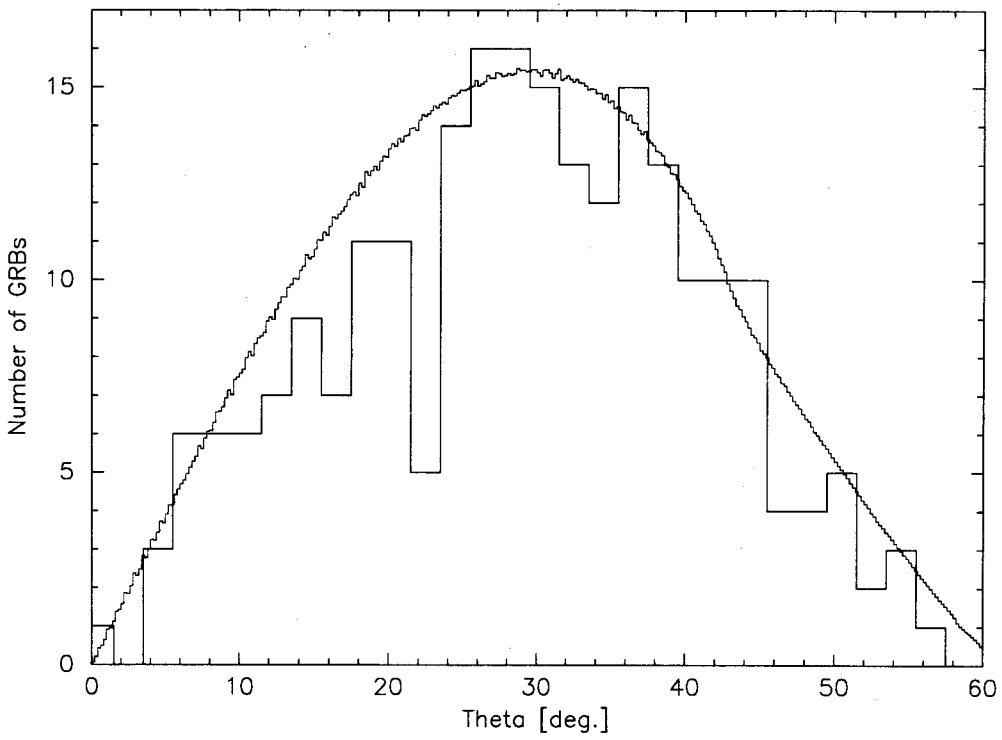

Fig. 7.— The incident angle (θ) distribution of the BAT GRBs. The red line shows the calculated θ distribution in the case of the uniform sky distribution.

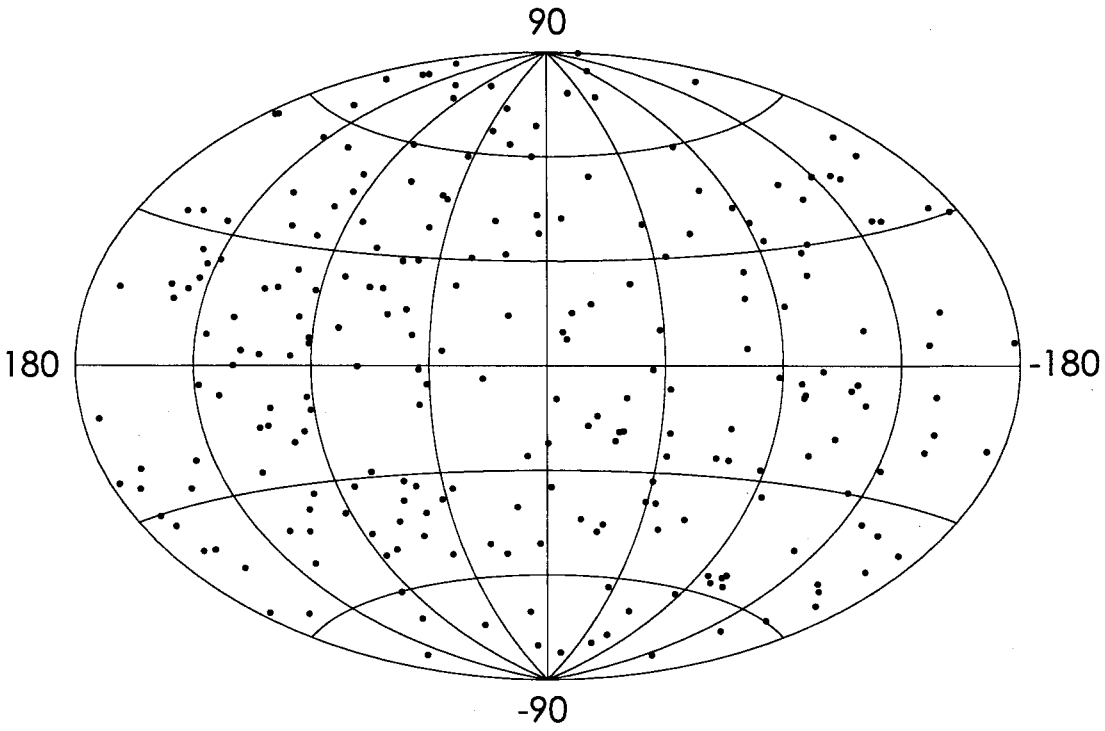

Fig. 8.— Sky distribution of the 237 BAT bursts in Galactic coordinates.

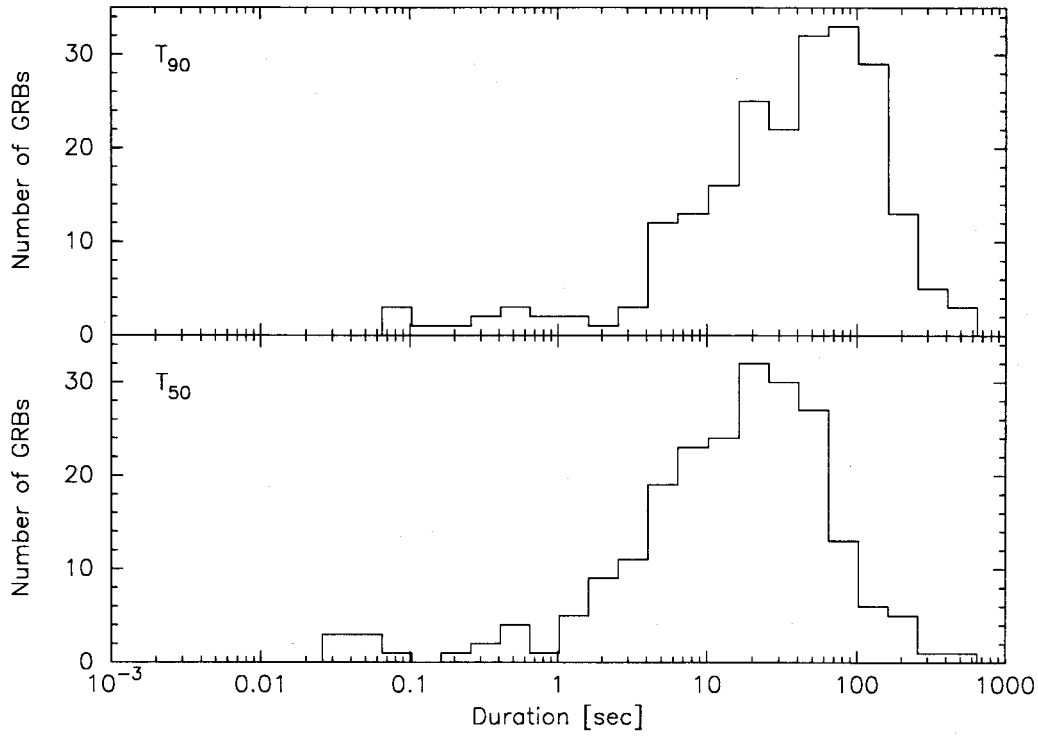

Fig. 9.— T_{90} (top) and T_{50} (bottom) distributions from the BAT mask-weighted light curves in the 15-350 keV band.

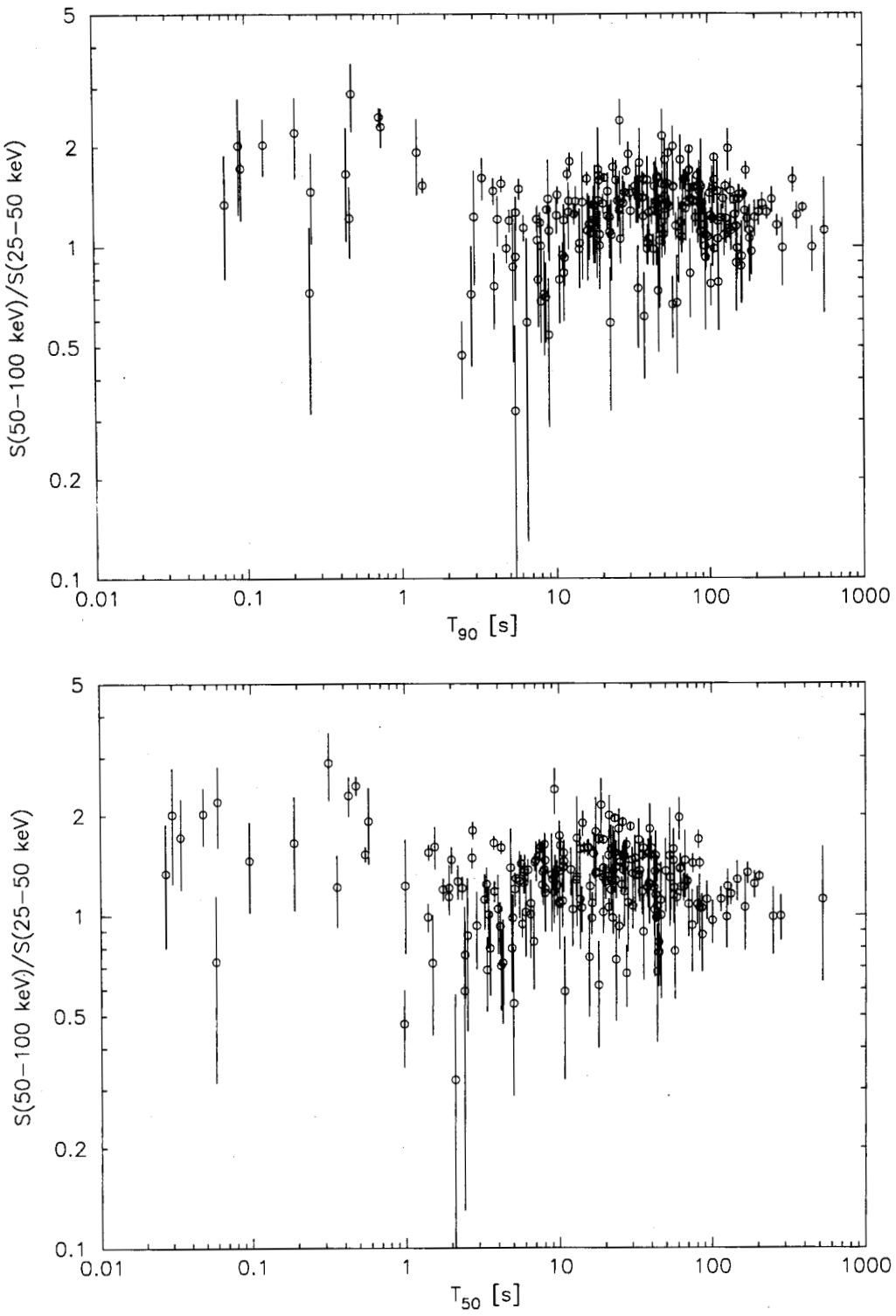

Fig. 10.— T_{90} (top) and T_{50} (bottom) versus the fluence ratio between the 50-100 keV and the 25-50 keV bands.

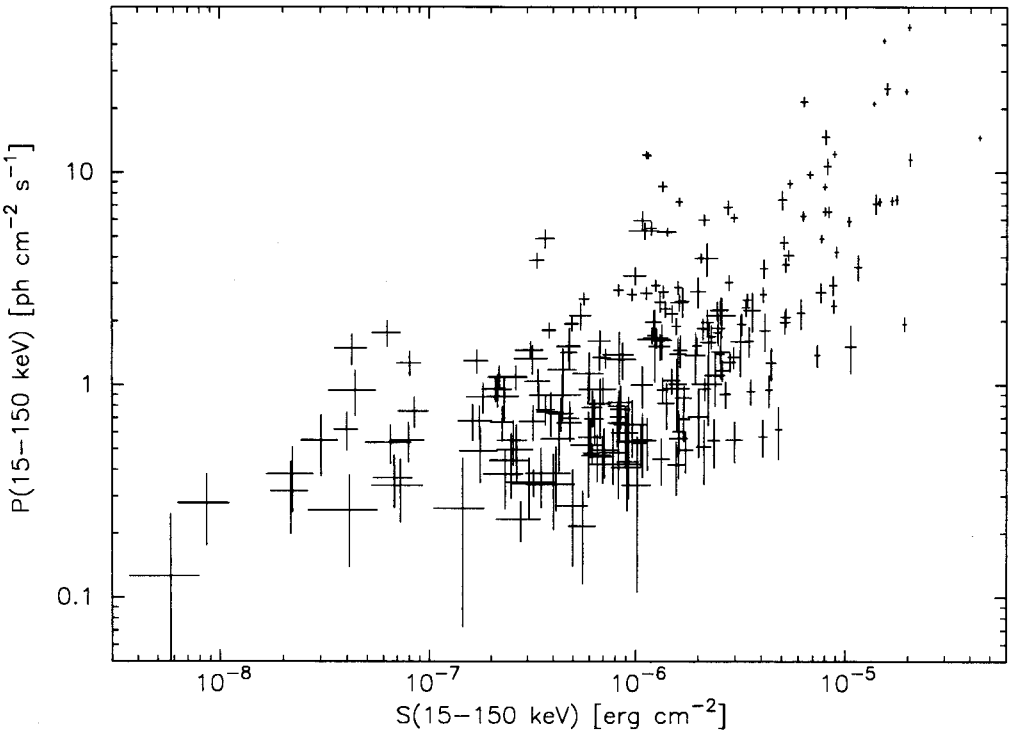

Fig. 11.— The distribution of the energy fluence in the 15-150 keV band versus 1-s peak photon flux in the 15-150 keV band.

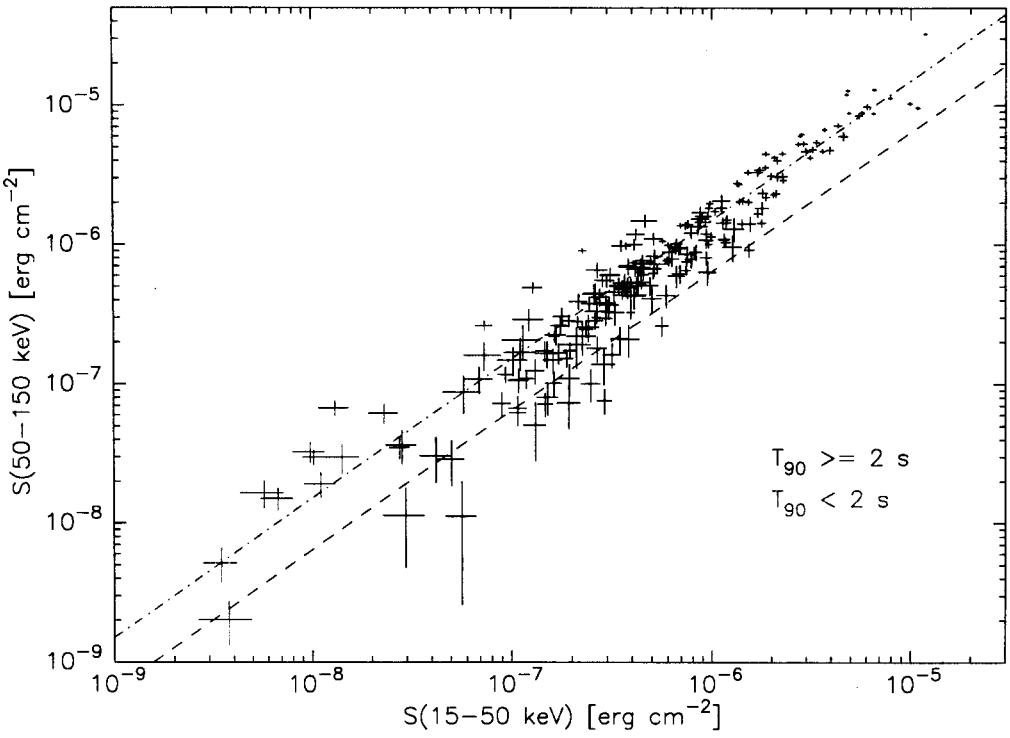

Fig. 12.— The distribution of the energy fluence in the 15-50 keV band versus that in the 50-150 keV band. Long GRBs ($T_{90} \geq 2$ s) are in black and short GRBs ($T_{90} < 2$ s) are in red. The blue dash-dotted line is the case of the Band function of $\alpha = -1$, $\beta = -2.5$, and $E^{\rm obs}_{\rm peak} = 100$ keV. The blue dashed line is the case of the Band function of $\alpha = -1$, $\beta = -2.5$, and $E^{\rm obs}_{\rm peak} = 30$ keV.

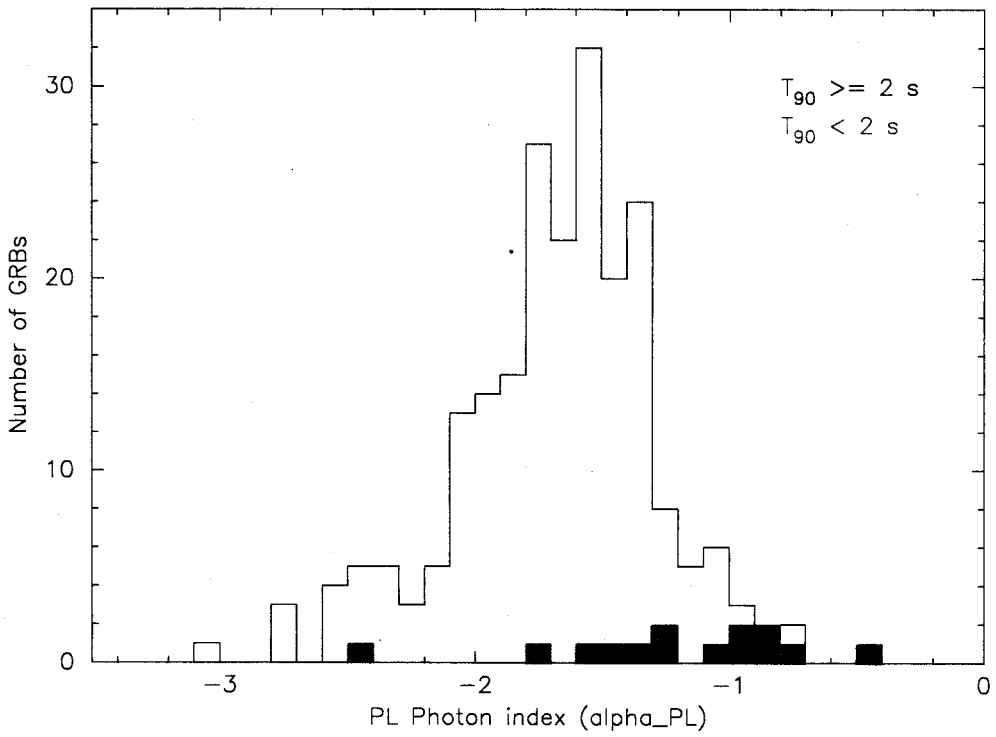

Fig. 13.— The histogram of the photon index in a PL fit for long GRBs (black) and short GRBs (red). The short GRB which has a PL photon index of −2.5 is GRB 050906.

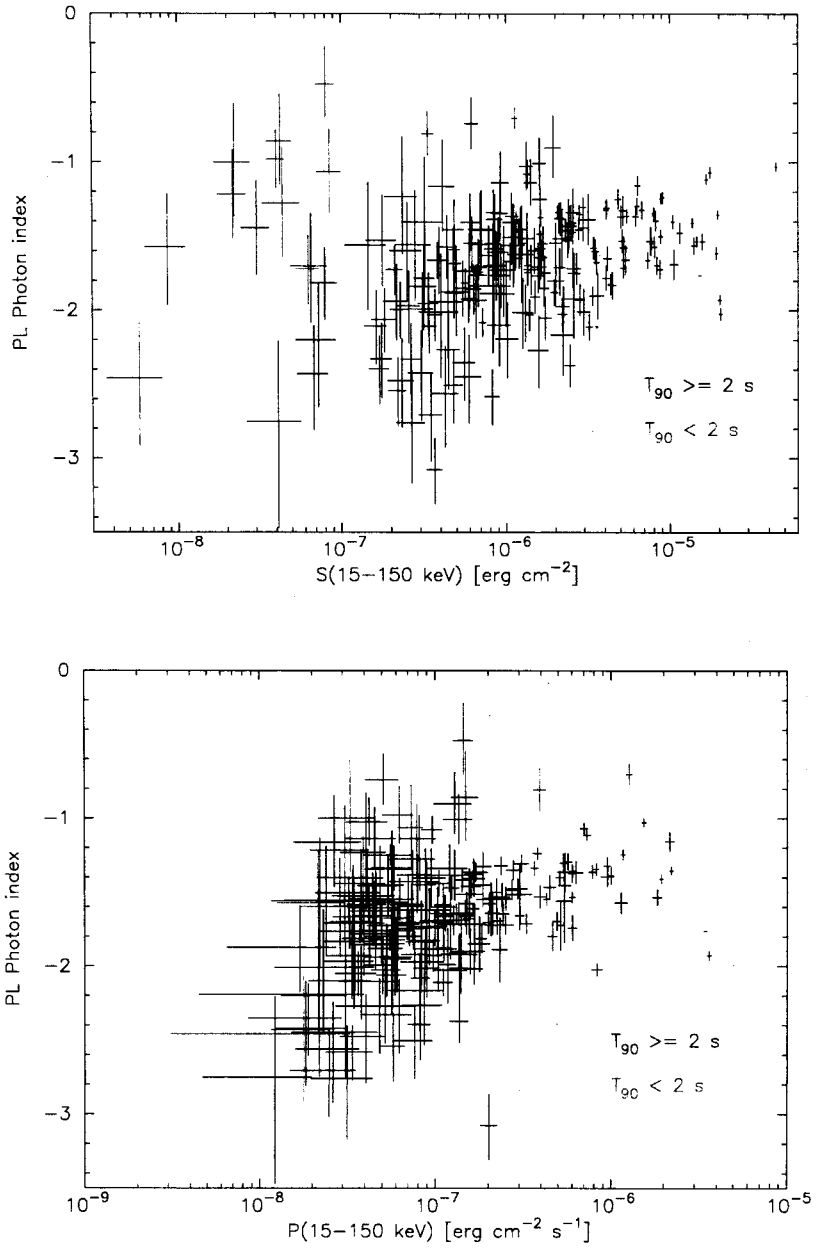

Fig. 14.— Top: The distribution of the PL photon index versus the energy fluence in the 15-150 keV band for long GRBs (black) and short GRBs (red). Bottom: The distribution of the PL photon index versus the 1-s peak energy flux in the 15-150 keV band for long GRBs (black) and short GRBs (red).

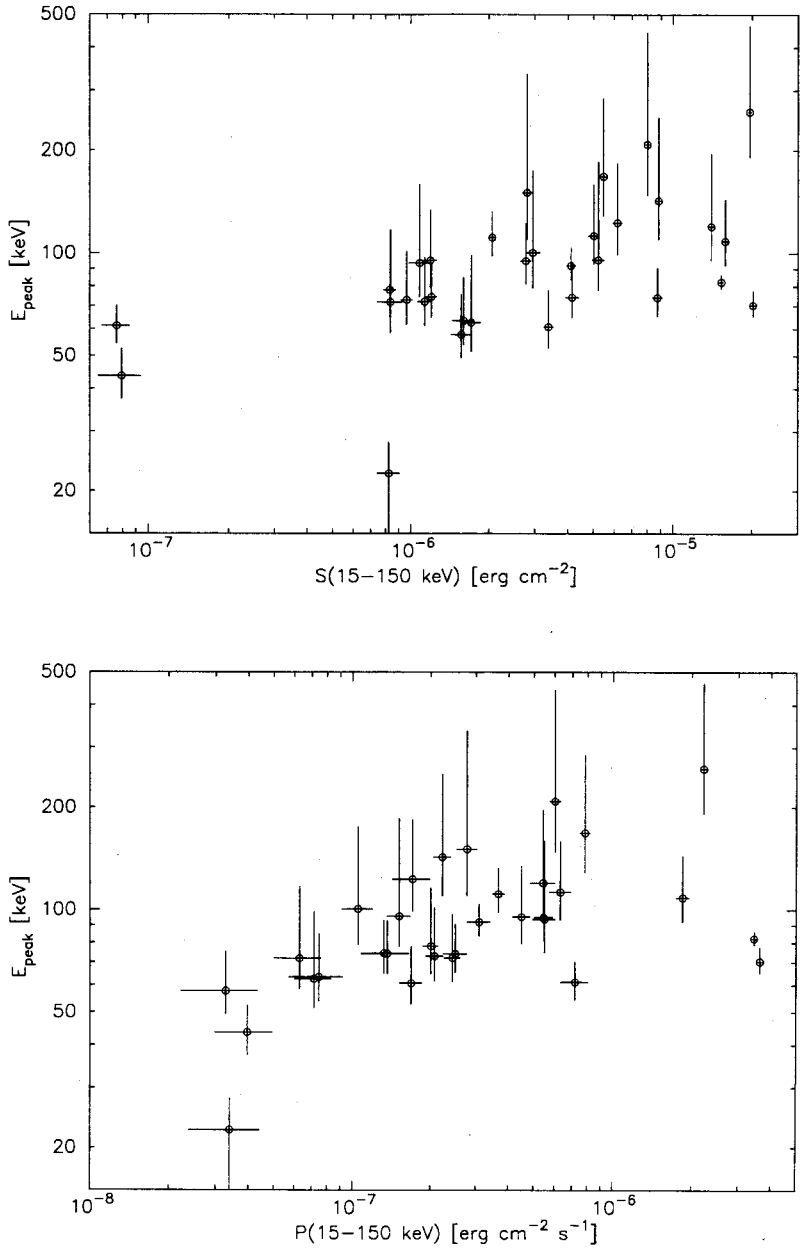

Fig. 15.— Top: The distribution of $E_{\rm peak}$ versus the energy flux in the 15-150 keV band. Two GRBs which locate in $\sim 7 \times 10^{-8}$ erg cm^{-2} are GRB 050815 and GRB 050925. One GRB which has $E_{\rm peak}$ of $\sim$ 20 keV is GRB 060428B. Bottom: The distribution of $E_{\rm peak}$ versus the 1-s peak energy flux in the 15-150 keV band.

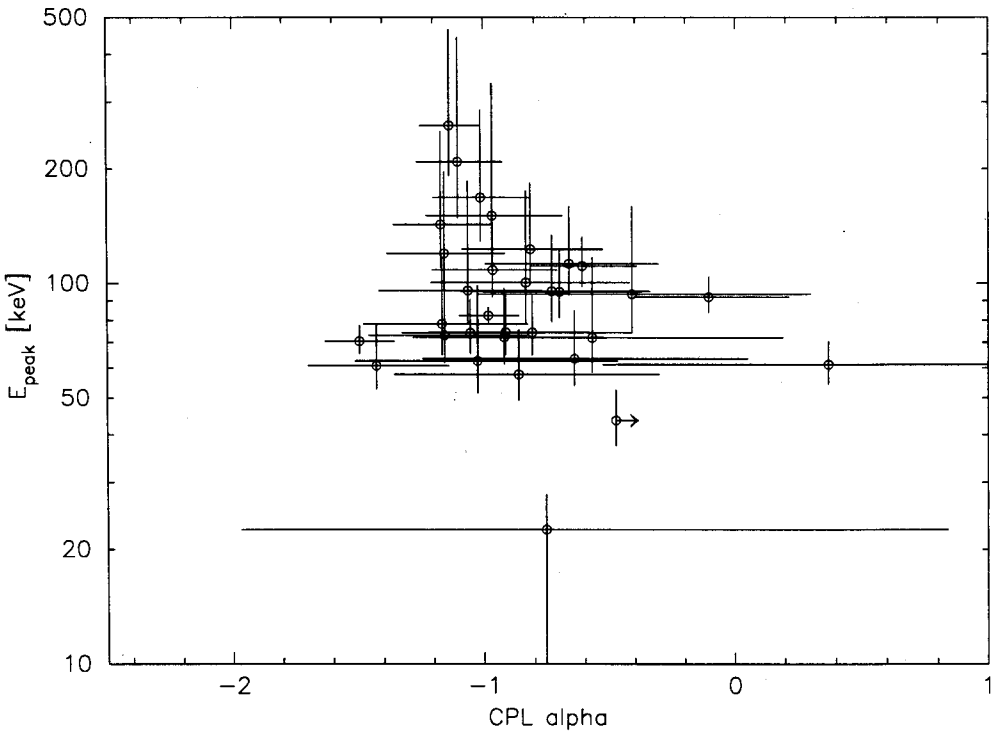

Fig. 16.— The distribution of $E^{\rm obs}_{\rm peak}$ versus the CPL photon index for 32 GRBs which have a significant improvement in χ^2 by a CPL fit over a PL fit.

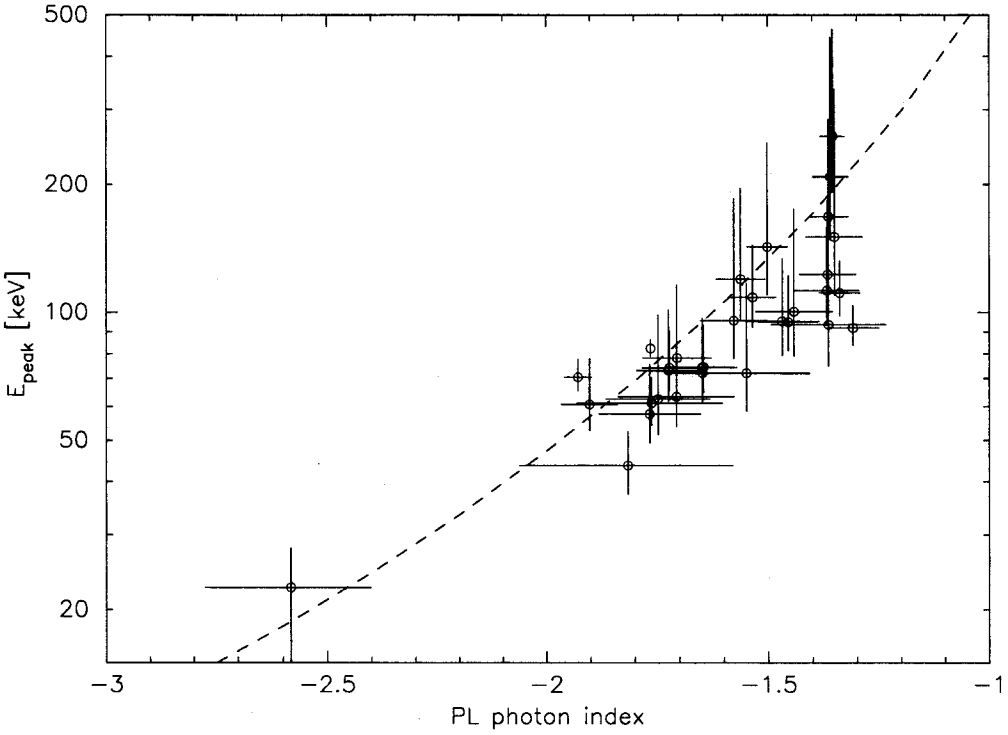

Fig. 17.— The distribution of $E_{\rm peak}^{\rm obs}$ versus the PL photon index for 32 GRBs. The dashed line is the PL photon index - $E_{\rm peak}^{\rm obs}$ correlation of Zhang et al. (2007): $\log E_{\rm peak}^{\rm obs} = 2.76 - 3.61 \log(-\alpha_{PL})$.